



VLÁKNA

TEXTIL

FIBRES AND TEXTILES



Volume **31**
June
2024

TECHNICAL
UNIVERSITY
OF LIBEREC

STU
FCHPT



Indexed in:

SCOPUS
Chemical Abstract
World Textile Abstracts
EBSCO Essentials

ISSN 1335-0617
print version

ISSN 2585-8890
online version



VLÁKNA A TEXTIL

<http://www.vat.ft.tul.cz>

PUBLISHED BY

Technical University of Liberec, Faculty of Textile Engineering
Slovak University of Technology in Bratislava, Faculty of Chemical and Food Technology
Alexander Dubček University of Trenčín, Faculty of Industrial Technologies
Slovak Society of Industrial Chemistry, Bratislava
Research Institute of Man-Made Fibres, JSC, Svit
Research Institute of Textile Chemistry (VUTCH) Ltd., Žilina
Chemosvit Fibrochem, JSC, Svit

EDITOR IN CHIEF

Maroš TUNÁK, Technical University of Liberec, CZ

EXECUTIVE EDITOR

Veronika TUNÁKOVÁ, Technical University of Liberec, CZ

EDITORIAL BOARD

Ľudmila BALOGOVIÁ, VUTCH Ltd., Žilina, SK
Marcela HRICOVÁ, Slovak University of Technology in Bratislava, SK
Vladimíra KRMELOVÁ, A. Dubček University of Trenčín, SK
Zita TOMČÍKOVÁ, Research Institute of Man-Made Fibres, JSC, Svit, SK
Maroš TUNÁK, Technical University of Liberec, CZ
Veronika TUNÁKOVÁ, Technical University of Liberec, CZ
Tomáš ZATROCH, Chemosvit Fibrochem, JSC, Svit, SK

HONOURABLE EDITORIAL BOARD

Vladimír BAJŽÍK, Technical University of Liberec, CZ
Martin BUDZÁK, Research Institute of Man-Made Fibres, JSC, Svit, SK
Anton GATIAL, Slovak University of Technology in Bratislava, SK
Ana Marija GRANCARIĆ, University of Zagreb, HR
Anton MARCINČIN, Slovak University of Technology in Bratislava, SK
Alenka M. LE MARECHAL, University of Maribor, SL
Jiří MILITKÝ, Technical University of Liberec, CZ
Darina ONDRUŠOVÁ, Alexander Dubček University in Trenčín, SK
Olga PARASKA, Khmelnytskyi National University, UA
Anna UJHELYIOVÁ, Slovak University of Technology in Bratislava, SK

PUBLISHER

Technical University of Liberec
Studentska 1402/2, 461 17 Liberec 1, CZ
Tel: +420 485 353615
e-mail: vat@tul.cz
IČO: 46747885

ORDER AND ADVERTISEMENT OF THE JOURNAL

Technical University of Liberec
Faculty of Textile Engineering
Studentska 1402/2, 461 17 Liberec 1, CZ
Tel: +420 485 353615
e-mail: vat@tul.cz

TYPESET AND PRINT

Vysokoškolský podnik, s.r.o., Voroněžská 1329/13, 460 01 Liberec 1, CZ

DATE OF ISSUE

June 2024

APPROVED BY

Rector's Office of Technical University of Liberec
Ref. no. RE 31/24, 12th June 2024

EDITION

First

PUBLICATION NUMBER

55-031-24

PUBLICATION

Quarterly

SUBSCRIPTION

60 EUR

VLÁKNA A TEXTIL

Volume 31, Issue 1, June 2024

CONTENT

- 3** **TRAN, THI MINH KIEU; TRAN, THI NGOC HUE; NGUYEN, THANH TUNG AND HOANG, SY TUAN**
ANALYSIS OF VIETNAMESE WOMEN'S BODY SHAPE FROM ANTHROPOMETRIC DATA
- 13** **SHAHIDI, SHEILA; MOAZZENHI, BAHAREH; KALAHROODI, HOSSEINI KIMIASADAT AND**
MONGKHOLRATTANASIT, RATTANAPHOL
WOUND DRESSING WITH TEXTILE DRESSING APPROACH: A REVIEW
- 26** **THO, LUU THI; PHUONG, DUONG THI AND HUONG, CHU DIEU**
EFFECT OF COMMERCIAL WATER REPELLENT AGENTS ON FUNCTIONAL PROPERTIES OF
POLYESTER WOVEN FABRIC USED FOR WASHABLE MEDICAL MASKS
- 37** **STEHLE, FRANZISKA; GILLNER CHRISTIANE; DILBA BORIS; KEUCHEL SÖREN AND HERRMANN, AXEL S.**
ANALYSIS OF AIRFLOW RESISTIVITY AND ACOUSTIC ABSORPTION OF FIBRE-REINFORCED
PLASTIC COMPOSITES MADE OF POLYLACTIC ACID AND NATURAL FIBRES

ANALYSIS OF VIETNAMESE WOMEN'S BODY SHAPE FROM ANTHROPOMETRIC DATA

TRAN, THI MINH KIEU^{1*}; TRAN, THI NGOC HUE^{1,2}; NGUYEN, THANH TUNG^{1,3} AND HOANG, SY TUAN⁴

¹ School of Material Science and Engineering, Hanoi University of Science and Technology, Vietnam

² Technical and technological college, Hanoi, Vietnam

³ Hanoi Industrial University, Vietnam

⁴ School of Mechanical Engineering, Hanoi University of Science and Technology, Vietnam

ABSTRACT

This study aims to classify and analyze the body shapes of Vietnamese women aged 18 to 50 using 3D anthropometric data. Research data was collected from 480 females across three regions: North, Central, and South. The five body types result from data analysis involving principal component analysis, K-means cluster analysis, numerical discriminant analysis, ANOVA test, and T-test comparison using SPSS software. Group 1, accounting for 15.23 %, represents the "short, thin, small-shouldered" body type with medium hip height and a bust-waist ratio higher than the hip-waist ratio. Group 2, accounting for 18.36 %, can be described as the "tall, slightly fat and large-shoulders" body type, characterized by high stature and hip height, with a bust-waist ratio smaller than the hip-waist ratio. Group 3, accounting for 35.94 %, falls under the category of the "Medium body type", with an average height stature and a fit body, and a bust-waist ratio equal to the waist-to-hip ratio. Group 4, representing 21.88 %, has a low hip height, a bust-waist ratio higher than the hip-waist ratio, and can be called the "short, fat, medium-shoulder" body type. Finally, group 5, which comprises 8.59 %, embodies the "too fat, average height, big shoulders" body type, featuring low hip height, and a bust - waist ratio higher than the hip-waist ratio. The method of body classification in this study is scientifically sound and reliable. The new research results can serve as a reference for the garment industry while contributing to the goal of building a virtual model library within 3D design software.

KEYWORDS

Analysis, classify, body shape, women, working age, Vietnamese.

INTRODUCTION

In today's rapidly evolving society, market competition has intensified, and new technologies continue to emerge, influencing various aspects of our social life. In the face of opportunities presented by the fourth Industrial Revolution and the challenges posted by the COVID-19 pandemic to the fashion industry, 3D technology has not only adapted but has also become stronger than ever before [1, 2]. As of today, 3D technology has covered all areas of society, offering growth opportunities for creativity, particularly in the fashion industry [3-5]. Additionally, 3D anthropometric data play a significant role in this ongoing development [6-8].

Furthermore, research into anthropometry serves as an important foundation for determining the precise details of costume design and body characteristics, which, in turn, profoundly influence the creation of

basic blocks [9,10]. It is essential to recognize that the human body's proportions do not follow a completely regular pattern as they evolve [11]. In fact, each geographical area has a different body shape, making body classification a significant consideration when tailoring garments to suit the specific needs and preferences of each locale, ultimately leading to cost savings, and ensuring a perfect fit during garment production [12]. According to the general laws of biology, every 10-15 years, changes in living conditions lead to alterations in size and physical strength of residents [13]. Therefore, research into shape characteristics and body classification should be regularly updated to accommodate these variations of anthropometry over time [14]. Thus, the study of 3D-supported body shape analysis remains extremely necessary in the present context, especially for women of working age [15].

* Corresponding author: Tran T.M.K., e-mail: kieu.tranthiminh@hust.edu.vn

Received October 3, 2022; accepted December 4, 2023

In Vietnam, there have been many researches focused on classifying female body shape, typically [16,17]. In the study [16], author categorized Vietnamese female students into 2 distinct body shape groups: Shape 1 characterized by a small waist, wide hips, a protruding belly, warped buttocks, straight legs, and short, small thighs; and Shape 2, characterized by a larger waist, small hips, a flat stomach, low hips, slightly curved long legs, and larger thighs. Meanwhile, the study titled "Study on Terms of Adjusting the Design of Vietnamese Women's Juniors According to Body Diversity using V-Stitcher 3-Dimensional Clothing Design Software" [9] identified seven body shapes: Triangle 1, Spoon shape, Hourglass Bottom 1, Rectangle 1, Rectangle 2, Hourglass Bottom 2, Triangle 2. Moreover, another study [11] conducted in 2012 on the same topic, classified Vietnamese women's physique into three groups: Group 1 includes short and slender women with small body lengths, thin bodies, narrow shoulders, a narrow chest circumference, and a large waist; Group 2 comprised taller, obese women with prominent bellies, broad shoulders, wide hips, and smaller busts; and Group 3 includes shorter women with thick, curvier bodies, large bust, medium shoulders, and narrow hips. The proportions of the human body were also analyzed specifically in the study [18] of Bunka University - Japan. In this study, the authors mentioned the ratio of head-to-body height with a standard ratio of 7.1, hip height ratio and the relationship between width, thickness, and height of the body. However, the proportions of the Vietnamese female human body have not been published.

The research in this article focuses on classifying the body shape of Vietnamese women between the age of from 18 and 55 who are of working age. This analysis aims to discern the distinct characteristics of body shapes and proportions, contributing to the development of a virtual model library in 3D design software within the context of the Fourth Industrial Revolution.

RESEARCH CONTENT, SUBJECTS AND METHODOLOGY

Subjects

The subjects of this study consist of women between the age of 18 and 55, classified as workers, students, civil servants, residing in the two major cities of Hanoi and Ho Chi Minh City. These participants are of Kinh ethnicity, exhibit normal body shapes and overall good health, and do not have any bodily deformities. The subjects working in these two metropolitan areas represent diverse regions across Vietnam, thus ensuring that the study's measurements encompass

the entire Northern, Central, and Southern regions of the country.

The sample size was determined by the formula:

$$n = \frac{(t SD)^2}{m^2} = \frac{(1.96 \cdot 5.5)^2}{0.5^2} \approx 464.83 \quad (1)$$

where: n is the minimum sample size; probability $p = 0.95$ corresponding to standard error $t = 1.96$; m is the required accuracy of the dimensions ($m = 0.5$ cm); SD is the standard deviation of the height size of Vietnamese women ($SD = 5.5$ cm) [16, 19]. Thus, the minimum sample size is 465 (sample). However, in fact, the study measured 480 (sample) for measurement errors precautions in the study.

Body measurements: The selected body measurements are the circumference, length, width, height, and body depth dimensions which are used to set avatar parameters in CLO3D software and establish typical sizes for classifying female body types. These dimensions in CLO3D correspond to the definition of anthropometric measurements from International Standard ISO 8559-1 [20, 21]. To investigate the classification of female body shapes among individuals aged 18 to 55 in the workforce, the author employed a 3D body scanner to collect a total of 36 anthropometric measurements. These measurements include 10 circumferences, 3 lengths, 9 widths, 11 heights and 3 thickness measurements, as detailed in Table 1.

Research Methodology

480 Vietnamese women were 3D measured by F6 Smart device. The body shape analysis method employed SPSS 26.0 software in this study involved the following steps:

- Determine the statistical characteristics of the measurement.
- Determining the main components in a total of 36 measurements, we conducted factor analysis using Varimax orthogonal rotation applied to rotate the components. We assessed the suitability of variables for PCA using the Kaiser-Meyer-Olkin (KMO) and Bartlett's tests to determine the dominant size [22, 23].
- Analysis of clustering by K-means cluster analysis and discriminant analysis. In case the final number of clusters is determined, one-way analysis of variance (ANOVA) and Scheffe - test will be performed to observe the difference in human body size for each body type because of the results. of the analytical cluster [11, 15, 22, 23, 24].
- Enter avatar size parameters in CLO3D software to display analyzed body shapes [1, 25].
- Analysis of body proportions of Vietnamese women's body groups through ANOVA results.

Table 1. Measurement used in the study.

Category	Measurement items	Number
Circumference	Neck-, Upper bust-, Bust-, Under bust-, Waist-, Abdomen-, Hip-, Thigh-, Bicep - circumference, Total rise	10
Length	HPS to apex, Center back neck to wrist, Shoulder length	3
Width	Head width, Neck width, Shoulder width, BP to BP, Across back, Across chest, Waist width, Hip width, Thigh width	9
Height	Total height, Head module, HPS to waist, Shoulder point to waist, Center back neck to waist, Center front neck to waist, Center front neck to bust, Bust to waist, Waist to hip, Hip height, Crotch height	11
Depth	Bust depth, Waist depth, Hip depth	3
Total		36

RESULTS AND DISCUSSION

Statistical analysis results

The results of the statistical analysis, including histograms with normal curve and the standard probability histogram (Normal Q-Q Plots), show that all 36 anthropometric sizes used in the study exhibit mean value that closely located near the median (Me) and dominant (Mo). At the same time, the reliability of these dimensions falls within the acceptable limits, with a Cronbach's Alpha reliability coefficient of 0.948 as shown in Table 2.

Results of the main factor analysis

After applying orthogonal rotation Varimax, the analysis showed the presence of three main components among the measurements, each with eigenvalues greater than 1 and cumulative value of 96.92%. The results in Table 3 also show that the waist circumference has the largest weight among the size factor groups at 0.990. The remaining variables after rotation have lower weight but are greater than 0.6. At the same time, the KMO and Bartlett's test results in Table 4 are 0.669, ranging from 0.5 to 1 ($0.5 < 0.669 < 1$), which assesses the appropriateness of the variables in the principal component analysis [22-24].

Factor 1 includes 22 measurements related to body volume, which including circumferences, widths and depths such as waist circumference, waist width, abdomen circumference, bust circumference, bicep circumference, neck circumference, over bust circumference, under bust circumference, waist depth, hip depth, bust depth, apex to apex, hip circumference, neck width, hip width, head width, HPS to apex, total rise, thigh circumference, across back, thigh width, chest width. The eigenvalue of the principal component 1 is 20.175, which explains 56.042% of the total variance and is the most explanatory factor among the 3 factors with Cronbach's α reliability of 0.964.

Table 2. Cronbach's Alpha reliability of anthropometric dimensions.

Reliability Statistics	
Cronbach's Alpha	N of Items
0.948	36

Factor 2 includes 12 measurements related to body height and length, which representing: center front neck to waist, center front neck to bust, shoulder point to waist, total height, HPS to waist, center back neck to waist, hip height, center back neck to wrist, crotch height, bust to waist, head module, waist to hip can be considered as representative for the length and height dimensions of the body. Specifically, the total height is 0.986, hip height is 0.964, center neck back to wrist is 0.954, crotch height is 0.947 and head module is 0.839, there is no systematic measurements factor load is less than 0.7. Principal component 2 has an eigenvalue of 13.392 which explains 37.199% of the total cumulative variance, is the second explaining factor with a Cronbach's α reliability of 0.914.

Factor 3 has the lowest eigenvalue 1.323, accounting for 3.675% of the total cumulative variance with a confidence level of 0.754, including 2 measurements: shoulder width (0.724), shoulder length (0.674). This is the main factor representing the measurement of the shoulder area of the body.

Results of cluster analysis by K-means cluster analysis

K-means cluster analysis is used in the case of expected clustering of 2-10 clusters [24]. The results of subgroup analysis using K-means cluster analysis of 10 groups can be clearly displayed as table 5. However, with the further support of Discriminant analysis could narrow the results of subgroup analysis by K-means cluster analysis and scatter plot as shown in Figure 1. It finally shows that the classification is correct with 97.3% in the case of samples classified into 5 groups, while the classifications are classified into 5 groups. 2 groups, 3 groups, 4 groups, 6 groups, 7 groups, 8 groups, 9 groups, 10 groups are 97.0%, 94.9%, 93.4%, 94.5%, 95.7%, respectively, 95.3%, 96.1% and 94.1%. Thus, classifying the samples into 5 groups appears to be the most appropriate method for achieving clear classification. These five groups will continue to be analyzed and compared by ANOVA and find out the body characteristics of each group [22 - 24].

Table 3. Main factor analysis results.

Main factor	Measurements	Factor loading	Eigen values	Cumulative %	Cronbach' α
Body volume	Waist circumference	0.990	20.175	56.042%	0.964
	Waist width	0.989			
	Abdomen circumference	0.988			
	Bust circumference	0.985			
	Bicep circumference	0.982			
	Neck circumference	0.979			
	Over bust circumference	0.977			
	Waist depth	0.976			
	Under bust circumference	0.976			
	Hip depth	0.973			
	Bust depth	0.946			
	Apex to apex	0.940			
	Hip circumference	0.924			
	Neck width	0.915			
	Hip width	0.901			
	Head width	0.898			
	HPS to apex	0.870			
	Total rise	0.841			
	Thigh circumference	0.817			
	Across back	0.806			
Thigh width	0.798				
Across chest	0.784				
Body height and length	Center front neck to waist	0.990	13.392	37.199%	0.914
	Center front neck to bust	0.988			
	Shoulder point to waist	0.988			
	Total height	0.986			
	HPS to waist	0.972			
	Center back neck to waist	0.968			
	Hip height	0.964			
	Center back neck to wrist	0.954			
	Crotch height	0.947			
	Bust to waist	0.927			
	Head module	0.839			
	Waist to hip	0.757			
	Shoulder area	Shoulder width			
Shoulder length		0.674			
Note: Rotation method: Varimax Extraction method: PCA (principal component analysis)					

Table 4. KMO and Bartlett's test results.

KMO and Bartlett's Test		
Kaiser-Meyer-Olkin Measure of Sampling Adequacy.	0.669	
Bartlett's Test of Sphericity	Approx. Chi-Square	33119.171
	df	231
	Sig.	0.000

Results of ANOVA test

The mean and standard deviation of the measurements are shown in the results of F-test in ANOVA analysis and Scheffe-test for 36 body measurements are presented in Table 6.

In ANOVA analysis the results show that the significance level of $0.00 < \text{Sig} < 0.001$ shows that the cluster analysis results are more significant, and the clusters are different from each other [22, 23]. The results of testing the difference in mean values for each body type of body sizes showed interesting insights. Human Type 1, accounting for 15.23% of the sample, represents the thinnest individuals with the smallest circumference measurements, including waist circumference (64.11cm), bust circumference (80.95 cm) and hip circumference (84.33 cm). This

group also features the shortest height (151.24 cm) and a small shoulder area with shoulder width (35.34 cm) and shoulder length (10.95). Meanwhile, Human Type 5, accounting for only 8.59% of the sample, consists of fat individuals with the largest circumference measurements, bust circumference (103.36 cm), waist circumference (87.33 cm), hip circumference (105.10 cm). However, there is a large average head modulus (21.51 cm), the largest distance from waist to hip (20.95 cm) and crotch height belongs to the low group (71.74 cm); Large shoulder size with shoulder width (37.98 cm) and shoulder length (11.88 cm). Human Type 3 has the highest proportion with 35.94% of the sample, representing the symmetrical humanoid with sizes close to the size of the sample mean. Human Type 4, accounting for 21.88% of the sample, is as slightly fat

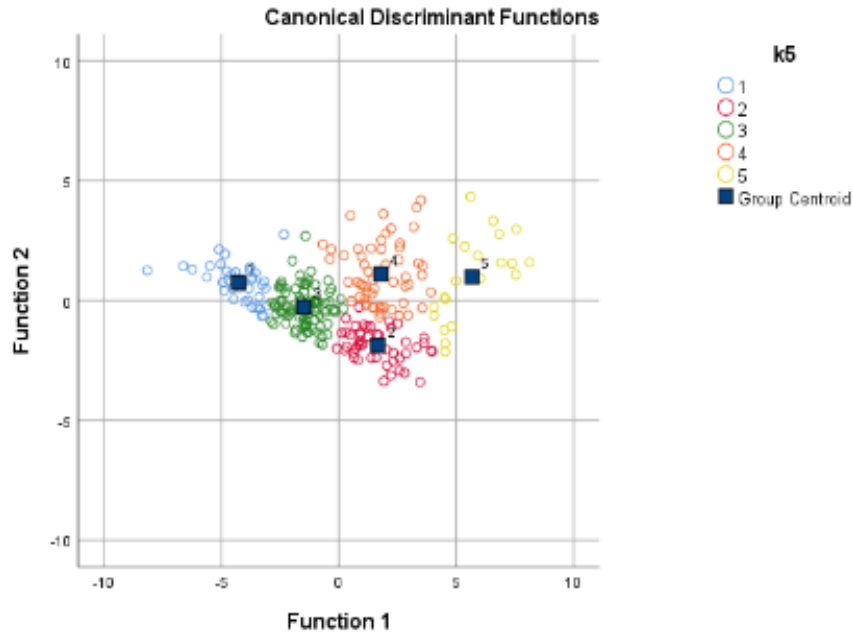


Figure 1. Scatter plot in case of analysis of 5 subgroups.

Table 5. Results of quantity and percentage of each sample.

Number of groups	Quantity and percentage of each sample									
2 group	195 40.63%					285 59.38%				
3 group	178 37.11%			139 28.91%			163 33.98%			
4 group	182 37.89%		71 14.84%		114 23.83%		113 23.44%			
5 group	73 15.23%		88 18.36%		173 35.94%		105 21.88%		41 8.59%	
6 group	26 5.47%	69 14.45%		152 32.64%		68 14.06%	86 17.97%		79 16.41%	
7 group	107 22.27%	62 12.89%		26 5.47%	58 12.11%	71 14.84%		86 17.97%	69 14.45%	
8 group	26 5.47%	94 19.53%	77 16.02%	77 16.02%	62 12.89%	69 14.45%	41 8.59%	34 7.03%		
9 group	39 8.20%	60 12.50%	60 12.50%	41 8.59%	66 13.67%	26 5.47%	34 7.03%	47 9.77%	107 22.27%	
10 group	56 11.72%	39 8.20%	84 17.58%	96 19.92%	15 3.13%	19 3.91%	45 9.38%	43 8.98%	56 11.72%	26 5.47%

person with waist circumference (79.04 cm), bust circumference (91.19 cm), hip circumference (96.73 cm). Yet, this group tends to have shorter heights with the average body height measurement (152.58 cm) and average shoulder size. Human Type 2, accounting for 18.36% of the sample, is the tall and large human body type, with the longest length measurements and larger circumferential measurements compare to the average group sizes.

Results of body proportion analysis of five body types

The simulation of body shapes is based on the measurements from each body group in Table 6. The shape of each human form is simulated in Figure 2 through CLO3D design software. Figure 3 shows a

distinct difference among the physique groups, partially in terms of body contour. When comparing height sizes, Group 5 and Group 3 show minimal difference, as do Group 4 and Group 1. However, Group 2, Group 5 and Group 4 show notable differences. In addition, clear differences can be seen among all body types when comparing body width and thickness. The results show that Group 1 represents individuals who are short, thin, and have small shoulders; Group 2 consists of taller individuals who are slightly overweight and have larger shoulders; Group 3 showcase well-proportioned figure; Group 4 includes shorter individuals who are heavier with medium-sized shoulders; Group 5 comprises individuals who are notably overweight, of average height, and possess large shoulders.


Table 6. Results of ANOVA analysis and Scheffe-test.

								<i>Unit: cm</i>
Main factor	Measurements	Mean (SD)						F
		Group 1 (n=73) 15.23% <SD>	Group 2 (n=88) 18.36% <SD>	Group 3 (n=173) 35.94% <SD>	Group 4 (n=105) 21.88% <SD>	Group 5 (n=41) 8.59% <SD>	Total (n=480) 100% <SD>	
Body volume: circumference, width and depth measurements	Waist circumference	64.11 A <2.90>	75.03 C <3.33>	69.39 B <2.64>	79.04 D <2.67>	87.33 E <3.82>	73.27 <7.19>	319.454***
	Waist width	22.86 A <0.91>	26.65 C <0.97>	24.62 B <0.68>	27.30 D <0.80>	29.92 E <0.99>	25.77 <2.14>	364.716***
	Abdomen circumference	79.12 A <2.79>	92.49 C <3.39>	85.77 B <2.48>	94.73 D <2.97>	104.21 E <3.88>	89.54 <7.51>	350.164***
	Bust circumference	80.95 A <2.77>	91.35 C <3.47>	85.89 B <2.74>	95.19 D <2.67>	103.36 E <3.91>	89.67 <7.00>	286.725***
	Bicep circumference	23.67 A <1.03>	27.85 C <1.28>	25.78 B <1.00>	28.99 D <1.13>	32.15 E <1.51>	27.09 <2.61>	272.294***
	Neck circumference	30.58 A <0.59>	33.42 C <0.66>	31.86 B <0.48>	33.63 C <0.62>	35.69 D <0.81>	32.67 <1.53>	361.142***
	Over bust circumference	80.03 A <2.08>	90.69 C <2.27>	85.29 B <1.43>	94.19 C <1.96>	101.94 D <2.49>	89.01 <5.08>	381.575***
	Waist depth	16.60 A <0.88>	19.65 C <1.04>	18.13 B <0.93>	21.09 D <0.89>	23.55 E <1.32>	19.29 <2.20>	261.032***
	Under bust circumference	68.54 A <2.85>	77.92 C <3.39>	73.12 B <2.77>	83.38 D <3.10>	91.76 E <4.85>	77.15 <7.37>	276.616***
	Hip depth	20.48 A <0.87>	24.37 C <1.05>	22.43 B <0.83>	24.97 C <0.97>	27.74 D <1.22>	23.50 <2.20>	280.268***
	Bust depth	21.13 A <0.95>	23.81 C <1.18>	22.53 B <1.11>	25.62 D <1.03>	27.99 E <1.57>	23.70 <2.27>	195.128***
	Apex to apex	15.42 A <0.50>	17.54 C <0.54>	16.35 B <0.36>	17.52 C <0.49>	18.92 D <0.54>	16.90 <1.08>	283.884***
	Hip circumference	84.33 A <2.53>	97.20 C <3.27>	90.68 B <2.49>	96.73 C <3.06>	105.10 D <3.89>	93.47 <6.37>	241.518***
	Neck width	9.92 A <0.21>	10.87 D <0.19>	10.32 B <0.13>	10.71 C <0.20>	11.32 E <0.20>	10.53 <0.43>	313.553***
	Hip width	30.51 A <0.84>	34.83 C <1.06>	32.63 B <0.82>	34.44 C <0.99>	37.06 D <1.30>	3.49 <2.04>	226.376***
	Head width	14.17 A <0.13>	14.86 D <0.14>	14.47 B <0.10>	14.72 C <0.15>	15.17 E <0.15>	14.61 <0.30>	316.647***
	HPS to apex	22.79 A <0.50>	25.44 D <0.58>	24.02 B <0.48>	24.92 C <0.60>	26.59 E <0.55>	24.51 <1.18>	244.884***
	Total rise	70.46 A <1.60>	78.43 D <1.88>	74.16 B <1.65>	76.49 C <2.01>	81.75 E <2.12>	75.54 <3.59>	188.262***
	Thigh circumference	49.85 A <1.24>	56.57 C <1.65>	53.18 B <1.38>	55.40 C <1.59>	59.41 D <2.05>	54.32 <2.68>	133.829***
	Across back	29.61 A <0.72>	32.26 D <0.54>	30.67 B <0.50>	31.48 C <0.67>	33.03 E <0.55>	31.18 <1.16>	183.730***
Thigh width	15.96 A <0.50>	18.14 C <0.67>	17.04 B <0.57>	17.74 C <0.65>	19.03 D <0.86>	17.40 <1.05>	117.473***	
Across chest	29.40 A <0.86>	32.33 D <0.65>	30.56 B <0.62>	31.44 C <0.80>	33.13 E <0.65>	31.12 <1.30>	152.401***	
Body height and length measurements	Center front neck to waist	30.49 A <0.76>	32.68 C <0.82>	31.36 B <0.88>	30.47 A <0.80>	31.39 B <0.75>	31.28 <1.13>	56.817***
	Center front neck to bust	17.94 A <0.53>	19.55 C <0.56>	18.60 B <0.60>	18.06 A <0.54>	18.71 B <0.48>	18.56 <0.78>	60.115***
	Shoulder point to waist	23.99 A <0.64>	25.97 C <0.67>	24.78 B <0.73>	24.12 A <0.67>	24.99 B <0.64>	24.75 <0.96>	61.776***
	Total height	151.24 A <4.29>	164.68 C <4.39>	156.73 B <4.97>	152.58 A <4.19>	157.95 B <3.88>	156.55 <6.34>	63.065***
	HPS to waist	31.80 A <0.74>	34.28 C <0.79>	32.81 B <0.84>	32.17 A <0.80>	33.31 B <0.70>	32.83 <1.14>	66.540***
	Center back neck to waist	32.36 A <0.75>	34.75 C <0.81>	33.35 B <0.86>	32.66 A <0.79>	33.75 B <0.71>	33.34 <1.13>	61.147***
	Hip height	76.71 A <3.05>	84.75 C <3.05>	79.93 B <3.57>	76.58 A <2.87>	79.24 B <2.78>	79.53 <4.27>	51.477***
	Center back neck to wrist	67.81 A <2.20>	74.87 D <2.17>	70.63 B <2.37>	69.26 B <2.01>	72.25 C <1.72>	70.82 <3.13>	68.552***
	Crotch height	70.64 A <2.96>	77.59 C <2.97>	73.34 B <3.48>	69.74 A <2.77>	71.74 A <2.77>	72.79 <4.09>	47.539***
	Bust to waist	12.55 A <0.26>	13.13 D <0.28>	12.76 C <0.30>	12.41 A <0.30>	12.68 B <0.29>	12.71 <0.37>	43.134***

	Head module	20.64 A <0.23>	21.58 C <0.25>	21.04 B <0.24>	21.01 B <0.25>	21.51 C <0.22>	21.11 <0.39>	100.083***
	Waist to hip	19.21 A <0.45>	20.92 C <0.46>	19.94 B <0.47>	19.94 B <0.52>	20.95 C <0.49>	20.10 <0.74>	
Shoulder area measurements	Shoulder width	35.34 A <0.78>	37.98 C <0.57>	36.36 B <0.62>	36.61 B <0.76>	37.98 C <0.59>	36.70 <1.10>	109.388***
	Shoulder length	10.95 A <0.27>	11.83 C <0.21>	11.30 B <0.22>	11.42 B <0.26>	11.88 C <0.19>	11.42 <0.38>	

*** p < 0.001

The alphabet is the result of a Post - hoc test (Scheffe test) (with A< B< C<D<E).

 : Size with the highest mean


 : Size with the lowest mean



Figure 2. Simulation of 5 types of women through CLO3D software.

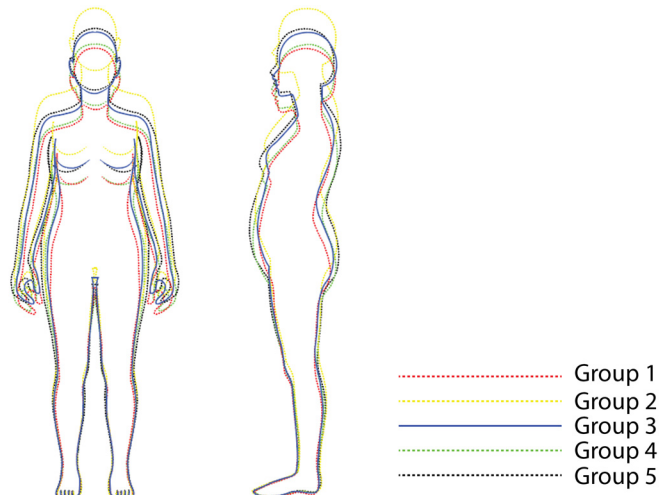


Figure 3. Compare the differences between body shapes.

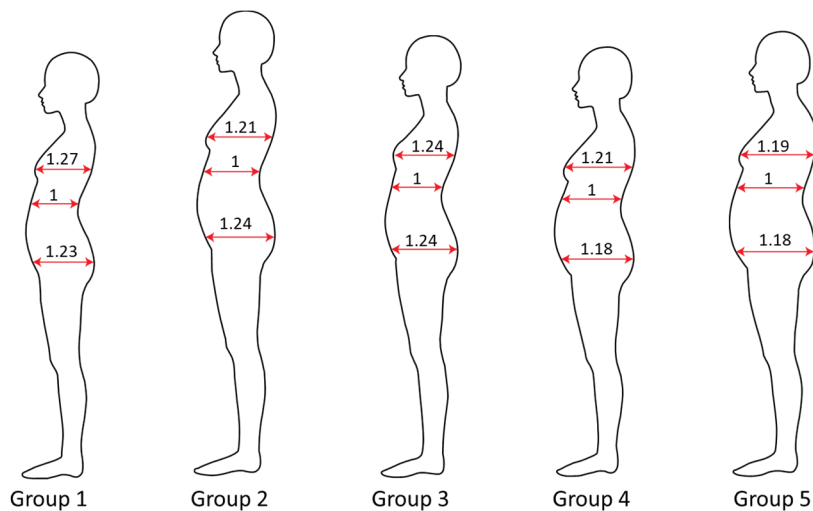


Figure 4. Body thickness ratio of 5 body shapes.

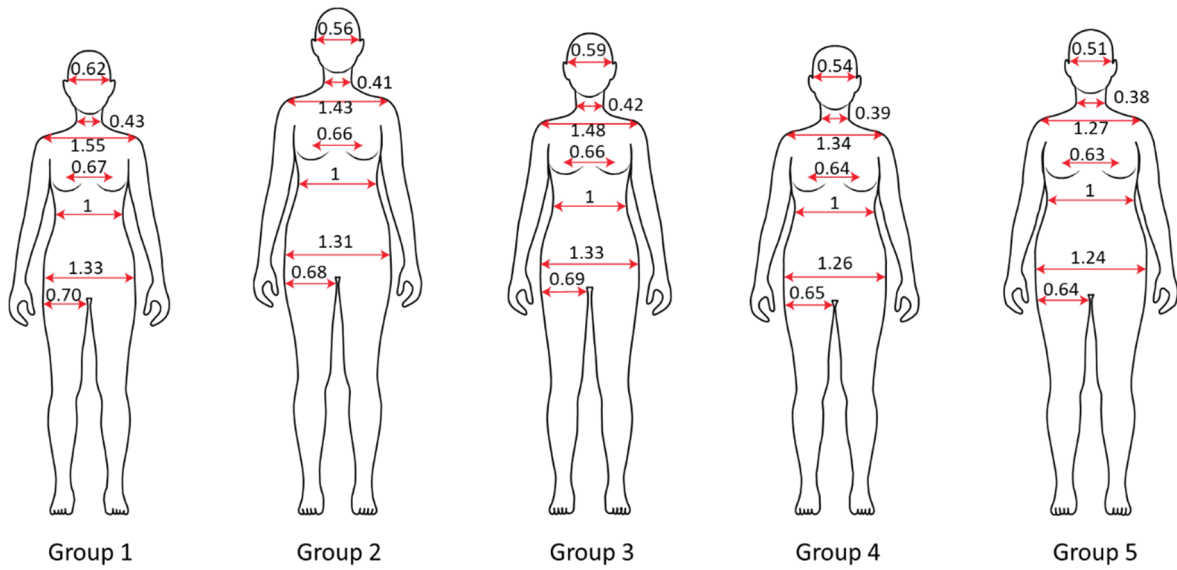


Figure 5. Body width ratio of 5 body types.

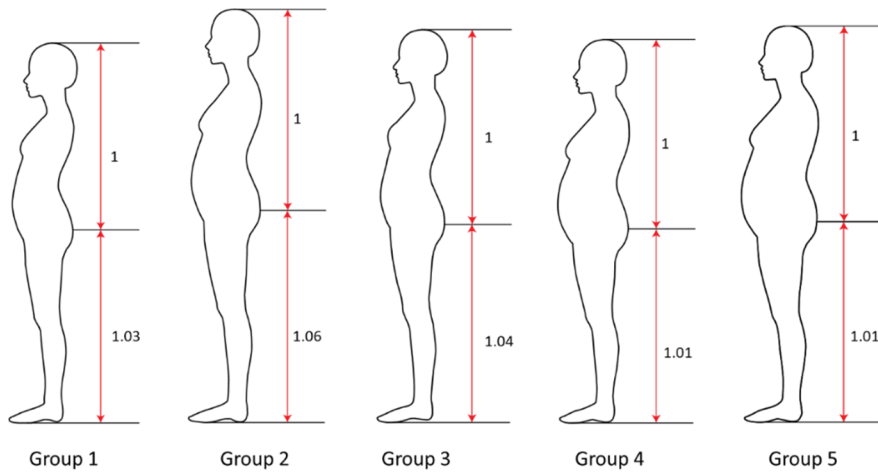


Figure 6. Hip height ratio of 5 body types.

In addition, the proportions of each body type are shown in Figures 4, 5, 6, 7, 8, 9, 10, 11, 12.

The body thickness ratio among the 5 body shape groups is shown in Figure 4. The results show that Group 3 is the body group with the bust - waist ratio equal to the hip waist ratio, indicating a symmetrical body shape. Conversely, Groups 1, 4 and 5 all display a larger bust - waist ratio than hip - waist ratio, while Group 2 showed a smaller bust waist ratio than the hip waist ratio.

Figure 5 shows the body width ratio among five body types. When compares to Group 3, which is the average group for width-to-waist sizes ratios, Group 2, 4 and 5 all have a smaller width-to-waist ratio. This explains more clearly that body groups 2, 4, 5 represent slightly fat, fat and over-fat bodies, respectively. The other group, Group 1, has a larger of width-to-waist ratio than Group 3, especially, the hip size has the same ratio as Group 3. This is the body group representing the thin group.

The ratio of hip height to the height from the top of the head to the hip of the five body shapes is shown in

Figure 6. Looking at the figure and the results of the ratio calculation, Group 2 has the highest hip height ratio at 1.06, representing a body type with higher hip position. In contrast, Group 4 and Group 5 have the lowest hip height ratios of 1.01, representing body types with sagging hips. The remaining groups, Group 1 and Group 3 have an average hip height ratio of 1.04 compared to the height from the top of the head to the hip.

Figures 7, 8, 9, 10, 11 analyze the height ratio measurement to the size of the body height for five body groups. From the analysis results, Groups 2 and 3 have the same ratio of height to standing height dimensions, while Groups 1, 4 and 5 have differences. Specifically:

- Group 1 matches Groups 2 and 3 in proportions for bust height, hip height, and crotch height but has a larger head modulus size ratio. Other measurements show smaller proportions than Groups 2 and 3.

- Group 4 has smaller proportions than groups 2 and 3, except for the head modulus, which matches Groups 1 and 5.

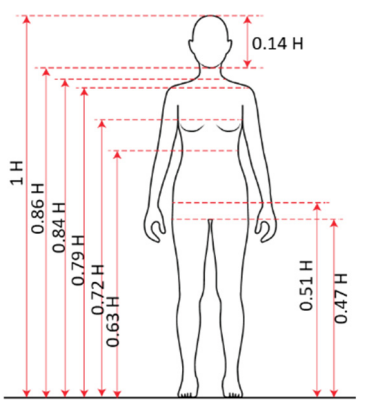


Figure 7. Ratio of height dimensions of group 1

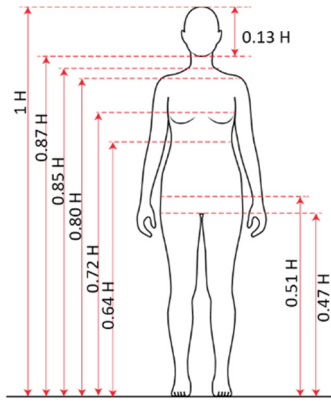


Figure 8. Ratio of height dimensions of group 2

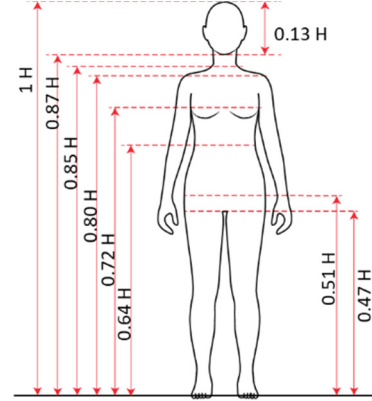


Figure 9. Ratio of height dimensions of group 3

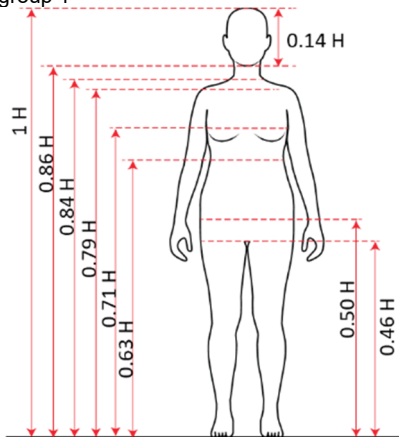


Figure 10. Ratio of height dimensions of group 4

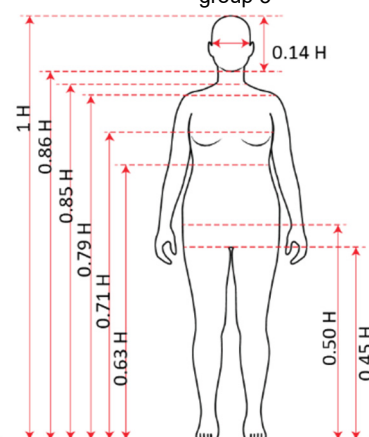


Figure 11. Ratio of height dimensions of group 5

- Group 5 has a first modulus ratio greater than Groups 2 and 3, similar to Groups 1 and 4, with neck height proportions matching Groups 2 and 3. Other measurements show smaller proportions than Groups 2 and 3.

- In addition, Groups 1, 4 and 5 share equal proportions for chin height, shoulder height, waist height and head modulus.

CONCLUSION

This study collected 36 anthropometric measurements from a sample of 480 Vietnamese women residing in major cities, representing three regions of North, Central, and South. The analysis results, including statistical characteristics, principal component analysis, K-means cluster analysis, discriminant analysis, ANOVA analysis and Scheffé-test showed the existence of five female body types: "short and thin with small shoulder" accounting for 15.23 %; "tall with slightly fat and large shoulders" accounting for 18.36 %; "Medium body type", with an average accounting for height stature and a fit body, and a bust-waist ratio equal to the waist-to-hip ratio, accounting for 35.94 %; "short with fat and medium-large shoulder" accounting for 21.88 %; and "too fat with average height, big shoulders" accounting for 8.59 %. The analysis of body thickness ratio of five body shapes showed results that: Group 3 had a

bust-waist ratio equal to the hip-waist ratio; Groups 1, 4 and 5 had a bust-waist larger than the hip-waist ratio; Group 2 exhibited a bust-waist ratio smaller than the hip-waist ratio. The analysis of body width ratio showed that: Group 2, 4 and 5 had a smaller width to waist ratio than Group 3. Group 1 had a width to waist ratio larger than Group 3, especially the hip size has the same ratio as Group 3. The results of analyzing the ratio of hip height to the height from the top of the head to the hips of the five body shapes showed that: Group 2 had the highest hip height ratio (1.06), representing a body types with a high hip position; Group 4, 5 had the lowest hip height ratio (1.01), representing the body type with sagging hip; Group 1 and 3 had an average hip height ratio of 1.04 compared to the body. The results of analysis of height dimensions ratio to body height for five body groups show that Groups 2 and 3 have the same height dimensions ratio to body height, the remaining Groups 1, 4 and 5 have significant differences in these ratios.

The research results can serve as a reference for the garment industry while contributing to the goal of building a virtual model library within 3D design software and mass-customization.

Acknowledgement: This research was supported by the Hanoi University of Science and Technology (HUST) under project number T2018-PC-048.

REFERENCES

1. White J., Scurr J.: Evaluation of professional bra fitting criteria for bra selection and fitting in the UK. *Ergonomics*, 55(6), 2012, pp. 704-711.
<https://doi.org/10.1080/00140139.2011.647096>
2. Smith R.L., Sandhya P., Lorraine A.F.: Evaluation and management of breast pain. *Mayo Clinic Proceedings*, 79(3), 2004, pp. 353-372.
<https://doi.org/10.4065/79.3.353>
3. Wood K., Cameron M., Fitzgerald K.: Breast size, bra fit and thoracic pain in young women: a correlational study. *Chiropractic & osteopathy*, 16(1), 2008, pp. 1-7.
<https://doi.org/10.1186/1746-1340-16-1>
4. Hardaker C.H.M., Fozzard G.J.W.: The bra design process - a study of professional practice. *International Journal of Clothing Science and Technology*, 9(4), 1997.
<https://doi.org/10.1108/09556229710175795>
5. Wang J. P., Wei Y. Z.: An approach to predicting bra cup dart quantity in the 3D virtual environment. *International Journal of Clothing Science and Technology*, 19(5), 2007.
<https://doi.org/10.1108/09556220710819546>
6. Benefits of bras for women - 2014. Available online:
<https://vnexpress.net/4-loi-ich-cua-ao-nguc-doi-voi-phu-nu-2952486.html> 2022/07/05
7. Page K.A., Julie R.S.: Breast motion and sports brassiere design. *Sports Medicine*, 27(4), 2012, pp. 205-211.
<https://doi.org/10.2165/00007256-199927040-00001>
8. McGhee D.E., Julie R.S.: Optimising breast support in female patients through correct bra fit. A cross-sectional study. *Journal of Science and Medicine in Sport*, 13(6), 2010, pp. 568-572.
<https://doi.org/10.1016/j.jsams.2010.03.003>
9. Triumph bra size charts- 2022. Available online:
<https://www.triumph.com/pages/size-charts/> 2022/07/10
10. Calvin Klein bra size chart – 2022. Available online:
<https://www.calvinklein.co.uk/bra-sizes-explained> 2022/07/08
11. Victoriasecret bra size – 2022. Available online:
<https://www.victoriasecret.com/vn/vs/bras/how-to-measure-bras/> 2022/07/05
12. Vera bra size charts – 2022. Available online:
<https://vera.com.vn/pages/huong-dan-chon-size/> 2022/07/02
13. Relax bra size charts – 2022. Available online:
<https://relaxunderwear.com/pages/huong-dan-chon-size/> 2022/07/04
14. Oh S., Chun J.: New breast measurement technique and bra sizing system based on 3D body scan data. *Journal of the Ergonomics Society of Korea*, 33(4), 2014.
15. Yu W., et al.: Innovation and technology of women's intimate apparel. Sawston: Woodhead Publishing, 2006, pp. 20.
16. Bra Size Charts and Conversions. Available online:
<https://www.evasintimates.com/blog/> 2022/07/03
17. Edward A. P.: Method for determining bra size and predicting post augmentation breast size. Chapter 11: Breast Augmentation. Berlin: Springer, 2009, pp. 77-83.
18. McGhee D.E., Julie R.S.: Breast volume and bra size. *International Journal of Clothing Science and Technology*, 23(5), 2011, pp. 351-360.
<https://doi.org/10.1108/09556221111166284>
19. Pechter E.A.: A new method for determining bra size & predicting post augmentation breast size. *Plastic and Reconstructive Surgery*, 102(4), 1998, pp. 1259-1265.
20. Bengtson B.P., Caroline A.G.: The standardization of bra cup measurements: redefining bra sizing language. *Clinics in plastic surgery*, 42(4), 2015, pp. 405-411.
<https://doi.org/10.1016/j.cps.2015.06.002>
21. Rong Z., Yu W., Fan J.: Development of a new Chinese bra sizing system based on breast anthropometric measurements. *International Journal of Industrial Ergonomics*, 37(8), 2007, pp. 697-705.
<https://doi.org/10.1016/j.ergon.2007.05.008>
22. Liu Y., Wang J., Cynthia L. I.: Study of optimum parameters for Chinese female underwire bra size system by 3D virtual anthropometric measurement. *The Journal of The Textile Institute*, 108(6), 2017, pp. 877-882.
<https://doi.org/10.1080/00405000.2016.1195954>
23. Shin K.: Patternmaking for underwear design. *The Journal of the Textile Institute*, 98(4), 2010.
<https://doi.org/10.1080/00405000701503006>
24. Avşar D. K., et al.: Anthropometric breast measurement: a study of 385 Turkish female students. *Aesthetic Surgery Journal*, 30(1), 2010, pp. 44-50.
<https://doi.org/10.1177/1090820X09358078>
25. Hoang T., Chu N. M. N.: Analysis of research data with SPSS, published in Hong Duc, 2008.
26. Hair J.F., et al.: *Multivariate Data Analysis: A Global Perspective*. 7th ed. Upper Saddle River: Prentice Hall, 2009.
27. Quatest 3, Directorate for standards, metrology and quality, 2017. Available online:
<http://quatest3.com.vn/Content/UserImages/Files/TNNT/2.1.%20Gi%E1%BB%9Bi%20thi%E1%BB%87u%20v%E1%BB%81%20TNNT.pdf>
28. Nikita E.: *Osteoarchaeology: A guide to the macroscopic study of human skeletal remains*. Cambridge: Academic Press, 2016.
29. International Standard (ISO 4416): Size designation of clothes – women's and girl's underwear, nightwear, foundation garments, and shirts. The International Organization for Standardization, 1981.
30. Amoena bra size charts. Available online:
<https://www.amoena.com/global/about-us/lingerie-and-swimwear-measuring-guide/>, 2022/07/01
31. Eva's Intimates bra size charts. Available online:
<https://www.evasintimates.com/bras/> 2022/07/01
32. Tran M.K., Park, S.J.: Somatotype Analysis and development size charts for Vietnamese women using 3D body scanner data. *Proceedings for 2011 Asian Textiles Conference ATC11*. 1PS-107, pp. 141.
33. Tran M.K.: Somatotype analysis and torso pattern development for Vietnamese women in their 30s using 3D body scan data. Ph.D. Dissertation, Yeungnam University Korea, 2012.
34. TCVN 5782: 2009. Standard sizing systems for clothes.
35. Nga B. T.: Research on building a hierarchy of size tables for some women's garment products. *Scientific research*, Ministry of Industry and Trade, 2010.
36. Nguyen T. T. T.: Building a sizing system for the lower body of women in Ho Chi Minh City aged 25 to 35. Master thesis, Hanoi University of Science and Technology, 2015.
37. Pham T. H.: Building a body size system for female students at Hanoi University of Industry, applying clothing design. Scientific research of Hanoi University of Industry, 2019.
38. Tiwari M., Noopur A.: *Development of Bottom-Wear Size Chart for Indian Male Youth*. Ergonomics for Improved Productivity. Singapore: Springer, 2021, pp. 43-56.
https://doi.org/10.1007/978-981-15-9054-2_5
39. Yadav S., Chanana B.: Developing standard size chart for teenage girls of 17-19 years using anthropometry. *International Research Journal on Advanced Science Hub 2*, 2020, pp. 15-20.
<https://doi.org/10.47392/IRJASH.2020.254>
40. Petrova A.: *Creating sizing systems*. Sizing in Clothing: Developing effective sizing systems for ready-to-wear clothing. 2007, pp. 57-87.
41. Gupta D., Gangadhar B. R.: A statistical model for developing body size charts for garments. *International Journal of Clothing Science and Technology*, 2004.
<https://doi.org/10.1108/09556220410555641>
42. Park S.J.: Upper garment sizing system for obese school boys based on somatotype analysis. *Journal of the Korean Home Economics Association*, 46(9), 2008, pp. 99-112.

WOUND DRESSING WITH TEXTILE DRESSING APPROACH: A REVIEW

SHAHIDI, SHEILA¹; MOAZZENHI, BAHAREH^{2,3}; KALAHROODI, HOSSEINI KIMIASADAT⁴ AND MONGKHOLRATTANASIT, RATTANAPHOL^{5*}

¹ Islamic Azad University, Arak Branch, Faculty of Engineering, Department of Textile, 38361-1-9131 6, Arak, Iran

² Amirkabir University of Technology, Textile Department, 15916-34311, Tehran, Iran

³ Atiyeh Hekmat Abtin Company, Research and Development Department, 19496-35879, Tehran, Iran

⁴ Alborz University of Medical Sciences, School of Pharmacy, 301-810 301-810, Karaj, Iran

⁵ Rajamangala University of Technology Phra Nakhon, Faculty of Industrial Textiles and Fashion Design, Department of Textile Chemistry Technology, 10300, Bangkok, Thailand

ABSTRACT

To help healing, protect and care the wound from additional damage, a sterile dressing is applied to wound and injured area. Wound dressing can be a sterile pad or compress that directly contact with the wound area. Nowadays, different models of wound dressings are used in the medical field. In this review paper different wound dressings and efforts made on the textile based wound dressings discussed.

KEYWORDS

Wound; Dressing; Healing; Textile; Antibacterial; Nanofibers.

INTRODUCTION

For reducing infection in different wound types, various models of wound dressings are used. Wound dressings should stop bleeding and start clotting, absorb excess blood and other fluid from the injured area and eventually debride the wound [1]. Wounds are classified as chronic or acute (Figure 1), due to the nature of the repair procedure [2].

Chronic wounds associated with tissue injury heal and heal very slowly and recur regularly as the trauma recurs, depending on the immunological problems, the patient's physiological situation and the persistent infection [3]. On the other hand, acute wounds are often tissue injuries that heal completely in the estimated time of 8-12 weeks with slight scarring. Acute wounds include mechanical injuries such as lacerations, abrasions, burns, cuts, and penetrations, as well as chemical injuries induced by chemical caustics [4]. In addition, wounds are categorized based on the number of layers of skin and the area of skin affected. In a superficial wound, the skin surface is only affected and contains the epidermis and the deeper layers of the skin with sweat glands, blood vessels and hair follicles, which is referred to as a partial wound [5]. Epidermis, dermis, and the underlying subcutaneous fat or deeper tissues are injured while full-thickness wounds occur. Based on

physiological conditions and appearance, wounds are divided into five groups (Figure 2).

Necrotic wounds are dry, hard, and tend to shrink. Leg ulcers, burns, and pressure sores are types of greasy wounds. In this situation, the necrotic plaque is removed from the wound surface and a sticky yellow plaque is formed. This tissue is a mixture of protein, fibrin, serous exudate, leukocytes and bacteria and is not dead. Granulating tissue is the fresh matrix through healing which appear on the wound surface with bright color and moist condition with many tiny blood vessels. In epithelializing wounds, epithelium is made on a denuded surface and wound surface seems as pink colored. Infected wounds are green, cloudy with smelling fluid drainage [6]. There are many different types of wounds [7] such as burns, malignant wounds, radiation wounds, pressure ulcers, vasculitic ulcers that need treatment [5]. In an open wound, an internal or external break in the body's tissue caused that generally reasoned by accidents involving rough or sharp objects that cut through the skin and trauma created which can exposes the skin and body to dangerous bacteria and infections [8]. In open wounds, minor cuts can be self-treated, but severe cases need emergency services. Some types of open wounds include Abrasion (When the skin rubs in contradiction of a rough surface, abrasions occur. In most cases, wound is not deep

* Corresponding author: Mongkholarattanasit, R., e-mail: rattanaphol.m@rmutp.ac.th

Received September 18, 2023; accepted March 5, 2024

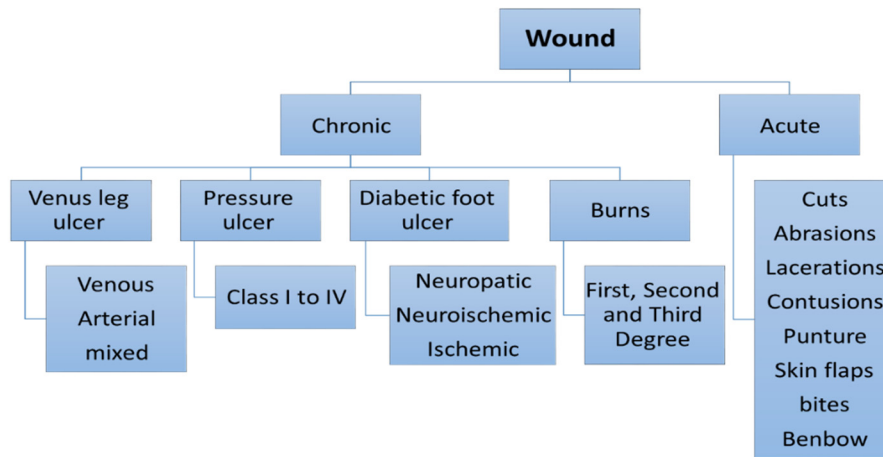


Figure 1. Wounds types due to the nature of the repair procedure.

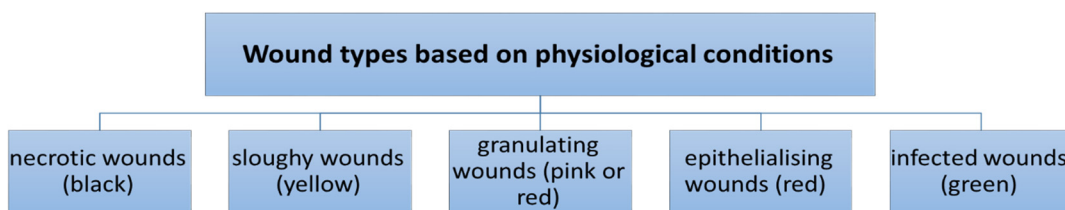


Figure 2. Wound types based on physiological condition.

and a little bleeding occurs), Puncture (There are hole-shaped wounds caused by pointy objects such as needles, gunshot and nails that called Punctures. Deep punctures necessitate urgent medical intervention.), Incision (A straight wound caused by any sharp object such as a knife or a broken glass is an incision), Laceration (A laceration is a sharp and deep cut those results in skin tears and caused heavy bleeding. Frequently it happens through machinery, mishandle knives, and other sharp tools.), Avulsion (A severe wound in the partial or complete tear of the tissues and skin that frequently occur during violent accidents like explosions, car crashes, and other incidents called avulsion that involve trauma.), Amputation (An amputation mentions to the loss of an extremity which can causes accidentally or also be done in a medical procedure to manage certain diseases such as gangrene) [9-10]. An infection caused if a major wound is not treated correctly or left on its own. Some symptoms of infection are fever (body temperature rising above 37.5°C), malaise (tiredness, lack of energy and general feeling of being unwell), redness, swelling, temperature rise in the area, body aches (persistent pain in and around the wound), vomiting and unpleasant odor. It is difficult to know why some ulcers are not healing and occasionally out of many local wound dressing materials, some dressing material works wonders [11].

COMMERCIAL WOUND DRESSING TYPES

Wound dressings should have several properties (Figure 3) including absorb exudates, alleviate pain, sustain non-toxicity, moist environment, prevent infection and contaminant, permeability, ease of application, flexibility, comfortability, antibacterial properties and biodegradability [12]. Wound dressings should have antibacterial properties and the growth of microorganisms should be controlled or eliminated in the presence of antimicrobial agents resident in the fibrous structure [13]. In the wound healing process, the dressing defends the injury and restores skin and epidermal tissue. For this purpose, natural polymers such as proteoglycans and proteins (e.g. fibrin, collagen, gelatin and keratin), polysaccharides and derivatives (e.g. CMC, chitosan, alginates and heparin) [14] are widely used, that are biodegradable and biocompatible [15]. For effective and fast wound healing, using the correct dressing is important. Several features such as the type, size, position, and harshness of injury impressed on the type of used wound dressing [16]. Some of the most commonly used dressings are shown in Figure 4.

Hydrocolloid dressing

The word hydrocolloid was invented in the 1960s with the development of mucoadhesives made by combining carboxymethyl cellulose, tackifiers and adhesives used to treat mouth ulcers. To prepare



Figure 3. Ideal wound dressing specifications [17].

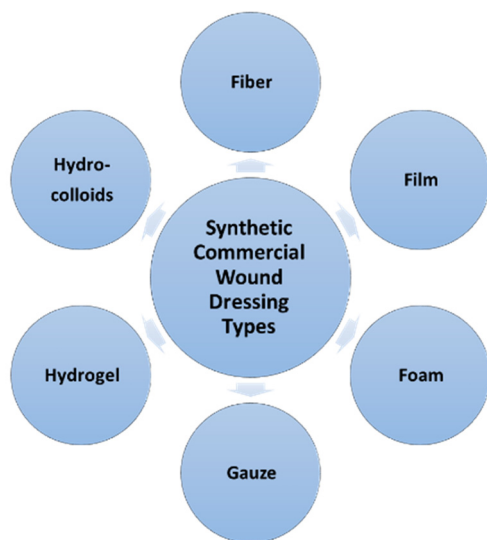


Figure 4. Synthetic commercial wound dressing type [16].

hydrocolloid dressings, a hydrophilic gellable mass in semi-solid form was applied to a flexible, semi-permeable support. The first formulation of this dressing was in the UK in 1982 and was later launched in 1983 as Duoderm in the US and other European markets. Hydrocolloid dressings are often associated with the treatment of chronic wounds. In addition, hydrocolloid dressings can be effective for treating various acute wounds. They can absorb excess fluid and help with debridement [18]. For wounds that are emitting liquid, burns, pressure and venous ulcers and necrotic wounds hydrocolloid dressings are useable. Hydrocolloid dressings are the most commonly used modern dressings and are self-adhesive, non-breathable, long-lasting, biodegradable, and easy to apply and need no taping. They made from comfortable and flexible materials that made them suitable for all skin types [19-21].

Hydrocolloid dressings made of a self-adhesive and hydrophilic colloid particle covered with a waterproof polyurethane film [22]. The surface of hydrocolloid dressings is coated with materials such as sodium carboxymethyl cellulose, pectin, gelatin, alginate or polysaccharides, which can absorb water and form a gel, which can protect the wound from infection and keep it clean and does not allow oxygen, water or bacteria entry on wounds. The outer layer protects the wound from environmental factors and bacteria and forms a gel-like phase on the surface of the wound, which preserves moisture and absorbs wound secretions and exudates [23]. The main advantage of hydrocolloid dressings is that they adapt to the patient's body and adhere well to different sites [24].

Hydrogel

In recent years there have been many advances in the management of wounds. Hydrogels are biocompatible with moisturizing properties and are widely used in wound dressings [25]. Hydrogel dressings are hydrophilic and semi-occlusive. They can hydrate wounds and re-hydrate eschar. Hydrogels are inexplicable polymers which are presented in different forms such as amorphous gel and sheet. Hydrogels absorb exudate and afford a moist environment for cell migration. One of the most benefit of hydrogel dressings is autolytic debridement deprived of damage and harm to granulation or epithelial cells [26].

This dressing allows moisture to stay at the surface of the wound. Hydrogel dressings can be a solution to these problems, exhibiting excellent properties such as tissue adhesion, swelling, and water absorption. In addition, these hydrogels can be formed in situ and, if necessary, dissolved by

chemical or physical reactions. For second-degree and minor burns, donor sites, infected wounds, pressure ulcers, sore or necrotic wounds and a variety of wounds that are no fluid or leaking little, hydrogel can be used. To reduce bleeding in liver and aortic models, hydrogels can be used as a dressing, which can then be easily removed. Still, there are many researches on diverse methods to synthesize these hydrogels. Lu et al. in 2018, investigated four strategies for dissolvable crosslinked hydrogels, supramolecular self-assembling hydrogels, and environmentally sensitive physically crosslinked hydrogels. They concluded that these hydrogels offer cheap and effective methods for in vivo applications [27]. Hydrogels are usually used for drug delivery or tissue/organ repairs. They are water or glycerin based products; crosslinked polymeric networks extended in biological fluid. They can absorb 30-90% of their mass in water. Some cooling gels like burn soothe in hydrogels can reduce pain and help to heal wounds and burns and accelerate the healing process. Hydrogel wound dressings keep the moist wound environment clean and healthy. Hydrogels are available in different forms, like film, injectable gels and spray. Furthermore, smart hydrogel dressings included sensors can transport real-time information about the wound healing status. In recent times, sprayable hydrogel-based wound dressings have developed as appropriate scaffolds for wound care. Many researchers studied on synthesis and fabrication of hydrogels and emerging new smart hydrogels for several biomedical applications [2, 28]. In 2019, various types of injectable self-healing conductive hydrogels using dextran graft aniline tetramer graft 4-formylbenzoic acid and N-carboxyethylchitosan were synthesized by Guo et al. Hydrogels revealed superb self-healing. The conductive and injectable self-healing hydrogels are admirable candidates as scaffolds or as carriers for cell delivery that can be used for skeletal muscle repair or cell therapy [29]. Jin et al. in a review paper discussed about hydrogels dressings. They reported, by utilizing hydrogels as substrates, it is possible to design hydrogel dressings with pH-sensitive, temperature sensitive, glucose-sensitive, and pressure-sensitive properties. The hydrogel dressings using wound-monitoring utilities may ease treatment, by monitoring the results [25].

Foam dressings

Polyurethane foam dressings have been used for exudate management in moist wound healing for the past 30 years. Foams have a porous structure that can absorb liquids into air-filled spaces by capillary action. Silicone foam is also used in the wound dressing but is often applied as an adhesive wound contact layer. Various thicknesses of foam dressings are made, which can be adhesive or non-adhesive. They are rich in film-backing that has the resolution to provide a water and microbe resistant barrier to the

environment. Overall, non-toxic and non-allergenic foam dressings are able to retain moisture at the wound bed and are easily removed, protecting the wound skin from bacteria. They can adopt and conform to body shape and maintained the temperature with a long shelf life. Foams can be used as a primary or secondary dressing [30]. Foam dressings are essential and important in the care of chronic and exuding wounds. Chronic wounds require the creation of a moist, warm wound healing environment and good exudate handling properties, and foam dressings are good candidates for treatment. Mostly, foams are made from polyurethane with smooth contact surface, thermal insulation, which are gas permeable. Foam dressings can absorb exudate in a number of ways. Some foams absorb exudate, some foams can breathe the moisture they absorb through a permeable backing. An absorbcency and the moisture-vapor permeability are very important factors for foam dressings [31]. Kowalczyk et al. in 2020, focused on developing a possibly antibacterial polyurethane foam wound dressing that was loaded with bismuth-ciprofloxacin [32]. Wang et al. investigated the wound healing efficacy of silver-releasing foam dressings in competition with silver-containing creams in the outpatient treatment of patients with diabetic foot ulcers in 2020. They concluded that silver-releasing foam wound healing in infected diabetic foot was more actual and effective than traditional silver sulfadiazine cream [33]. Susy Pramod describes in 2021 the use of the Kliniderm foam silicone dressings for wound management in oncology. Kliniderm foam silicone dressing is safe, acceptable and effective for chronic and acute wounds [34]. Foam dressings play a key role in the medical management of chronic wounds and in moist wound healing.

Films (Transparent dressings)

Transparent dressings are more comfortable than bulky gauze and tape [35]. Semi-permeable sheet is a sterile polyurethane sheet coated with acrylic adhesive. Transparent dressings are breathable, flexible, impermeable to bacteria and comfortable to wear and keep the wound dry and clean. These dressings covered the wound with a clear film and wound healing can be monitored and detecting prospective problems much easier and earlier. Transparent dressings can be ideal for surgical incision sites, ulcers and burns and conform easily to the patient's body. Due to the film-like structure, they are semi-blocking and can trap moisture. They can create a moist environment for wound healing [36]. Transparent polyurethane dressings have become popular cause of their consistently secures the catheter, it permits immediate visual inspection of the catheter insertion site. Transparent polyurethane dressings do not have to be changed repeatedly and enables the patient to wash and shower with no worry about wetting the dressing. They have significant

adhesion, cost effective and easy to use [37]. Efficiency and success of a transparent film dressing for peripheral intravenous catheters was studied by Atay and Yilmaz Kurt in 2021. They concluded that the use of a transparent film dressing for addition of peripheral intravenous catheter may increase catheter indwelling time and reduce the incidence of complications [38]. The effectiveness of transparent compression bandages in inhibiting pain, discomfort and hematoma was reviewed by Sharma et al. checked. They reported that transparent dressing is a superior choice in patients with femoral/groin dressings after cardiac catheterization. Also, they reported that transparent dressings are more comfort and effective in prevention of pain [39].

Gauze dressings

Gauze dressings are produced in extensive range of shapes and sizes which made of non-woven or woven materials. These can be used for infected wounds, draining wounds, wounds which need packing and very frequent dressing changes. Gauze dressings are available readily and are cheaper than other wound dressing types and can be used on almost all wound types. In the other hand, gauze dressings should frequently combine with another wound dressing and often is not effective for moist wound healing. Gauze dressing is still routinely used for long-term wound care in hospitals and clinics [40]. Balasubramanian et al. in 2013 studied about carboxymethylated cotton gauze dressing. Moist conditions are maintained by increasing surface carboxyl content. The samples were padded with different concentrations of ornidazole and ofloxacin as antibacterial agents. Carboxymethylated cotton gauze treated with antibacterial agents may be suitable for the manufacture of antibacterial wound dressings [41]. Soares et al. in an integrative review in 2020, reported that sterile gauze with Vaseline, reduced the amount of pain after the bandages. This bandage provided pain relief, increased mobility, and improved sleep patterns, offer the client more comfort and more willingness and energy for self-care [42]. Paraffin gauze dressing helps keep the skin graft moist, reduces adhesion and allows for non-traumatic removal, and creates a moist environment that facilitates migration of epithelial cells. In addition, paraffin gauze dressings have some disadvantages, such as: B. the need for a secondary dressing, they do not absorb exudate and require frequent dressing changes to ensure they do not dry out and damage good cells when the dressing is removed [43]. Fang et al. in 2021 developed a reusable ionic liquid-grafted antibacterial cotton gauze wound dressing using 3-aminopropyltriethoxysilane, glycidyl methacrylate, 1-vinyl-3-butylimidazolium bromide and butyl acrylate. They reported that the treated gauze pad is reusable and showed good antibacterial activity even after three repeated antibacterial tests [44]. Traditional wound dressings such as gauzes and

felt is keeping the wounds dry and warm. One of the biggest problems with traditional dressings was their adhesion to the wound and the difficulty of removing them from the wound surface [45]. In recent times, by impregnating paraffin onto the gauze, coating viscose fiber with polypropylene or adding polyamide contact layer, the adherence of traditional dressings were fixed [24].

TEXTILE DRESSINGS FOR WOUND HEALING

Textile materials have numerous superior features and are used in various industries. Textile materials have different properties such as compatibility, good mechanical properties, non-allergenic, hydrophilic/hydrophobic properties, air and moisture permeability etc. and can be used in all types of dry and wet dressings. For human existence, healthcare is very essential, and in recent years developing textile materials for biomedical purpose have increased extensively. Wound healing is a complex process and the manufacture of wound dressings for complex unhealed wounds requires further investigation. For caring open wounds or broken skin areas such as cuts, grazes or areas of delicate skin in minor injuries, cloth dressings are used widely. Cloth dressings are available in different shapes and sizes, in addition to pre-cut dressings, in a roll choice that can be cut to suitable size. According to the cause, textile wound dressings can be used as protective layers, drug carriers, contact layers and reinforcements of wound healing composites. Textile wound dressing structures can be changed by using different raw materials and changing production parameters [4]. Porosity, strength, flexibility, capillarity, absorption, three-dimensional structures, moisture permeability, air permeability, drape ability, extensibility, different fiber types and lengths, cross-sectional shape and geometry, fineness, combinability with medicines, etc. are the major and significant properties to produce an effective textile wound dressings. Natural fibers such as cotton and silk and synthetic fibers such as polyester, polyamide, polypropylene, polyurethane, etc. can be used as the wound dressing. The key benefits of new dressings are exudate transport, wound closure and on-demand drug delivery to the wound environment. Recently, innovative fibers and gels have been made from natural polymers such as polysaccharides (alginates, chitin and chitosan), proteins, polyglycolic acid, regenerated cellulose, etc. [6].

Wound dressings play a critical role in wound care and wound healing. Chitosan-based wound dressings are biodegradable, biocompatible and antibacterial and have increased significant attention in recent years. Chitosan is a natural polymer derived from chitin, which is originate in crustacean shells and has been widely considered in diverse presentations [46-47].

Recently, many researchers have focused on using biological materials such as chitin and chitosan [48]. Chitosan acetate theoretically has extensive biologically valuable properties such as antimicrobial activity, homeostasis and stimulation of healing, drug delivery, and tissue engineering scaffolds. Chitosan is the soluble form of chitin, which is mainly in marine arthropod shells and is a biopolymer consisting of poly-N-acetylglucosamine and prevalent in nature. The antimicrobial properties of chitosan depend on the degree of chitosan polymerization, substrate chemical and/or nutrient composition; type (plain or derivative); environmental conditions like moisture and host natural nutrient constituency. The site of action of chitosan is on the microbial cell wall and the antimicrobial effect occurs immediately on fungi and algae and then on bacteria [32]. The use of chitosan accompanied by various antibacterial agents such as Ag, Zn, CuO, TiO₂ and Fe has been studied by many researchers in recent years [48]. Antimicrobial and scar-preventive wound dressings were developed by coating a mixture of chitosan, polyethylene glycol and polyvinylpyrrolidone on the cotton fabric and subsequent freeze drying by Anjum et al. in 2016 [49]. Multilayered or composite dressings are frequently a mixture of the described dressings. Blend of a semi/non-adherent layer with an extremely absorbent fibrous layer such as cotton is typically useful for burns, lacerations, abrasions or surgical incisions [31]. The wound healing has different phases and different wound dressing can be used in each phase of healing procedure. As a primary or secondary dressing, combination dressings can be used. Composite dressings are combination of dressing types and are simply a combination of a gauze dressing and a moisture retentive dressing. Depends on the type of dressing, it is useable on different wound. Although it is easy for clinicians to use and is available extensively. The composite dressing may contain hydro-fiber inner layer and a viscoelastic hydrocolloid outer layer, which can be used for post-operative applications, such as following a total knee replacement procedure [50]. Zhang et al. in 2021 engineered a nontoxic, biocompatible, and antibacterial chitosan-collagen dressing with water retention property [51]. Effect of alginate/chitosan hydrogel with different amounts of hesperidin on wound healing was reviewed in 2020 by Bagher et al. examined. They concluded that the produced hydrogel has suitable properties for wound healing applications and shows promise overview for successful wound treatment [52]. Purwar et al. made a composite wound dressing by embedding hydrogel on cotton fabric for drug release in 2014. The prepared dressing showed drug release at different pH values with maximum drug release in acidic medium [53]. A therapeutic and cost-effective chitosan–Vaseline gauze dressing was industrialized by Fang et al. in 2020 through coating the Vaseline and chitosan on sterile gauze following drying. They

reported that chitosan–Vaseline dressing is useful for wound healing [54]. The treatment of cotton gauze with a nanocomposite of Ag/chitosan/ZnO can also improve wound care ability, increased wicking, drying time and water absorption capacity on the way to modern wound dressings [48]. Pinho et al. reported in 2018 on composite wound dressings obtained by crosslinking between cotton fabric and cyclodextrin-cellulose-based hydrogels. They reported that it is possible to synthesize antimicrobial composite wound dressings with natural compounds and eco-friendly techniques using gallic acid [55].

As it was mentioned before, hydrogels are developing as one of the best dressings because of their biocompatibility, drug loading capability and extracellular matrix imitating structure. Though, current hydrogel dressings reveal unfortunate environmental compliance, limited breathability, probable drug resistance, and partial drug options, which particularly confine their working conditions and therapeutic result. Jiang et al. presented the first model of hydrogel textile dressings by innovative gelatin glycerin hydrogel (glyhydrogel) fibers invented by the Hofmeister effect through wet spinning method. Through the exceptional knitted structure, the textile dressing features admirable breathability and stretchability ($535.51 \pm 38.66\%$). Totally these properties can not be reachable via traditional hydrogel dressings and offer a novel tactic for the growth of hydrogel dressings [56].

An innovative bio-printed textiles based on fish skin decellularized extracellular matrix (dECM) for wound healing was presented in 2023. Due to the good biocompatibility of fish-derived dECM, bioprinted textiles show excellent functionality due to cell adhesion and proliferation. Considering that the dECM-based hydrogels are produced by the bio printing method, the bio printed textiles exhibit a suitable and tunable porous structure with good air permeability throughout the fabric. Furthermore, a variety of active molecules can be loaded onto the hydrogel skeleton according to the porous structure, and increasing the wound healing effect [57].

Alginate dressings which are easy removal, have extremely great absorbing effectiveness and can remove great amounts of exudate. Alginate dressings can be used also in clean or infected wounds [58].

For higher state pressure ulcers, packing wounds, burns, venous ulcers and wet wounds with high liquid drainage, alginate dressings are suggested as primary dressings. Alginate is an ionic polysaccharide which can be used in different wound dressings and can improve the wound healing procedure. Alginate cross-link with various organic or inorganic materials, which can aid in healing properties. Bioactive alginate has hydrogel properties such as biodegradability, optimal water vapor permeability, exudate absorption and intrinsic swelling properties. These properties are beneficial for a sterile dressing and wound healing

[59]. Alginate dressings can contain some medicines like sodium and seaweed fibers, that can absorb high amounts of fluid, and more they are biodegradable after use. Alginates are mixed water-soluble Na and/or K, Ca and Mg salts of alginic acid. Alginates are mostly gained from brown sea algae. Biocompatibility, biodegradability, gelation, high absorbency, non-irritating, non-toxic, easy application and blending and swelling are the superior properties of alginate fiber. The alginate can absorb 15 to 20 times its weight in liquid. Many researchers have worked on applications of alginate in wound dressings. Alginate can be mixed with other textile fibers like cotton and chitosan [60]. Commoto et al. in 2019 produced an alginate-based hydrogel with implanted biologically active materials that was breathable for at least 72 hours and had excellent mechanical properties. Curcumin and t-resveratrol as antioxidants were individually encapsulated in the alginate-based hydrogel. The prepared hydrogel was biocompatible and was not toxic for human keratinocytes. The hydrogel encapsulated with curcumin was more effective against bacterial growth. The hydrogel dressings produced are useful in many skin diseases and can modulate the immune response while controlling bacterial growth [61].

Hydro fiber Technology (HT) was founded on a new sodium CMC hydrocolloid fiber material. Definitely, it was industrialized for wound care to include the required features of more traditional dressings (cotton gauze, alginates and foams) and for increasing aspects of exudate controlling. Mike Walker and David Parsons in 2010 reported that the initial material is advanced form of cellulose. In wound care, usually cotton gauze used as natural form. Cotton is very useful but its absorbency or the ability to retain fluid is not enough because of the physical spaces in cotton fabrics tightly bounding in the cellulose. Changing the macroscopic fiber structure and introducing several pathways for moisture permeability and fiber gelation confirm that improvements in both absorption and retention properties are being achieved in hydrofiber dressings. Number of sodium carboxymethyl groups in the molecular structure should be controlled. Subsequently, HT dressings afford hydration properties which make them different from other wound dressing [62]. Hydro fiber based dressings are able to lock in wound exudate and have antibacterial properties and removed bacteria and proteolytic enzymes which may presence in the fluid from the wound area. Hydrofiber products have wonderful properties such as gel blocking, high fluid absorption capacity, fluid retention under pressure (e.g. >90%) and are easy to apply and allow for non-traumatic dressing removal as demonstrated by in vivo and in vitro studies [63]. After achievements of alginate wound dressings, a gel-forming CMC fiber was produced as wet healing dressing under the name of Hydro-Fiber. This hydrofiber made from the solvent-

spun cellulose fiber (Tencel), by replacing the -OH group in cellulose by sodium carboxymethyl groups. Fiber is insoluble in water, yet the sodium carboxymethyl groups draw enough water into the fibers and cause the fibers to swell and form a gel. Hydrofiber nonwoven felts are strong, soft and conformable, unlike the alginate fibers which are brittle, weak and light brown. Hydro-fibers gel wound dressings are highly absorbable and can be easily removed after use [64]. Aquacel Ag® (ConvaTec, Princeton, NJ, USA) is a hydro-fiber wound dressing made from soft, non-woven fibers of sodium carboxymethylcellulose that incorporate ionic silver. It is antimicrobial and is a moisture retaining wound dressing and forms a gel on contact with wound fluid. In 2009, Barnea et al. reported on the use of hydro-fiber dressings with silver (Aquacel Ag®) in wound care. They concluded that Aquacel Ag® is an effective, antibacterial and safe dressing for acute and chronic wounds [65].

Collagens are the greatest abundant protein originate in the body. For wound healing, these collagens are created by fibroblasts and improved into different morphologies. Wound healing and tensile strength of healed skin depend on the amount, type and organization of collagen [66]. Collagen-based biomaterials have been used for wound dressings cause of easy to apply, low immunogenicity, biocompatibility and ability to reactivate wound healing responses. Typically, the normal sources of collagen are bovine, equine, avian, or porcine. The use of animal-based collagen products is associated with allergic problems, microbial contamination and the spread of prion diseases. In addition, other natural (marine) or genetically engineered (recombinant human collagen from bacterial or plant material) sources of collagen have been considered. Collagen has been used as matrices/scaffolds for tissue engineering, hemostats, soft tissue repair, and in recent years as a drug delivery system. Collagen can be combined with natural and synthetic polymers such as hyaluronic acid, poly(L-lactic acid), polyethylene oxide, elastin and silk fibroin, alginate, chitosan. Some additives such as insulin, antibiotics or nanoparticles have been added for wound healing. Biocompatible nanocollagen is a fairly new material produced by electrospinning processes and this nanosize offers a higher surface area to volume ratio that can be used for therapeutic drug delivery systems [67].

Chitosan and collagen are used as natural polymers along with textiles for wound dressing. In a research work, a collagen-containing wound dressing was prepared using non-woven fabric with a collagen layer.

For burns, chronic, surgical or stalled wounds, transplant sites, pressure sores, ulcers and injuries; collagen dressing can be offered. Collagen dressings may remove dead tissue, grow fresh blood vessels, and help to bring the wound edges together and act

as a scaffold for new cells. Santhanam et al. in 2020 reported about the role of collagen for wound treatments [68]. Doillon and Silver in 1986 were determined the effect of hyaluronic acid and fibronectin in a collagen-based wound dressing [69]. Amirah et al. studied antibacterial collagen dressings for diabetic foot ulcers in 2020. Encouraging results have been reported using a collagen-based dressing with integrated antibacterial components such as polyhexamethylene biguanide and silver for diabetic foot ulcer wound healing [70].

In the other point of view, nanofibers are widely used in numerous biomedical uses for example cancer therapy, gene delivery, drug delivery, cell therapy, tissue engineering and regenerative medicine [71]. Nanofiber composites can be used efficiently for wound healing and conformal tissue regeneration. Currently electrospinning, phase separation, self-assembly, and template synthesis are main methods for nanofibers preparation [72]. Among others, electrospinning is a modern, cheap and efficient method for large scale production of continuous fine nanofibers with tunable diameter and can process both natural and synthetic polymers to solve specific wound problems.

These fibers can be used in filtration, composite materials, wound dressing and membrane industry. Nanofibers are favorable materials for assisting wound healing and skin regeneration. Electrospun meshes have high surface area and microporosity which can be loaded by biomolecules or drugs and can be used as scaffolds for tissue engineering. Subsequently, different materials such as chitosan, gelatin, collagen, fibrinogen, poly lactic acid, polyurethane, poly caprolactone and polyvinyl alcohol can be electrospun and used as appropriate wound dressing [73-74]. The electrospun nanofibers have specific properties such as large surface areas, changeable morphologies, high porosities, and manageable mechanical properties and can be used for drug delivery applications [75]. Various antibiotics and anticancer drugs can be combined into electrospun polymeric nanofibers for making desirable wound dressings. Usually, these active ingredients are incorporated into nanofibers by mixing them into the polymer and then electrospinning the mixture or core-shell electrospinning. Iacob et al. described in 2020 a summary of widely used polysaccharides of animal, plant, fungal and bacterial origin for the production of nano-wound dressings. Drugs and biological molecules can be encapsulated in electrospun nanofibers and wound healing processes can be improved and accelerated. They concluded that electrospun polysaccharide nanofiber dressings had more desirable and appropriate properties such as cost-effectiveness, ease of preparation, efficient drug delivery, and better wound healing time compared to traditional dressings [75]. Recently, many researchers are investigating electrospun polymeric wound dressings with fiber

diameters in the nanometer and micrometer range. These wound dressings have different properties that can accelerate the wound healing process. In a 2021 review, Akhmetova and Heinz gave an overview of cytocompatible and biodegradable fibrous wound dressings produced by electrospinning proteins and peptides of animal and plant origin [76]. Campa-Siqueiros et al. in 2020 described electrospun nanofibers from gelatin, chitosan and chitosan-polyvinyl alcohol that made through electrospinning method. The produced nanofibers provide good antimicrobial efficiency and can be used as wound healing dressings [77]. Multifunctional nanofiber dressings are effective for wound healing process due to their great biocompatibility, biodegradability and bioactivity, and can be produced by mixing various natural or synthetic polymers and combining drugs, nanoparticles and bioactive agents through the electrospinning process. Electrospinning of natural and synthetic biopolymers has larger structures for making wound dressings and tissue engineering scaffolds, and hence is valued for modern wound care and medical industry and other specific structures [78]. Wound dressings based on hydrophilic polyurethane with peppermint extract as a natural and herbal anti-inflammatory and antimicrobial agent were prepared through electrospinning method. Prepared nanofibers have potential wound healing property for diabetic ulcers [79].

Natural polymers such as glucan and galactan-based carbohydrate are inexpensiveness, natural, biocompatible, biodegradable and are good candidate for using in wound healing dressings process. In addition, nanofibrous mesh have great surface area and are similar to the ECM (extracellular matrix) and supports fine proliferation and migration of fibroblasts. Therefore, nanostructured dressings derivative from glucans and galactans like chitosan, pullulan, carrageenan, agar or agarose and curdlan do not have the problems of traditional wound dressings [80].

In the other research work nanofibrous wound dressings with synergistic antibacterial activity were developed. The process involves the layerwise co-assembly of benzalkonium chloride (BC) and metal-organic framework nanoparticles (MOFs, PCN-224) onto poly(ϵ -caprolactone) (PCL) electrospun nanofibrous membranes (ENMs) using a tannic acid (TA)-assisted adhesion strategy. The prepared nano composite presents a novel method for enhancing wound disinfection in clinical settings [81].

The inappropriate managing of wound exudate around the diabetic wound bed is one of the key parameters leading to delay diabetic wound healing. Zhuo et al., introduced a new diabetic wound dressing for achieving fast wound healing by electrospinning hydrophobic nanofibers on a hydrophilic modified non-woven fabric. The double-layer structure of the

self-pumping dressing divert excessive exudate away from diabetic wounds, ultimately promoting wound healing [82].

ANTIMICROBIAL WOUND DRESSING

With a global market of US\$20.4 billion by 2021, skin wound dressings are a core part of the wound care industry. Natural polymeric nanofibers loaded with antibacterial and biofunctional agents are intelligent classes of bioactive wound dressings and can be replaced by classic wound dressings [83]. In order to manufacture antimicrobial dressings, several performance criteria are important, such as wound surface protection, absorption of wound exudate, and ease of application and removal. Usually, textile wound dressings can combine with antimicrobial agents through different methods such as 1) antimicrobial creams and ointment (betadine solution and betadine cream or silver antimicrobial wound gel), 2) textile fabric impregnated with antimicrobial active ingredients, 3) antimicrobial coated textile substrate, 4) textile fibers containing antimicrobial active ingredients, 5) textile composite containing antimicrobial fibers. Wound dressings come in direct contact with injured skin and should be safe, non-toxic and free from allergy problems. It must be effective on broad-spectrum of bacteria without bacteria resistance and antimicrobial effect should sustained during the shelf time.

Studying about functional wound dressings with rapid hemostasis and antimicrobial efficiency is necessary for the managing of severe bleeding wounds. In general, cotton dressings are used in clinical practice; but, few number of dressings may concurrently have antimicrobial properties and fast hemostasis. Zeng et al. in 2023 developed a versatile cotton dressing in name of (GCQCNF-5) by deposition catechol modified quaternary chitosan (CQCS) and gelatin onto a cotton nonwoven fabric surface. They reported, cause of presence of a gelatin sponge layer with suitable thickness and porosity on its surface, GCQCNF-5 exhibits a particular enhanced hemostatic effect compared to raw nonwoven fabric both in vitro and in vivo, which is even somewhat superior to a commercial gelatin hemostatic sponge. They reported by exerting a rapid hemostasis effect, GCQCNF-5 can exploit catechol modified quaternary chitosan to apply excellent immediate antimicrobial and long-lasting bacteriostatic properties. By in vivo wound healing experiments they indicated that GCQCNF-5 could significantly promote rapid healing of infected wounds by effectively sterilizing, absorbing exudates, and providing moist healing environments [84].

Generally fibrous biomaterials are used for manufacturing of antibacterial wound dressings. Antibacterial and probiotic therapies can be used for preparing anti-infective dressings may have side-effects and biotoxicity. Zhang et al. in 2023 reported a method for fabricating wound dressings to combat

infection. They claimed that Poly(4-methyl-1-pentene) (PMP) fabric can remove bacteria from infectious wounds through dressing changes based on its efficient bacterial adhesion. Also, they reported PMP fabric could inhibit the twitching motility of bacteria, which is beneficial for inhibiting infection. In a rat wound model, ability of the Poly(4-methyl-1-pentene) fabric was demonstrated in vivo for wound healing acceleration. They reported, by treating with the PMP fabric dressing, pathogenic bacteria in the wound were removed through dressing change; therefore, the wound exhibited better healing speed than when the commercial dressing was used. The low bacterial concentration effectively stimulated the expression of growth factors and inhibited wound inflammation and accelerating wound healing. They claimed that PMP fabric has been approved for use in clinical treatment by the Food and Drug Administration, no antibacterial agent or probiotics were used for preparation and the fabric could be manufactured through an industrial production process [85].

Clove (*Syzygium aromaticum*) is one of the useful herbal medicines to prevent the bacteria infection. The extract of Clove has phenolic compounds such as eugenol and this plant have great antioxidant, antimicrobial and anti-inflammation properties. Parham et al. endeavored to develop the flexible cellulosic textile nanocomposite by dipping the cellulosic textile in a nano emulsion containing clove herbal medicine (32%wt). This clove treated textile improve the in vitro cellular compatibility and in vivo wound healing and approximately 85% of the procedure of wound was mended in 14 days [86].

In the other research in 2019, a wound dressing able to release chlorhexidine (CHX) as antiseptic agent, ensuring long-lasting antibacterial efficacy during the healing was designed by Aubert-Viard et al [87]. In similar research, the sandwich-like composite hydrogel wound dressings were settled by adding nonwoven fabrics for interior layer and chitosan and gelatin hydrogel treated with *Centella asiatica* as a base material. After treating with *Centella asiatica*, the treated wound dressing revealed brilliant antibacterial activity and drug release properties. This work indicates that the nonwoven composite hydrogels have wide application in the field of medical care in the future [88].

APPLICATIONS OF SMART MATERIALS IN WOUND CARE

Topical improvements on dressings like hydrogel dressings using combined treatment functions and monitoring, using intelligent materials or sensors to sense modifications in the wound situation and wound healing are ongoing. These dressings support reactive treatment for wound healing and are able to carry out dynamic treatment soon enough to successfully help wound healing. Some dressings can monitor and observe wound status and afford

tailored treatment, for example temperature, pressure, pH and glucose sensitive dressings [25]. Developing smart dressing integration can help prevent amputations and ulcers and speed up the healing process. Recently, for smart wound dressings, researchers suggested bio-sensing technique for chronic wound environment condition. Some biomarkers recognized as probable indicators for treatment of non-healing chronic wounds. Biochemical and physical biomarkers are the two main categories. Biochemical marker classified as cytokine, enzyme, metabolic byproduct and pH and some physical markers classified as temperature, pressure, moisture content that can be converted into calculable electrical signals. Ginanini et al. reported that the chronic wound environment can be sensed in real time and the creation of a feedback system can measure the healing process [89]. Magnetization of cellulose fiber using CoFe₂O₄ as smart wound dressing was studied by Williams et al. in 2019 for healing monitoring ability. They concluded that prepared magnetic dressing can be used as a smart wound dressing concerning wireless magnetic announcement for tele-monitoring wound healing procedures [90]. Ghaderi and Afshar in 2004 [91] reported about honey application for skin wound treatment. Honey can accelerate the wound healing process and improve the formation of granulation tissue, keratinization of the wound surface, and the thickness of the basement membrane and epidermis. Honey can decrease inflammation, infection, edema, and improved resilience, ultimate tensile strength and toughness of wound. Nazeri et al. in 2015 reported about a honey-based alginate hydrogel for wound dressing [92]. Silver and silver derivatives have been used as an antimicrobial agent for many years, and the medicinal use of silver is not a new tactic. Metallic silver or silver nitrate was used for skin infection treatments and chronic wounds. Silver in ionized form and nanosilver shows excellent antimicrobial and antifungal properties and can be used to coat medical devices. Silver can be used in wound dressing's compound for healing the contaminated wounds [93]. Elsaboni et al. in 2022 focused on the design and fabrication of flexible textile-based protein sensors to be embedded in wound dressings. Chronic wounds need continuous monitoring for preventing additional difficulties and determining the best treatment in the case of infection. For the progression of wound healing, proteins are necessary and can be used as an indicator of wound status. By measuring protein concentrations, the sensor can monitor the wound condition continuously as a function of time. The protein sensor has electrodes printed on polyester fabric by silver and carbon composite inks. Currently, this is a collective backing fabric used for wound dressings. They concluded that, the best sensor design is comprised of silver conductive tracks but a carbon layer as the working and counter electrodes at the interface zone [94]. At least, much more

research is needed for wound dressing and effective materials for wound healing.

CONCLUSION

Newer wound dressings create an ideal atmosphere in which cells can move freely. Because oxygen circulates efficiently throughout the wound in a moist atmosphere, bacterial growth is low and tissue renewal is faster. Large series of wound dressings have been developed because no single dressing is suitable for the treatment of different wounds. Wound healing procedures have different phases that require different dressings for each phase. In moist wound controlling, textile dressings can be used as advanced fibers like chitosan or alginate fibers, or the textile dressing can be coated and modified with several ingredients such as hydrogels or honey for achieving distinctive properties such as drug release or better hydrophilicity. Generally, different types of textiles such as nanofibers, filaments, yarns, woven, nonwoven and composite textiles can be used in wound-dressing products. In summary, textile materials and composite structures will continue to be one of the physical solutions for the care of people with wounds.

Acknowledgement: *The authors gratefully acknowledge the help and support of Department of Textile, Arak Branch, Islamic Azad University, Arak, Iran for performing the study and development work. Authors gratefully acknowledge the help of Rajamangala University of Technology Phra Nakhon (RMUTP), Thailand, for supporting this research.*

REFERENCES

1. Kubera S.K.S., Prakash C., Subramanian S.: Study on performance of different wound dressings on surgical non infected wounds, *Journal of Natural Fibers* 18(2), 2021, pp. 161-174.
<http://doi.org/10.1080/15440478.2019.1612812>
2. Tavakoli S., Klar A.S.: Advanced hydrogels as wound dressings, *Biomolecules* 10(8), 2020, pp. 1-20.
<http://doi:10.3390/biom10081169>
3. Andrews K.L., Derby K.M., Jacobson T.M., et al.: Prevention and management of chronic wounds. In: Cifu D.X., editor. *Braddom's physical medicine and rehabilitation*, Pennsylvania: Elsevier, 2021, pp. 469-484.
<http://doi:10.1016/B978-0-323-62539-5.00024-2>
4. Ramazan E.: Advances in fabric structures for wound care. In: Rajendran S., editor. *Advanced textiles for wound care*, Cambridge: Woodhead Publishing, 2019, pp. 509 – 540.
<http://doi:10.1016/B978-0-08-102192-7.00018-7>
5. Vachhrajani V., Khakhar P.: *Science of wound healing and dressing materials*, Springer Nature Singapore, Gateway East, 2020.
http://doi:10.1007/978-981-32-9236-9_7
6. Voncina B., Fras L.Z., Ristic T.: Active textile dressings for wound healing. In: Langenhove L.V., editor. *Advances in smart medical textiles: Treatments and health monitoring*, Cambridge: Woodhead Publishing, 2016, pp. 73-92.
<http://doi:10.1016/B978-1-78242-379-9.00004-9>
7. Cutting K.F., White R.J., Legerstee R.: Evidence and practical wound care—an all-inclusive approach, *Wound Medicine* 16, 2017, pp. 40-45.
<http://doi:10.1016/j.wndm.2017.01.005>
8. Milne K.E., Penn-Barwell J.G.: Classification and management of acute wounds and open fractures, *Surgery (Oxford)* 38(3), 2020, pp.143- 149.

9. <http://doi:10.1016/j.mpsur.2020.01.010>
Sen C.K.: Human wounds and its burden: an updated compendium of estimates, *Advances in wound care* 8, 2019, pp. 39-48.
10. <http://doi:10.1089/wound.2019.0946>
Guest J.F., Fuller G.W., Vowden P.: Cohort study evaluating the burden of wounds to the UK's National Health Service in 2017/2018, update from 2012/2013, *BMJ Open* 10(12), 2020, pp. 1-15.
11. <http://doi:10.1136/bmjopen-2020-045253>
Tottoli E.M., Dorati R., Genta I., et al.: Skin wound healing process and new emerging technologies for skin wound care and regeneration, *Pharmaceutics* 12(8), 2020, pp. 1-30.
12. <http://doi:10.3390/pharmaceutics12080735>
Rizani N.: Modern wound dressing for wound infection: An overview, *Indonesian Journal of Tropical and Infectious Disease* 3(1), 2012, pp. 39-59.
13. <http://doi:10.20473/ijtid.v3i1.201>
Kuo F.C., Hsu C.W., Tan T.L., et al.: Effectiveness of different wound dressings in the reduction of blisters and periprosthetic joint infection following total joint arthroplasty: A systematic review and network meta-analysis, *The Journal of Arthroplasty* 36(7), 2021, pp. 2612- 2629.
14. <https://doi:10.1016/j.arth.2021.02.047>
Kumar K.S., Prakash C., Ramesh P., et al.: Study of wound dressing material coated with natural extracts of *Calotropis Gigantea*, *Eucalyptus Globulus* and buds of *Syzygium Aromaticum* solution enhanced with rhEGF (REGEN-DTM 60), *Journal of Natural Fibers* 18(12), 2021, pp. 2270-2283.
15. <http://doi.org/10.1080/15440478.2020.1726239>
Prakash C., Sukumar N., Ramesh P., et al.: Development and characterization of wound dressing material coated with natural extracts of curcumin, aloe vera and chitosan solution enhanced with rhEGF (REGEN-DTM), *Journal of Natural Fibers* 18(12), 2021, pp. 2019-2032.
16. <http://doi.org/10.1080/15440478.2019.1710738>
Shi C., Wang C., Liu H., et al.: Selection of appropriate wound dressing for various wounds, *Frontiers in Bioengineering and Biotechnology* 8, 2020, pp. 1-17.
17. <http://doi:10.3389/fbioe.2020.00182>
Vivcharenko V., Przekora A.: Modifications of wound dressings with bioactive agents to achieve improved pro-healing properties, *Applied Sciences* 11(9), 2021, pp.1-16.
18. <http://doi:10.1111/j.1742-481X.2008.00541.x>
Thomas S.: Hydrocolloid dressings in the management of acute wounds: a review of the literature, *International Wound Journal* 5(5), 2008, pp. 602-613.
19. <https://clhgroupp.co.uk/learning-centre/guides/7-types-of-wound-dressings-when-to-use-each>
CLH Healthcare, 7 Types of Wound Dressings & When to Use Each.
20. <https://doi.org/10.1111/j.1742-481X.2008.00541.x>
Thomas S.: Hydrocolloid dressings in the management of acute wounds: a review of the literature, *International wound journal* 5(5), 2008, pp. 602-613.
21. <http://doi:10.3390/ijerph17217881>
Kamińska M.S., Cybulska A.M., Skonieczna-Żydecka K., Augustyniuk K., Grochans E., Karakiewicz B.: Effectiveness of hydrocolloid dressings for treating pressure ulcers in adult patients: A systematic review and meta-analysis, *International Journal of Environmental Research and Public Health* 17(21), 2020, pp. 1-19.
22. <https://doi.org/10.1039/D2RA07673J>
Nguyen H.M., Le T.T.N., Nguyen A.T., et al.: Biomedical materials for wound dressing: Recent advances and applications, *RSC advances* 13(8), 2023, pp. 5509-5528.
23. <https://doi.org/10.3390/pharmaceutics15010042>
Ahmad N.: In vitro and in vivo characterization methods for evaluation of modern wound dressings, *Pharmaceutics* 15(1), 2022, pp. 1-47.
24. <http://doi:10.1016/j.compositesb.2021.109134>
Long C., Qing Y., Li S., et al.: Asymmetric composite wound nanodressing with superhydrophilic/ superhydrophobic alternate pattern for reducing blood loss and adhesion, *Composites Part B: Engineering* 223, 2021, pp. 1-10.
25. <https://doi.org/10.3390/gels9090694>
Jin S., Newton M.A.A., Cheng H., et al.: Progress of hydrogel dressings with wound monitoring and treatment functions, *Gels* 9(9), 2023, pp. 1-26.
26. <https://doi.org/10.1016/B978-0-08-102192-7.09001-9>
Asdasd Weller C., Team V.: Interactive dressings and their role in moist wound management. In Rajendran R., editor. *Advanced textiles for wound care* Cambridge: Woodhead Publishing, 2019, pp. 105-134.
27. <http://doi:10.11846/s1038-018-0138-8>
Lu H., Yuan L., Yu X., et al.: Recent advances of on-demand dissolution of hydrogel dressings, *Burns & Trauma* 6, 2018, pp.1-13.
28. <https://doi.org/10.5339/qcsp.2013.38>
El-Sherbiny I.M., Yacoub M.H.: Hydrogel scaffolds for tissue engineering: Progress and challenges, *Global Cardiology Science and Practice* 2013(3), pp. 1-27.
29. <http://doi:10.1016/j.actbio.2018.12.008>
Guo B., Qu J., Zhao X., et al.: Degradable conductive self-healing hydrogels based on dextran-graft-tetraaniline and N-carboxyethyl chitosan as injectable carriers for myoblast cell therapy and muscle regeneration, *Acta Biomaterialia* 84, 2019, pp. 180-193.
30. <http://doi:10.12968/bjcn.2015.20.Sup9.S17>
Nielsen J., Fogh K.: Clinical utility of foam dressings in wound management: A review, *Chronic Wound Care Management and Research* 2, 2015, pp. 31-38.
31. <http://doi:10.12968/bjcn.2015.20.Sup9.S17>
Bullough L., Johnson S., Forder R.: Evaluation of a foam dressing for acute and chronic wound exudate management, *British Journal of Community Nursing* 20 (Sup9), 2015, pp. S17-S24.
32. <http://doi:10.3390/molecules25215096>
Kowalczyk D., Miazga-Karska M., Gładysz A., et al.: Characterization of ciprofloxacin-bismuth-loaded antibacterial wound dressing, *Molecules*, 25(21), 2020, pp. 1-13.
33. <http://doi:10.3390/jcm10071495>
Wang Y.C., Lee H.C., Chen C.L., et al.: The effects of silver-releasing foam dressings on diabetic foot ulcer healing, *Journal of Clinical Medicine* 10(7), 2021, pp. 1-9.
34. <http://doi:10.12968/bjon.2021.30.1.40>
Pramod S.: A soft silicone foam dressing that aids healing and comfort in oncology care, *British Journal of Nursing* 30(1), 2021, pp. 40-46.
35. [http://doi:10.1016/0195-6701\(93\)90015-R](http://doi:10.1016/0195-6701(93)90015-R)
Wille J.C., Alblas A.B.V.O., Thewessen E.A.P.M.: A comparison of two transparent film-type dressings in central venous therapy, *Journal of Hospital Infection* 23(2), 1993, pp.113-121.
36. <https://doi.org/10.1177/112972980400500205>
Silveira R.C.D.C.P., Braga F.T.M.M., Garbin L.M., et al.: The use of polyurethane transparent film in indwelling central venous catheter, *Revista Latino-Americana de Enfermagem* 18, 2010, pp.1212-1220.
37. <http://doi:10.1177/1129729820927238>
Gallieni M.: Transparen film dressings for intravascular catheter exit-site, *The Journal of Vascular Access* 5(2), 2004, pp. 69-75.
38. <http://doi:10.1177/1129729820927238>
Atay S., Kurt F.Y.: Effectiveness of transparent film dressing for peripheral intravenous catheter, *The Journal of Vascular Access* 22(1), 2021, pp.135-140.
39. <http://doi:10.34172/jcs.2021.019>
Sharma S.K., Thakur K., Mudgal S.K., et al.: Efficacy of transparent vs. pressure pressing in prevention of post-cardiac catheterization pain, discomfort and hematoma: A systematic review and meta-analysis of RCTs, *Journal of Caring Sciences* 10(2), 2021, pp. 103-110.
40. <http://doi:10.1046/j.1524-475x.2001.00050.x>
Edwards J.V., Yager D.R., Cohen I.K., Diegelmann R.F., Montante S., Bertoniere N., Bopp A.F.: Modified cotton gauze dressings that selectively absorb neutrophil elastase activity in solution, *Wound Repair and Regeneration* 9(1), 2001, pp. 50-58.
41. <https://doi.org/10.1016/j.compositesb.2021.109134>
Balasubramanian E., Balasubramanian V., Babu G., et al.: Moist wound dressing fabrications: Carboxymethylation of

- antibacterial cotton gauze, *Journal of Engineered Fibers and Fabrics* 8(4), 2013, 78-87.
<http://doi.org/10.1177/155892501300800402>
42. Soares H.P.L., Brandão E.D.S., Tonole R.: Primary bandages for people with pemphigus vulgaris lesions: An integrative literature review, *Revista Gaúcha de Enfermagem* 41, 2020, pp. 1-8.
<http://doi.org/10.1590/1983-1447.2020.20190259>
 43. Edwards H., Finlayson K., Parker C., et al.: *Wound dressing guide*. Brisbane: Queensland University of Technology, 2019.
 44. Fang H., Li D., Xu L., et al.: A reusable ionic liquid-grafted antibacterial cotton gauze wound dressing, *Journal of Materials Science*, 56, 2021, pp.7598-7612.
<http://doi.org/10.1007/s10853-020-05751-8>
 45. Qin Y.: Antimicrobial textile dressings in managing wound infection. Rajendran S., editor. *Advanced textiles for wound care*, Oxford: Woodhead Publishing, 2009, pp. 179-197.
http://doi.org/10.1533/9781845696306_1_179
 46. Atay H.Y.: Antibacterial activity of chitosan-based systems, *Functional chitosan: drug delivery and biomedical applications 2019*, pp. 457-489.
https://doi.org/10.1007/978-981-15-0263-7_15
 47. Yang M., Wang H., Li K., et al.: A new soft tissue constructed with chitosan for wound dressings-incorporating nanoparticles for medical and nursing therapeutic efficacy, *Regenerative Therapy* 24, 2023, pp. 103-111.
<https://doi.org/10.1016/j.reth.2023.06.005>
 48. Abbasipour M., Mirjalili M., Khajavi R., et al.: Coated cotton gauze with Ag/ZnO/chitosan nanocomposite as a modern wound dressing, *Journal of Engineered Fibers and Fabrics* 9(1), 2014, pp. 124-130.
<http://doi.org/10.1177/155892501400900114>
 49. Anjum S., Arora A., Alam M.S., et al.: Development of antimicrobial and scar preventive chitosan hydrogel wound dressings, *International Journal of Pharmaceutics* 508(1-2), 2016, pp. 92-101.
<http://doi.org/10.1016/j.ijpharm.2016.05.013>
 50. Ghomi E.R., Khalili S., Khorasani S.N., et al.: Wound dressings: Current advances and future directions, *Journal of Applied Polymer Science* 2019, 136(27), pp. 1-12.
<http://doi.org/10.1002/app.47738>
 51. Zhang M.X., Zhao W.Y., Fang Q.Q., et al.: Effects of chitosan-collagen dressing on wound healing in vitro and in vivo assays, *Journal of Applied Biomaterials & Functional Materials* 19, 2021, pp.1-10.
<http://doi.org/10.1177/2280800021989698>
 52. Bagher Z., Ehterami A., Safdel M.H., et al.: Wound healing with alginate/chitosan hydrogel containing hesperidin in rat model, *Journal of Drug Delivery Science and Technology* 55, 2020, pp.1-34.
<http://doi.org/10.1016/j.jddst.2019.101379>
 53. Purwar R., Rajput P., Srivastava C.M.: Composite wound dressing for drug release. *Fibers and Polymers* 15, 2014, pp.1422-1428.
<http://doi.org/10.1007/s12221-014-1422-2>
 54. Fang Q.Q., Wang X.F., Zhao W.Y., et al.: Development of a chitosan–vaseline gauze dressing with wound-healing properties in murine models, *The American Journal of Tropical Medicine and Hygiene* 102(2), 2020, pp. 468-475.
<http://doi.org/10.4269/ajtmh.19-0387>
 55. Pinho E., Calhelha R.C., Ferreira I.C.F.R., et al.: Cotton - hydrogel composite for improved wound healing: Antimicrobial activity and anti - inflammatory evaluation— Part 2, *Polymers for Advanced Technologies* 30(4), 2019, pp. 863-871.
<http://doi.org/10.1002/pat.4519>
 56. Jiang S., Deng J., Jin Y., et al.: Breathable, antifreezing, mechanically skin-like hydrogel textile wound dressings with dual antibacterial mechanisms, *Bioactive Materials* 2, 2023, pp. 313-323.
<https://doi.org/10.1016/j.bioactmat.2022.08.014>
 57. Lin X., Zhang H., Zhang H., et al.: Bio-printed hydrogel textiles based on fish skin decellularized extracellular matrix for wound healing, *Engineering* 25, 2023, pp. 120-127.
<https://doi.org/10.1016/j.eng.2022.05.022>
 58. Froelich A., Jakubowska E., Wojtylko M., et al.: Alginate-based materials loaded with nanoparticles in wound healing, *Pharmaceutics* 15(4), 2023, pp. 1142-1181.
<https://doi.org/10.3390/pharmaceutics15041142>
 59. Stoica A.E., Chircov C., Grumezescu A.M.: Nanomaterials for wound dressings: an up-to-date overview, *Molecules* 25(11), 2020, pp. 1-25.
<http://doi.org/10.3390/molecules25112699>
 60. Ip, M.: Antimicrobial dressings. In: Farrar, D., editor. *Advanced wound repair Therapies*. Cambridge: Woodhead Publishing; 2011, pp. 416-449.
http://doi.org/10.1533/9780857093301_3_416
 61. Comotto M., Saghadzadeh S., Bagherifard S., et al.: Breathable hydrogel dressings containing natural antioxidants for management of skin disorders, *Journal of Biomaterials Applications* 33(9), 2019, pp. 1265 – 1276.
<http://doi.org/10.1177/0885328218816526>
 62. Walker M., Parsons D.: Hydrofiber® technology: Its role in exudate management, *Wounds UK*. 6(2), 2010, pp. 31- 88.
 63. Walker M., Lam S., Pritchard D., et al.: Biophysical properties of a Hydrofiber® cover dressing, *Wounds UK*. 6(9) 2010, pp. 16-29.
 64. Qin Y.: Advanced wound dressings, *The Journal of The Textile Institute* 92(2), 2001, pp. 127-138.
<http://doi.org/10.1080/00405000108659563>
 65. Barnea Y., Weiss J., Gur E.: A review of the applications of the Hydrofiber dressing with silver (Aquacel Ag®) in wound care, *Therapeutics and Clinical Risk Management* 6, 2010, pp. 21- 27.
 66. Rangaraj A., Harding K., Leaper D.: Role of collagen in wound management, *Wounds UK*. 7(2), 2011, pp. 54-63.
 67. Mathew-Steiner S.S., Roy S., Sen C.K.: Collagen in wound healing, *Bioengineering*. 8(5), 2021, pp. 1-15.
<http://doi.org/10.3390/bioengineering8050063>
 68. Santhanam R., Rameli M.A.P., Effri A.A., et al.: Bovine based collagen dressings in wound care management, *Journal of Pharmaceutical Research International* 32(33), 2020, pp. 48-63.
<http://doi.org/10.9734/jpri/2020/v32i3330949>
 69. Doillon C.J., Silver F.H.: Collagen-based wound dressing: Effects of hyaluronic acid and firponectin on wound healing, *Biomaterials* 7(1), 1986, pp. 3-8.
[http://doi.org/10.1016/0142-9612\(86\)90080-3](http://doi.org/10.1016/0142-9612(86)90080-3)
 70. Amirrah I.N., Wee M.F.M.R., Tabata Y., et al.: Antibacterial-integrated collagen wound dressing for diabetes-related foot ulcers: an evidence-based review of clinical studies, *Polymers* 12(9) 2020, pp. 1-17.
<http://doi.org/10.3390/polym12092168>
 71. Guo W., Yang Z., Qin X., et al.: Fabrication and Characterization of the Core-Shell Structure of Poly (3-Hydroxybutyrate-4-Hydroxybutyrate) Nanofiber Scaffolds, *BioMed Research International* 2021, 2021, pp. 1-11.
<http://doi.org/10.1155/2021/8868431>
 72. Gao C., Zhang L., Wang J., et al.: Electrospun nanofibers promote wound healing: theories, techniques, and perspectives, *Journal of Materials Chemistry B* 9(14), 2021, pp. 3106-3130.
<http://doi.org/10.1039/D1TB00067E>
 73. Abrigo M., McArthur S.L., Kingshott P.: Electrospun nanofibers as dressings for chronic wound care: advances, challenges, and future prospects, *Macromolecular Bioscience* 14(6), 2014, pp. 772-792.
<http://doi.org/10.1002/mabi.201300561>
 74. Fatahian R., Mirjalili M., Khajavi R., et al.: Recent studies on nanofibers based wound-dressing materials: A review. *Proceedings of 7 th International Conference on Engineering & Applied Science*, 2018, pp.1-12
 75. Iacob A.T., Drăgan M., Ionescu O.M., et al.: An overview of biopolymeric electrospun nanofibers based on polysaccharides for wound healing management, *Pharmaceutics* 12(10), 2020, pp. 1-49.
<http://doi.org/10.3390/pharmaceutics12100983>

76. Akhmetova A, Heinz A.: Electrospinning proteins for wound healing purposes: opportunities and challenges. *Pharmaceutics* 13(1), 2021, pp. 1-22.
<http://doi:10.3390/pharmaceutics13010004>
77. Campa-Siqueiros P., Madera-Santana T.J., Ayala-Zavala J.F., et al.: Nanofibers of gelatin and polyvinyl-alcohol-chitosan for wound dressing application: fabrication and characterization, *Polimeros* 30, 2020, pp.1-11.
<http://doi:10.1590/0104-1428.07919>
78. Azimi B., Maleki H., Zavagna L., et al.: Bio-based electrospun fibers for wound healing, *Journal of Functional Biomaterials* 11(3), 2020, pp. 1-36.
<http://doi:10.3390/jfb11030067>
79. Almasian A., Najafi F., Eftekhari M., et al.: Preparation of polyurethane/pluronic F127 nanofibers containing peppermint extract loaded gelatin nanoparticles for diabetic wounds healing: Characterization, in vitro, and in vivo studies, *Evidence-Based Complementary and Alternative Medicine* 2021, pp. 1-16.
<http://doi:10.1155/2021/6646702>
80. Latiyan S., Kumar T.S., Doble M., et al.: Perspectives of nanofibrous wound dressings based on glucans and galactans-A review, *International Journal of Biological Macromolecules* 244, 2023, pp. 1-20.
<https://doi.org/10.1016/j.ijbiomac.2023.125358>
81. Li Y., Xu Z., Tang L., et al.: Nanofibers fortified with synergistic defense route: A potent wound dressing against drug-resistant bacterial infections, *Chemical Engineering Journal* 475 (1), 2023, pp. 146492.
<https://doi.org/10.1016/j.cej.2023.146492>
82. Zhou L., Xu P., Dong P., et al.: A self-pumping dressing with in situ modification of non-woven fabric for promoting diabetic wound healing, *Chemical Engineering Journal* 457, 2023, pp.141108.
<https://doi.org/10.1016/j.cej.2022.141108>
83. Homaeigohar S., Boccaccini A.R.: Antibacterial biohybrid nanofibers for wound dressings, *Acta Biomaterialia* 107, 2020, pp. 25-49.
<http://doi:10.1016/j.actbio.2020.02.022>
84. Li L., Chen D., Chen J., et al.: Gelatin and catechol-modified quaternary chitosan cotton dressings with rapid hemostasis and high-efficiency antimicrobial capacity to manage severe bleeding wounds, *Materials & Design* 229, 2023, pp. 1-18.
<https://doi.org/10.1016/j.matdes.2023.111927>
85. Zhang H., Wan H., Hu X., et al.: Antimicrobial-free knitted fabric as wound dressing and the mechanism of promoting infected wound healing, *Science China Technological Sciences* 66, 2023, pp. 2147-2154.
<https://doi.org/10.1007/s11431-022-2260-x>
86. Parham S., Kharazi A.Z.: Cellulosic textile/clove nanocomposite as an antimicrobial wound dressing: In vitro and in vivo study, *Colloids and Surfaces B: Biointerfaces* 217, 2022, pp. 1-9.
<https://doi.org/10.1016/j.colsurfb.2022.112659>
87. Aubert-Viard F., Mogrovejo-Valdivia A., Tabary N., et al.: Evaluation of antibacterial textile covered by layer-by-layer coating and loaded with chlorhexidine for wound dressing application, *Materials Science and Engineering: C* 100, 2019, pp. 554-563.
<https://doi.org/10.1016/j.msec.2019.03.044>
88. Wang L., Li D., Shen Y., et al.: Preparation of Centella asiatica loaded gelatin/chitosan/nonwoven fabric composite hydrogel wound dressing with antibacterial property, *International Journal of Biological Macromolecules* 192, 2021, pp. 350-359.
<https://doi.org/10.1016/j.ijbiomac.2021.09.145>
89. Gianino E., Miller C., Gilmore J.: Smart wound dressings for diabetic chronic wounds, *Bioengineering* 5(3), 2018, pp. 1-26.
<http://doi:10.3390/bioengineering5030051>
90. Williams S., Okolie C.L., Deshmukh J., et al.: Magnetizing cellulose fibers with CoFe₂O₄ nanoparticles for smart wound dressing for healing monitoring capability, *ACS Applied Bio Materials* 2(12), 2019, pp. 5653-5662.
<http://doi:10.1021/acsabm.9b00731>
91. Ghaderi R., Afshar M.: Topical application of honey for treatment of skin wound in mice, *Iranian Journal of Medical Sciences* 29(4), 2015, pp. 185-188.
92. Nazeri S., Ardakani E.M., Babavalian H., et al.: Evaluation of effectiveness of honey-based alginate hydrogel on wound healing in rat model, *Journal of Applied Biotechnology Reports* 2(3), 2015, pp. 293-297.
93. Konop M., Damps T., Misicka A., et al.: Certain aspects of silver and silver nanoparticles in wound care: a minireview, *Journal of Nanomaterials* 2016, pp.1-10.
<http://doi:10.1155/2016/7614753>
94. ElSaboni Y., Hunt J.A., Stanley J., et al.: Development of a textile based protein sensor for monitoring the healing progress of a wound, *Scientific Reports* 12, 2022, pp. 1-12.
<https://doi.org/10.1038/s41598-022-11982-3>

EFFECT OF COMMERCIAL WATER REPELLENT AGENTS ON FUNCTIONAL PROPERTIES OF POLYESTER WOVEN FABRIC USED FOR WASHABLE MEDICAL MASKS

THO, LUU THI¹; PHUONG, DUONG THI¹ AND HUONG, CHU DIEU^{2*}

¹ Hanoi University of Industry, Hanoi, Vietnam

² Hanoi University of Science and Technology, Hanoi, Vietnam

ABSTRACT

Water repellent fabrics are always used for washable medical mask production to keep them from the bacterial liquid during use. Choosing the right water repellent which is efficient and suitable for fabric is important in washable medical mask production. The water-resistant treated fabric needs to keep its water repellent for many washed cycles. Moreover, their physico-mechanical properties such as air permeability and thickness must be less changed. In this study, four commercial water-resistant chemicals (Ruco-Coat BC 7068, TP – Phob FC 2904, Phobotex RHP Hydrophobic Agent, Ruco-guard AFB60) were used to treat the 100% polyester woven fabric to examine the influence of the type and concentration of the water-resistant chemicals on water repellent capability of the polyester woven fabric. The fabric thickness and the air permeability of the untreated and treated fabric were investigated. The SEM, FE-SEM analysis, and the FTIR spectra were used to find the differences between the initial and treated fabric. The results showed that the water-resistant type influenced the water repellent capability of fabrics and their duration. Among four investigated water resistance, the TP – Phob FC 2904 presented the best water resistance for treatment of the 100% polyester woven fabric, and its concentration of 50 g/l has maintained 85 % fabric water repellent capability after 25 washed cycles.

KEYWORDS

Water repellent fabric; Woven fabric; Water resistant chemicals; Air permeability.

INTRODUCTION

Medical textiles are considered personal protective clothing for healthcare in the medical sector, specifically to mitigate the risks from exposure to hazardous substances including body fluids, and to minimize the risk of cross-infections. Medical protective clothing, usually made from synthetic fabric such as polyester because of better liquid barrier properties, could be manufactured using nonwoven, weaving, or knitting technologies. Fluid repellent finishing can be used for getting water repellent fabrics [1, 2].

Water repellent textiles are often high-density woven fabric which is made of very fine yarns or common fabrics with treated hydrophobic surface to keep the fabric pores which are not filled during the treatment processes. A water repellent fabric may be quite permeable to air and water vapor so in a wet environment, it can keep the wearer dry due to their water repellent capability. Water repellent garments are designed for use that protects the human body from the water and many harmful agents and but let

effective transmission of moisture vapor from the inner to the outside atmosphere. The applications may range from their well-known use in leisure clothing, and industrial and military applications to specialized medical products such as washable medical masks [1-4].

Many researchers have investigated the different kinds of water resistant agents for fabric [5-9]. Weixia Zhu et al. have fabricated the fluorine-free breathable poly(methylhydrosiloxane)/ polyurethane fibrous membranes with water resistant capability based on the hydrophobic matrix and small pore size [5]. The authors have studied the morphologies, porous structure, surface wettability also tensile strength of the fabric. Indrajit Bramhecha et al. have used the citric acid-based polyol to synthesis waterborne polyurethane for antibacterial and water-repellent cotton fabric [6]. The author has reported that waterborne polyurethane coated cotton fabric was unchanged in tensile strength and crease recovery angle but it's excellent water repellency (100+ cm of water pressure by test using Shirley hydrostatic head tester in cm of water pressure as prescribed in ASTM

* Corresponding author: Huong, Ch.D., e-mail: huong.chudieu@hust.edu.vn

Received November 26, 2023; accepted April 25, 2024

D4491) was obtained. Guangming Pan et al. have studied the stable polydimethylsiloxane (PDMS) - copper stearate (CuSA2) coating on cotton fabric by a simple in-situ growth and dip-coating method [7]. The sample has inherent mechanical durability, UV resistance, and high oil-water separation efficiency. Y Su et al. have investigated the effect on the thermal protective performance of single- and double-layer fabric systems [8]. In their work, a hot water and steam tester was used to examine the thermal protective performance of treated fabric against hot water and steam hazards. P. De et al. have used the perfluoroalkyl-type fluorocarbon-based compound and fluorocarbon resin-type compound are used as water-repellent, chemicals are applied by different concentrations [9]. It was found that fluorocarbon resin-type compound gives the best results for a water-repellent finish. The water resistant agents in these investigations were not the commercial type which was always used in textile industries for the production of washable medical masks.

Besides, the influence of fabric structure such as the density, the used yarn, roughness, and the water repellent type and their concentrations on the fabric water repellent capacity have been reported [10-14]. Dunja Šajn Gorjanc et al. have investigated the influence of elastane incorporation in the weft direction of cotton fabrics, and the structural properties such as fabric density and type of weave (plain and twill) on the water vapor resistance of the elastic and conventional cotton woven fabrics [11]. Gulay Ozcan has investigated the effects of water repellent finishes on plain woven fabrics in two blends (100% cotton and 50/50 cotton/polyester) [12]. The research has studied the influence of three kinds of commercial water repellent (Fluorocarbon-based water repellent, Chromstearylchlorur-based water repellent, and 3XDRY smart water repellent) on the woven fabric properties such as breaking strength, abrasion resistance, pilling, light fastness, wetting time. The author reported that the water repellent type and their concentrations were very important parameters that effect on woven fabric properties: Fluorocarbon-based water repellent showed the most efficacy on fabric water repellent of both fabrics (100% cotton and 50/50 cotton/polyester). However, the research did not report the air permeability of the treated fabric which was always an important property for the water repellent fabric. Alain M. Jonas et al. has studied the theoretical and experimental methods to quantitatively evaluate the water repellency of woven fabrics coated by hydrophobic formulations (Wax-modified melamine resin, Silicone rubber, Perfluorobutyl-modified polyurethane) [13]. The research was based on the relationship between the woven fabric roughness and its water repellency. The authors have investigated the surface roughness of eight different woven fabrics and their water

repellency after having been coated by wax-based, silicone-based, or perfluorobutyl-based commercial polymer formulations. The result showed that the fabrics with roughness lower than the critical value (which was 1.22 in the research conditions) have partially wet state with a substantial pinning of the droplets on their surface and an absence of roll-off whatever the type of hydrophobic coating. Above this critical value, the fabrics became superficially wet with contact angle controlled by the amount of air trapped in the texture which depends on the wetting hysteresis of the coating material. Beysim Garip et al. have studied the water repellency of woven fabrics prepared from polyester filament yarns [14]. Yarns containing water repellent additives (0%, 3 %, 5 %, and 8% in weight) were produced by melt spinning method using polyester chips. Eight different yarns were produced that included 4 types of polyester yarn (P0, P3, P5, P8) and 4 types of textured yarns (T0, T3, T5, T8). Plain woven fabrics were weaved from these yarns. Then, the water repellency, tensile, and air permeability tests of the fabrics were measured. The authors reported that the yarns added water-repellent additive did not show an effective water repellency performance. The reason was the low percentage of additives in the yarns. Meanwhile, when the coating repetition increased (1, 3, and 5 times water-repellent finishing), the water repellency of the fabrics improved and air permeability decreased by approximately 80% as the number of coatings increased to 5 times.

Even though research papers can be found that compare the effectiveness of commercial water-repellents, most authors do not emphasize the preservation of breathability and water vapor permeability of fabrics, as well as the resistance in the washing of the applied treatment.

That is why the scope of this paper is to investigate the water-repelled capability of polyester fabric treated by chosen commercially water-repellent chemical solutions. The effect of the type of water-repellent solution on fabric water-repellent capability, fabric thickness, and fabric air-permeability is studied. Moreover, the effect of the type of water-repellent chemical on the durability of the applied treatment was analyzed. Based on the results, the most effective chemical concerning fabric repellent capacity and fabric air permeability was chosen and different concentrations of this chosen water-repellent chemical were studied concerning fabric repellent capacity and durability of the applied treatment during washing cycles. As a substrate polyester fabric was chosen and the treatment was applied by the pad-dry-cure method, described as commercial water-resistant chemicals are often used on textile industrial scale, especially for the washable medical mask.

Table 1. Technical parameters of the investigated polyester fabric.

Fabric density mass [g/m ²]	Fabric thickness [mm]	Yarn count [tex]		Fabric density [yarns/10 cm]	
		Warp filament yarn	Weft staple yarn	Warp	Weft
235.00	0.54	16.66/2	19.68/2	321	232

MATERIAL AND METHODS

Materials

The 100% polyester woven fabric (twill weave 2/1 Z) has been used for this investigation. Their technical parameters are presented in Table 1.

The study used four water repellent chemicals: Ruco – Coat BC 7068, a non-fluorocarbon hyperbranched and linear cationic polymer from Rudolf Group (Germany) [17]; TP – Phob FC 2904, a fluorocarbon-based water repellent from Truongphat JSC (Vietnam) [18]; Ruco-guard AFB6 conc from ODG Company (Taiwan) [19], Phobotex RHP Hydrophobic Agent, a non-fluorinated water repellent from the Huntsman (Germany) [20] and the cross link Phobol extender xan, a dispersion of an oxime-blocked polyisocyanate from Huntsman (Germany) [21]. The chemicals were used as supplied without any further purification.

Methods

The pad-dry-cure method has been used in the research. The woven fabric (100% polyester) was pre-treated (desizing and washing at 80 °C for 20 minutes) and then cut into samples of 40 cm x 20 cm. The samples were then kept in the standard condition (temperature at 21 ± 2 °C (70 ± 4 °F), relative humidity of 65 ± 5%) for at least 4h before testing.

Water repellent chemicals with suitable concentration, the cross link Phobol extender xan (15 g/l), and 0.15 ml of acid acetic were added to the padding solution to obtain the pH of 5 to form the padding solution. The concentration of water repellent chemicals was prepared depending on every investigation.

The padding machine model Rapid (Taiwan) was used. Every fabric sample was passed the padding solution then they were pressed with the pressure of 0.8 kg/cm² (80% pressure level) followed by a drying process at 150 °C for 60 seconds. After that, the fabric samples were cured at 190 °C for 60 seconds. The padding conditions were chosen based on the textile industrial scale (Textile Namdinh factory, Vietnam) where the washable medical masks were fabricated.

Influence of the water-repellent type on the fabric treated water repellent capability and its duration after washed cycles

To investigate the influence of water repellent chemical type on the water resistant capability and its duration of fabric treated water repellent, four water

repellent chemicals were used with the same concentration of 30 g/l for every padding solution. The padding conditions were as described in the above section.

The fabrics treated with the water-repellent chemical then have been washed by the standard ISO 6330:2012 using washing machine Type C (Vertical axis, top-loading pulsator machine) with the washing procedure 4M (washing at 40 °C ± 3 °C, 40 liters of water for 6 minutes, spinning for 3 minutes; rinsing with 40 liters of water for 2 minutes, spinning for 3 minutes). The water repellent capability of the treated fabric was evaluated after 5, 10, 15, 20, and 25 washed cycles by the Spray Test AATCC 22-2017 to choose the best water resistant chemical for further research.

The SEM image, the thickness, and the air permeability of initial and treated fabrics were investigated to examine their differences. The fabric thickness was measured by ASTM D1777- 96 (2011), each sample was measured in ten positions and their mean value was taken. Fabric air permeability had been determined by the standard ASTM D 737: 2004. SDL Atlas AirPerm Air Permeability Tester was used with a 20 cm² test head and pressure of 100 Pa. Each sample had been measured in five positions and their mean value was taken.

The ATR-FTIR analysis of the chemicals and the fabric before and after being treated by the best water repellent was carried out using an FTIR spectrometer (Thermo Scientific Nicolet iS50, USA) by recording 64 scans in transmittance mode [%].

Influence of the concentration of water repellent on the water repellent capability and duration of treated fabric after washable cycles

The best water repellent chosen from the first investigation would be used with 5 different concentrations (10 g/l, 20 g/l, 30 g/l, 40 g/l, and 50 g/l) for treating the woven fabric (table 1) with the same concentration of the cross link Phobol extender xan (15 g/l) and 0.15 ml of acid acetic was added to obtain the pH of 5 for the padding solution. The padding conditions were described above.

The fabric treated by water repellent chemicals has been then washed by the standard ISO 6330:2012. The water repellent capability of the fabric was evaluated after 5, 10, 15, 20, and 25 washed cycles by the Spray Test AATCC 22-2017.

Table 2. Ratings of the water repellent by Spray Test AATCC 22-2017 standard.

Ratings	Signification
100	Not sticking or wetting of the specimen face
90	Slight random sticking or wetting of the specimen face
80	Wetting of the specimen face at the spray points
70	Partial wetting of the specimen face beyond the spray points
50	Complete wetting of the entire specimen face beyond the spray points
0	Complete wetting of the entire specimen face

Table 3. Influence of the water repellent type on the fabric water repellent capability.






Order	Water resistant chemical	Fabric water repellent capability [%]	Image
1	Before treating	0	
2	Ruco – Coat BC 7968	85	
3	TP – Phob FC 2904	100	
4	Phobotex RHP Hydrophobic Agent	70	
5	Ruco-guard AFB6 conc	95	

Table 4. Influence of the water resistant type on the fabric water repellent capability after washed cycles.

Order	Water resistant chemical	Washed cycles (time)					
		0	5	10	15	20	25
		Fabric water repellent capability					
1	Ruco – Coat BC 7068	85	80	80	75	70	65
2	TP – Phob FC 2904	100	100	90	85	80	75
3	Phobotex RHP Hydrophobic Agent	70	70	65	60	60	50
4	Ruco-guard AFB6 conc	95	85	85	80	75	70

Evaluation of the water repellent capability fabric

The water repellent capability of the fabric was evaluated by the Spray Test AATCC 22-2017 standard (Table 2).

Verification of water repellent chemicals in treated fabric

The morphology of fabric surface was analyzed by Scanning electron microscope (SEM) and by Field emission scanning electron microscopy (FE-SEM). SEM was used to examine the change of the fabric surface after treating water resistant and FE-SEM (model JSM 7600 USA) was used to determine the presentation of Flour element. Scanning electron microscope (SEM) JEOL JSM7600F, USA was used at working conditions of 5.0 kV; LM mode; WD 4.4 mm. The observation was captured at magnifications of x1000 to observe the fabric surface before and after treating water repellent then the capture at magnifications of x 50 000 was carried out for the detail examination of the fabric surface.

RESULTS AND DISCUSSION

Influence of the water repellent type

Influence of the water repellent type on fabric water repellent capability

The 100% polyester woven fabric was treated with four types of water resistant (Ruco – Coat BC 7068, TP – Phob FC 2904, Phobotex RHP Hydrophobic Agent, Ruco-guard AFB6 CONC) with the same protocol described in the methodology part where four water resistant chemicals were used with the same concentration of 30 g/l. The fabric water repellent capability was evaluated by the AATCC 22-2017 standard (Table 2).

The fabric water repellent capability before and after treatment by four water-resistant chemicals is presented in Table 3.

The results showed the effect of the water resistant type on fabric after treatment (table 3). All the water resistant treated fabrics have increased their water

repellent capability from 70% to 100% in comparison to the initial fabric sample which had the fabric water repellent capability of 0 %. The water resistant TP – Phob FC 2904 demonstrated the best with its fabric water repellent capability of 100%. The fabric treated by the Ruco-guard AFB6 conc, Ruco – Coat BC 7968, and Phobotex RHP Hydrophobic Agent showed the fabric water repellent capability of 90%, 85%, and 70%, respectively.

Influence of the water resistant type on fabric water repellent capability after washed cycles

After water resistant finishing, the fabric samples were washed by standard AATCC 187 – 2013 for 5 times, 10 times, 15 times, 20 times, and 25 times to evaluate the influence of the water resistant type on fabric water repellent capability after washed cycles. The test was important for washable medical mask production, where the fabric water repellent capability needs to be kept as long as possible during use. The results were shown in Table 4.

It could be seen that the increase in the number of washed cycles caused the diminution of the fabric water repellent capability which was influenced by the type of water resistant chemical. After washing cycles 5 and 25, the fabric water repellent capability was 70% and 50%; 80% and 65%; 85% and 70%; 100% and 75% for the Phobotex RHP Hydrophobic Agent, Ruco – Coat BC 7068, Ruco-guard AFB6 conc and TP – Phob FC 2904, respectively. The water resistant TP – Phob FC 2904 showed the most efficacy in water repellent capability for 25 washed cycles.

The initial fabric and the treated fabrics were then observed by SEM to examine the change in the fabric surface after treatment (Fig. 1).

In the surface of the fabric sample treated by Ruco – Coat BC 7068 and Ruco-guard AFB6 conc water resistant, a number of small particles could be observed (Fig. 1). These particles appeared less in the fabric sample treated by Phobotex RHP Hydrophobic Agent and by TP – Phob FC 2904 water resistant.

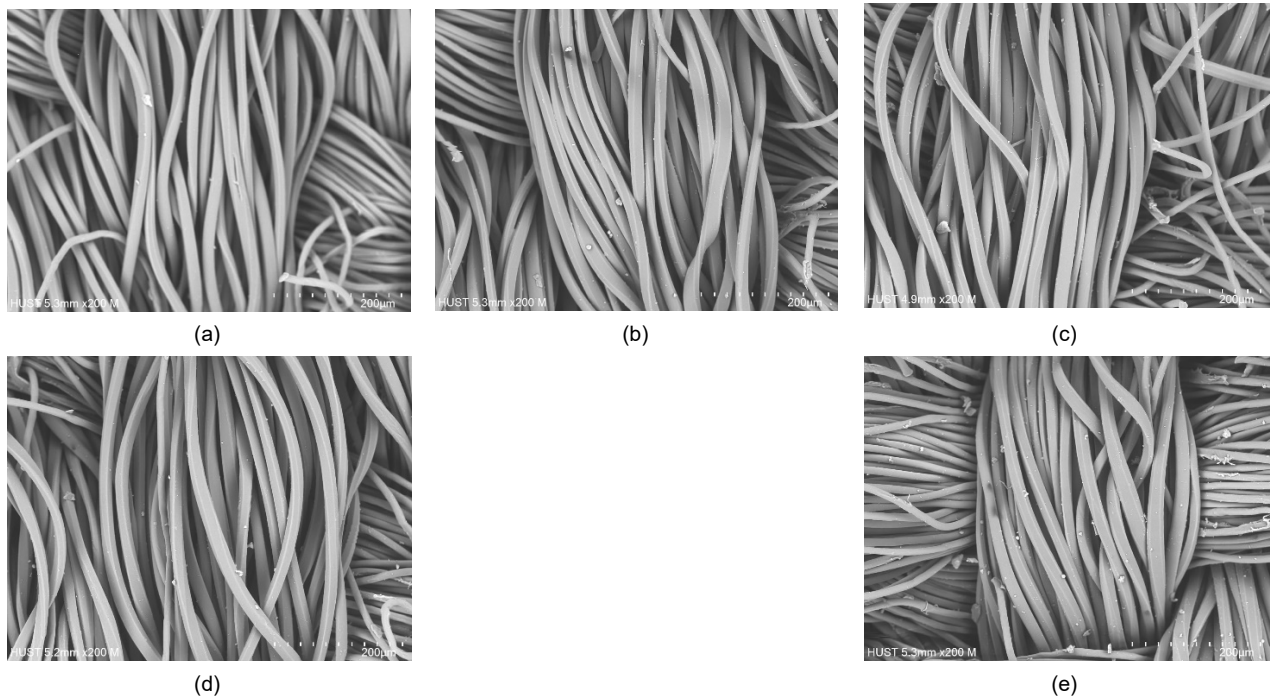


Figure 1. SEM images of fabric surface before and after treatment by the water resistant: (a) initial fabric, fabric treated by (b) TP – Phob FC 2904, (c) Phobotex RHP Hydrophobic Agent, (d) Ruco – Coat BC 7068, (e) Ruco-guard AFB6 conc.

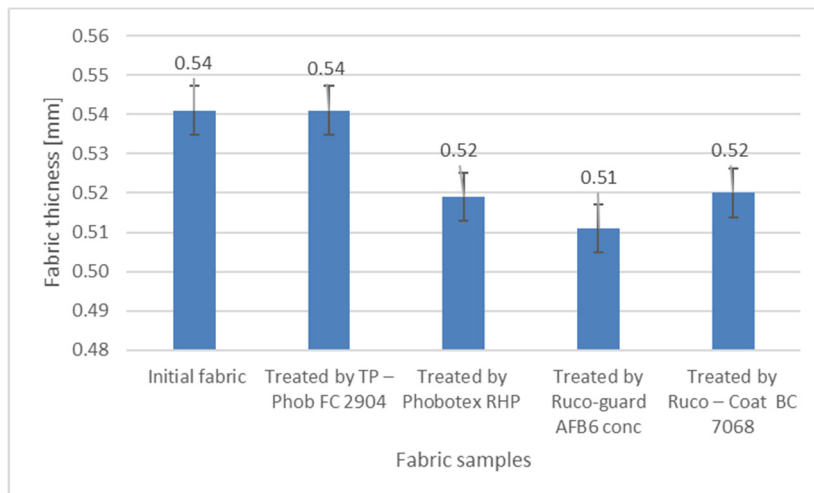


Figure 2. The fabric thickness before and after treatment by the water resistant.

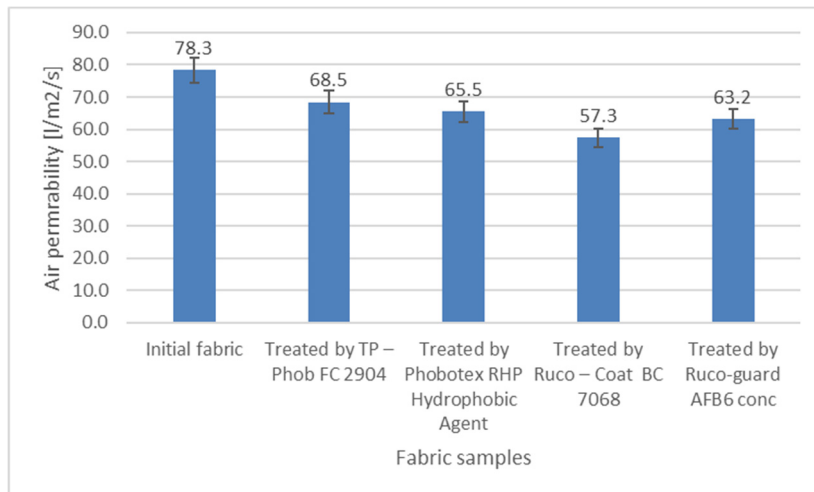




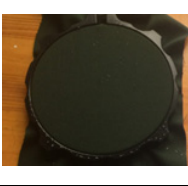



Figure 3. The fabric air permeability before and after treatment by the water resistant.

Table 5. Fabric water repellent capacity using different concentrations of TP-Phob FC 2904 chemical.

Order	Water resistant concentration [g/l]	Fabric water repellent capability [%]	Image
1	0	0	
2	10	80	
3	20	90	
4	30	100	
5	40	100	
6	50	100	

There were nearly no particles observed in the initial fabric surface. The water repellent may not be well reacted with fabric, and they rested in the fabric surface as small particles. By this hypothesis, the fabric sample treated by TP – Phob FC 2904 water resistant was considered the best, and the water-resistant chemical could become the thin membrane in the fibre surface, which improved the best fabric water resistant capability as the above results (table 3 and table 4). Further tests and explanations were carried out in the following sections to demonstrate this supposition.

The fabric thickness (Fig. 2) and the air permeability (Fig. 3) were examined to evaluate the influence of four water resistant types on the fabric properties after water repellent finishing.

The fabric thickness was diminished from an initial 0.54 mm to 0.52 mm, 0.51 mm, and 0.52 mm for the fabric treated by Phobotex RHP Hydrophobic Agent, Ruco – Coat BC 7068, and Ruco-guard AFB6 respectively (Fig. 2). Meanwhile, it rested unchanged while the treatment was carried out by the TP – Phob FC 2904 water resistant. So, the fabric may keep its soft and porosity after finishing by TP – Phob FC 2904 because its volume was almost unchanged. The test of air permeability could verify this hypothesis (Fig. 4).

The initial fabric showed a low level of air permeability with 78.3 l/m²/s which lightly decreased to 68.5 l/m²/s when treated by TP – Phob FC 2904. The values diminished strongly to 65.5 l/m²/s, 57.3 l/m²/s, and 63.5 l/m²/s when fabric was treated by the Phobotex RHP Hydrophobic Agent, Ruco – Coat BC 7068 and Ruco-guard AFB6, respectively. The fabric air

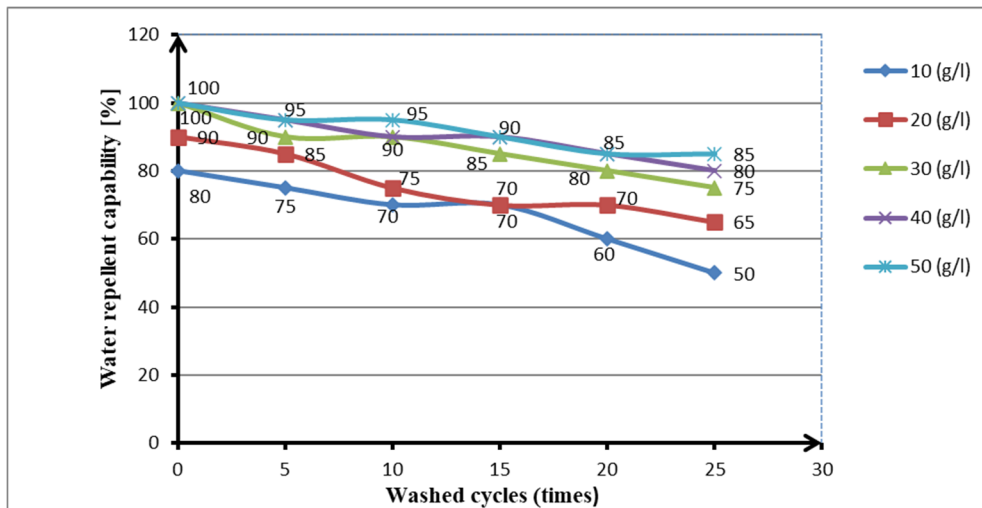


Figure 4. Influence of the water resistant concentration on fabric water repellent capability after washing cycles.

permeability demonstrated that the fabric treated by TP – Phob FC 2904 had the most porosity, so it showed the highest thickness as discussed above. We supposed that the TP – Phob FC 2904 reacted only to the fibre surface but not between fibres and yarns, so it may prevent water absorption throughout the fibres while the fabric thickness and porosity were kept unchanged.

The result showed that the water resistant TP – Phob FC 2904 was the most effective among the four investigated water resistants with the highest water repellent and air permeability as explication above. The order of the water repellent capability of the fabric samples (Table 3 and Table 4) was the same order of quantity of the appeared particles on the fabric surface (Fig. 1), which unified to the order of the fabric thickness (Fig. 2) and fabric air permeability (Fig. 3). So that the water resistant TP – Phob FC 2904 was chosen for our further research.

Influence of the water resistant concentration

Influence of the water resistant concentration on fabric water repellent capability

In this research the fabric samples were treated by the water resistant TP – Phob FC 2904 with 5 concentrations of 10 g/l, 20 g/l, 30 g/l, 40 g/l, and 50 g/l in the same technological conditions: pressure level of 80%, drying at 150 °C for 60 seconds and curing at 190 °C for 60 seconds. The fabric water repellent capability was evaluated by the standard AATCC 22-2017 before and after treatment by the water resistant TP – Phob FC 2904. The results are presented in Table 5.

The results showed that in applying the water resistant TP – Phob FC 2904 at a concentration of 30 [g/l] the fabric water repellent capability reached 100% and the same level was obtained for the concentration of 40 g/l and 50 g/l. The influence of the water resistant concentration on fabric water repellent capability after washed cycles has been carried on in

the following research to find the suitable concentration.

Influence of the water resistant concentration on fabric water repellent capability after washed cycles

The 100% polyester fabric samples were treated by water resistant TP – Phob FC 2904 with 5 different concentrations (10 g/l, 20 g/l, 30 g/l, 40 g/l, and 50 g/l) and by the same technological condition: the pressure of 0.8 kg/cm² (80% pressure level); drying process at 150 °C for 60 seconds; curing at 190 °C during 60 seconds. The fabric samples were washed by the standard AATCC 187 – 2013 with a different number of cycles: 5, 10, 15, 20, and 25 times to evaluate the influence of the water resistant concentration on fabric water repellent capability after applied washing cycles (Fig. 4).

The results showed that the water resistant concentration had influenced the fabric water repellent capability which decreased after washed cycles. The fabric water repellent capability before washing, after 5 washed cycles, and after 25 washed cycles were 80%, 75%, and 50 %; 90%, 80%, and 65%; 100%, 95%, and 75%; 100%, 90%, and 80%; 100 %, 90% and 85% for the water resistant concentration of 10 g/l, 20 g/l, 30 g/l, 40 g/l, 50 g/l respectively. So, the concentration of 50 g/l presented the best duration of fabric water repellent.

Morphology and EDX analyses of the fabric surface

Morphology analyses of the fabric surface before and after treatment by the water resistant

The 100% polyester fabric samples were analyzed by SEM with magnification x1000 (Fig. 5(a) and Fig. 5(c)) and x50 000 (Fig. 5(b) and Fig. 5(d)) to observe the fabric surface change after water resistant treatment. In fact, with the magnification scale x 1000 and x 50 000, only the fibre surface of yarn from fabric could be observed.

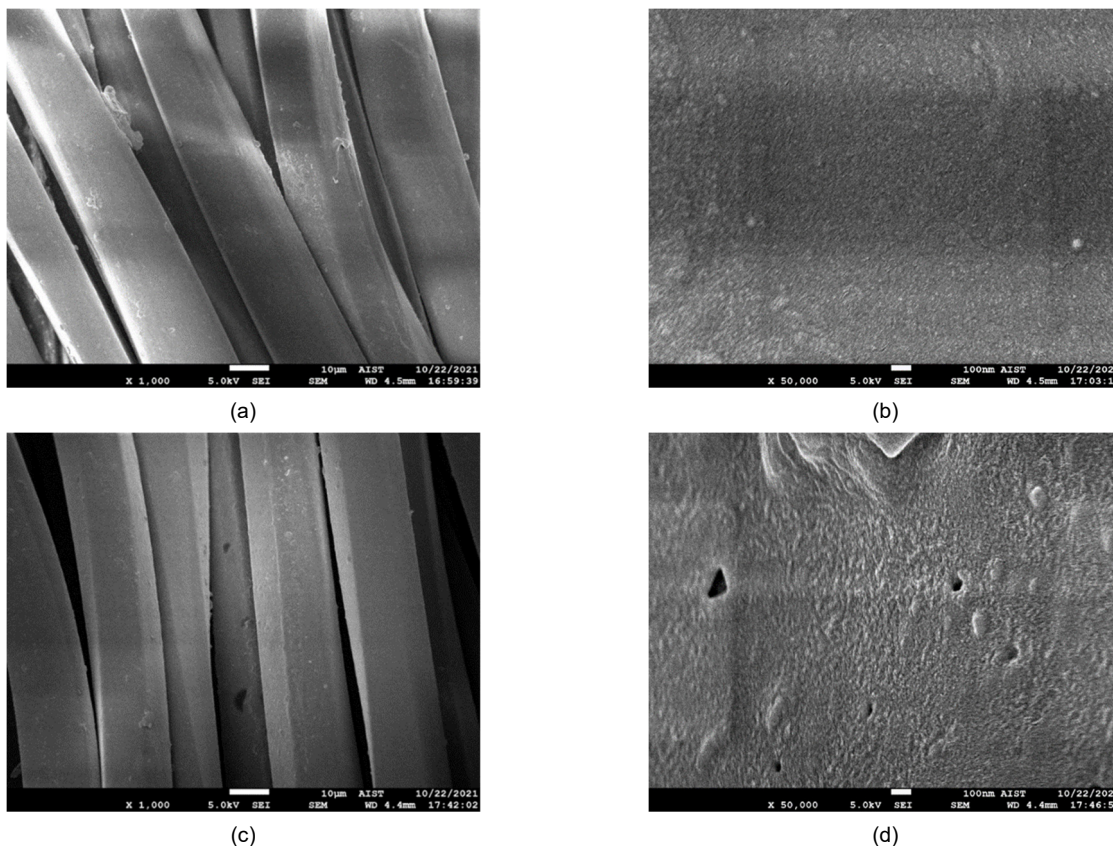


Figure 5. SEM images of: (a,b) the initial fabric and (c,d) TP – Phob FC 2904 water resistant treated fabric.

The results showed that there was no clear difference between the treated fibre surface and the initial fibre in the SEM image with a magnification of 1000, but at the magnification of 50 000, the fibre surface smooth could be observed before treatment and a thin polymer membrane was appeared in the fibre surface after treating. The thin polymer membrane may be the water resistant chemical that helps to improve the fabric water repellent capability as the hypotheses indicated above.

To demonstrate the presentation of TP – Phob FC 2904 water resistant chemical in the fabric surface, the treated sample fabric then was measured the chemical element content by FE-SEM analysis (Fig. 6).

EDX analysis of the fabric surface before and after being treated by the water resistant

EDX is proven as an effective technique for the elemental analysis of a given material. In this case, the EDX spectrum of the initial fabric showed that before water resistant treatment, the fabric sample surface consisted of only carbon and oxygen elements with 69.4 % and 30.6 %, respectively. They are the chemical contents of polyester fabric. The element content fabric became 74.1%, 20.9 %, and 5.0 % for carbon, oxygen, and fluor, respectively after water resistant treatment. The fluor element was the content of the water resistant TP – Phob FC 2904,

and the apparition of this element at 0.35 keV in the treated fabric sample demonstrated the membrane in the fabric was the water resistant TP – Phob FC 2904 as observed by the SEM images. That was the reason which improved the fabric water repellent.

FTIR spectra were obtained for TP-Phob FC 2904 water resistant, cross link P E xan, initial fabric, and the treated fabric to examine the chemical differences between the blank and the treated fabric (Fig. 7). The FTIR spectrum revealed that the intensity of the band frequency at 1504 cm^{-1} which were assigned to the C–H stretching vibration of the skeletal vibration of the aromatic systems in the polyester chains was almost not different for the initial fabric and the treated fabric. The peak at 1715 cm^{-1} showed C=O vibration, at 1409 cm^{-1} of the aromatic ring, 1338 cm^{-1} showed carboxylic ester, and at 1021 cm^{-1} indicated the presence of O=C–O–C or secondary alcohol. The peak at 967 cm^{-1} was attributed to the C=C stretching vibration [15-16].

The assignments of FTIR spectra of untreated fabric and TP-Pho FC 2904 water resistant treated polyester fabric with the same intensity of the typical pick of polyester fabric suggested that there were no clear chemical interactions during fabric padding or the concentration of TP – Phob FC 2904 chemicals was too small to reveal the chemical differences between the blank and the treated fabric.

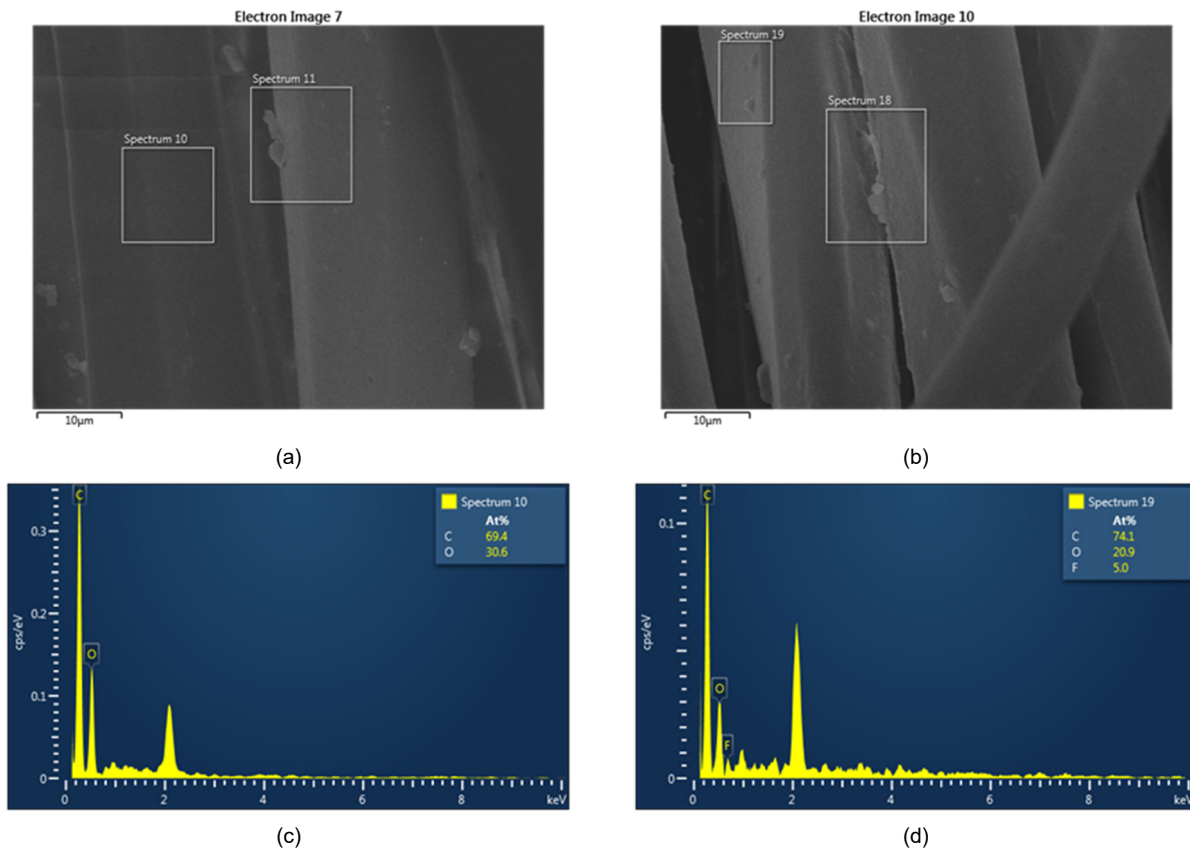


Figure 6. EDX spectra of 100% polyester fabric before (A) and after water resistant treatment (B).

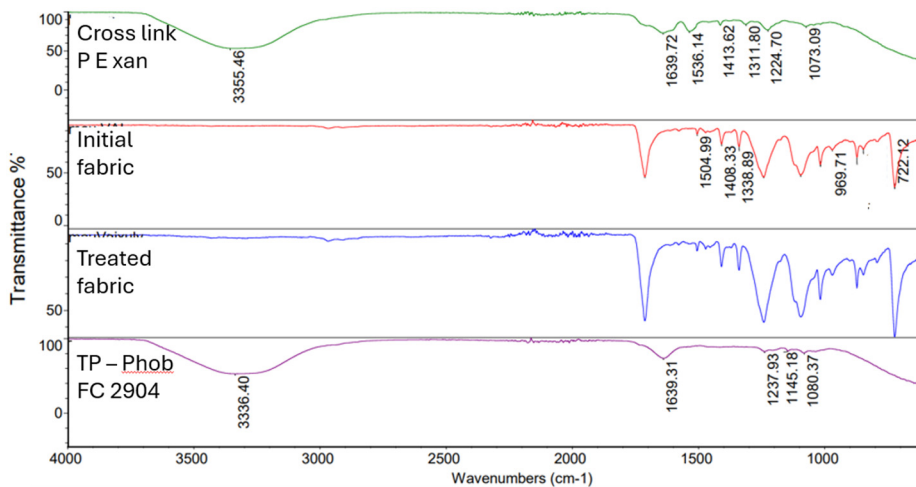


Figure 7. FT-IR spectra of initial chemicals and of the fabric before and after TP- Phob FC 2904 water resistant treatment.

CONCLUSION

The water resistant type influenced the water repellent capability of fabrics and their duration. Among four investigated commercial water resistance, the TP – Phob FC 2904 gave fabric the best water repellent characteristic and the best air permeability with almost unchanged fabric thickness for the 100% polyester woven fabric. The water resistant TP – Phob FC 2904 concentration of 50 g/l was the most efficacy with 85 % water repellent capability after 25 washed cycles. The SEM image showed the membrane in the surface fabric after

water resistant treatment and EDX spectra demonstrated the apparition of flour element (5% in w/w proportion) which came from water resistant TP – Phob FC 2904 in the treated fabric. So, we could conclude that the water resistant TP – Phob FC 2904 was presented in the fabric surface, even in the fibre surface and it improved the efficacy of the water repellent characteristic for the 100% polyester woven fabric in the study.

Acknowledgement: The authors are thankful to the Ministry of Science and Technology (Vietnam) for funding this research by the project number ĐTĐLCN.48/21.

REFERENCES

1. Nazmul K., Shaila A., Lloyd K., et al.: Sustainable Personal Protective Clothing for Healthcare Applications: A Review. *ACS Nano*, 2020, 14, pp. 12313–12340. <https://dx.doi.org/10.1021/acsnano.0c05537>
2. Ejajul H., Tran P., Unique J., et al.: Antimicrobial Coatings for Medical Textiles via Reactive Organo-Selenium Compounds. *Molecules*, 2023, 28, pp. 6381. <https://doi.org/10.3390/molecules28176381>
3. Mukhopadhyay A., Midha V.K.: Waterproof breathable fabrics. *Handbook of Technical Textiles. Volume 2: Technical Textile Applications*, 2016, pp. 27-55.
4. Carmen L., Lumina C., Dorin I., et al.: Introduction to waterproof and water repellent textiles. *Waterproof and Water Repellent Textiles and Clothing*, 2018, pp. 3-24. <http://doi.org/10.1016/B978-0-08-101212-3.00001-0>
5. Weixia Z., Jing Z., Xianfeng W., et al.: Facile fabrication of fluorine-free breathable poly(methylhydrosiloxane)/polyurethane fibrous membranes with enhanced water-resistant capability. *Journal of Colloid and Interface Science*, Volume 556, 2019, pp. 541-548. <https://doi.org/10.1016/j.jcis.2019.08.092>
6. Indrajit C. B., Javed S.: Development of Sustainable Citric Acid-Based Polyol to Synthesise Waterborne Polyurethane for Antibacterial, Breathable Waterproof Coating of Cotton Fabric, *Industrial & Engineering Chemistry Research*, 2019, pp. 1-31. <https://doi.org/10.1021/acs.iecr.9b05195>
7. Guangming P., Xinyan X., Zhihao Y.: Fabrication of stable superhydrophobic coating on fabric with mechanical durability, UV resistance and high oil-water separation efficiency. *Surface & Coatings Technology*, Vol. 360, 2019, pp. 318-328. <https://doi.org/10.1016/j.surfcoat.2018.12.094>
8. Su Y., Li R., Song G., Li J.: Application of waterproof breathable fabric in thermal protective clothing exposed to hot water and steam, *Materials Science and Engineering*, 254, 2017. <http://doi:10.1088/1757-899X/254/4/042027>
9. P De., Sankhe M. D., Chaudhari S. S., Mathur M. R.: UV-resist, Water-repellent Breathable Fabric as Protective Textiles, *Journal of Industrial Textiles*, 34 (4), April 2005, pp. 209-222. <https://doi.org/10.1177/1528083705051453>
10. Chinta S. K., Darbastwar S.: Studies in Waterproof Breathable Textiles. *International Journal of Recent Development in Engineering and Technology*, ISSN 2347-6435 (Online), 3 (2), 2014, pp. 16-20.
11. Gorjanc D.Š., Dimitrovski K., Bizjak, M.: Thermal and water vapor resistance of the elastic and conventional cotton fabrics, *Textile Research Journal*, 82(14), 2012, pp. 1498–1506. <https://doi.org/10.1177/0040517512445337>
12. Gulay O.: Performance Evaluation of Water Repellent Finishes on Woven Fabric Properties. *Textile Research Journal* Vol 77(4), 2007, pp. 265–270. <https://doi.org/10.1177/0040517507080619>
13. Alain M. J., Ronggang C., Romain V., et al.: How roughness controls the water repellency of woven fabrics. *Materials & Design*. Volume 187, 2020, pp. 1-17. <https://doi.org/10.1016/j.matdes.2019.108389>
14. Beysim G., Ayten N. Y. Y., Seda Ü., Ayşe Ç. B.: Improving the Water Repellency of Polyester, *Tekstil ve Konfeksiyon*, 33 (2), 2023, pp. 161-168. <https://doi.org/10.32710/tekstilvekonfeksiyon.1065250>
15. Ingrida P., Donatas P.: Effect of Abrasion on the Air Permeability & Mass Loss of Breathable-Coated Fabrics, *FIBRES & TEXTILES in Eastern Europe*, 2009, 17 (73), pp. 50-54.
16. Mazeyar P., Izadyar E.: Influence of atmospheric-air plasma on the coating of a nonionic lubricating agent on polyester fiber, *Radiation Effects & Defects in Solids*, 166 (6), June 2011, pp 408–416. <http://dx.doi.org/10.1080/10420150.2011.553230>
17. <https://www.scribd.com/document/541974746/BC7068-E-TDS-converted-pigment>
18. <https://truongphat-jsc.com/>
19. <https://www.oqd.com.tw/en/product/ruco-guard-afb6-conc/>
20. <https://www.huntsman.com/news/special-announcements/detail/9564/huntsman-ramps-up-production-of-products-required-for>
21. <https://3.imimg.com/data3/OH/AA/MY-3907742/phobol-xan.pdf>

ANALYSIS OF AIRFLOW RESISTIVITY AND ACOUSTIC ABSORPTION OF FIBRE-REINFORCED PLASTIC COMPOSITES MADE OF POLYLACTIC ACID AND NATURAL FIBRES

STEHLE, FRANZISKA^{1*}; GILLNER, CHRISTIANE²; DILBA, BORIS²; KEUCHEL, SÖREN² AND HERRMANN, AXEL S.¹

¹ Faserinstitut Bremen e.V., FIBRE, Bremen, Germany

² Novicos GmbH, Hamburg-Harburg, Germany

ABSTRACT

This study compares the airflow resistivity and acoustic properties of fibre-reinforced plastic composites (NFRP) with different mixing ratios of polylactic acid (PLA) and the natural fibres flax and cotton for the application in construction as lightweight structures, car door linings or seat pans. The composites are made from the binder fibre PLA, the bast fibre flax and two different kinds of cotton. Nonwovens are consolidated with a thermoforming process to manufacture the NFRP. The addition of cotton improves the absorption by increasing the number of air pockets (pores) and reducing their shape due to the fineness of the cotton. The airflow resistivity of samples with different mixing ratios were analysed and compared. The airflow resistivity is modelled with different calculation models that use distinct material parameters and the transferability is assessed. Further, the absorption coefficient is analysed and compared to the airflow resistivity. The study shows that there is a dependency of the two parameters.

KEYWORDS

Natural fibres; PLA; Fibre-reinforced composites; Thermoforming; Airflow resistivity; Acoustic

INTRODUCTION

Fibre-reinforced plastics made from degradable and renewable raw materials are gaining popularity as sustainable alternatives to materials derived from petrochemicals. Natural fibres contain better hydrothermal properties than petrochemical-based materials [1]. Furthermore, materials derived from petroleum are susceptible to price fluctuations of crude oil, are not renewable, and are predominantly non-biodegradable. On top of that fossil-based products are finite, which creates a need for alternatives [2, 3]. The production of petrochemical materials, as well as their recycling, requires a great deal of energy.

The construction industry is a major consumer of raw materials with 50% of the total consumption, while generating around 60% of the total waste. Only about 10% of the total amount of construction materials needed annually can be recovered [4]. The life-cycle impacts of natural fibres are significantly lower compared to synthetic materials [5]. Acoustic materials made from cellulose and other natural fibres have less embodied energy than polystyrene [6]. The

primary energy demand of cellulose fibres is approximately 90% less than of polyurethane rigid foam and 60% less than of rock wool [7].

This highlights the urgent need for a structural shift from petroleum-based products to a bio-based industry. The demand for products made from renewable raw materials is steadily rising in order to create more independence from fossil raw materials.

This study focuses on the development of industrially compostable composites based on renewable resources for the application in architecture as lightweight structures, car door linings or seat pans. The fibres utilized in this research are made of renewable resources: the bioplastic polylactic acid is produced from lactic acid through a fermentation of sugar or starch [8]. The use of renewable raw materials in the form of biopolymers offers the possibility to reduce dependence on petroleum and to use renewable resources instead [9–11]. Another advantage of the bioplastic is the processing on commercially available machinery [12]. Polylactide can be composted in industrial composting plants under the influence of defined moisture and temperature. This produces mainly carbon dioxide

* Corresponding author: Stehle F., e-mail: Stehle@Faserinstitut.de

Received November 30, 2023; accepted June 3, 2024

and water, which can be returned to the natural cycle [13]. Cotton and flax as natural fibres are also biodegradable. Thus, the composite can be easily composted on an industrial scale without the need of prior separation. Combining natural fibres and PLA has many advantages such as an improved tensile and flexural strength, elastic modulus and heat distortion [14].

Porous absorbers reduce the sound energy by viscous effects and thermal losses. Throughout the sound absorption, the energy of the sound migrates through the component and viscous effects cause the sound to be dissipated into heat, which is triggered by friction, impulse losses and temperature fluctuations. The developed absorber improves the acoustic by effectively absorbing the sound within the component. Finer fibres improve the viscous losses due to air vibration, since they can shift easier when air vibration occurs [15].

Absorbers partially reflect and absorb sound waves. When sound waves impinge on a surface and are not completely absorbed or reflected, transmission occurs [16]. This principle is shown in the figure 1.

A parameter to classify the acoustic absorbency is the absorption coefficient α . This value is defined by the ratio of the absorbed and the occurred sound energy. When $\alpha = 0$ no sound energy is absorbed, the highest possible number 1 means, that all the energy is absorbed [18].

This active principle is enhanced alongside the thickness and fibre orientation by using an increased fineness of the fibres, which increases the specific surface area, whereby cotton with its unique properties contributes to significant improvements: Compared to other natural fibres cotton is finer, making it an ideal choice for achieving an overall weight reduction in the material [19]. The finer fibres also influence the morphology of the material. The application of fibres with a smaller diameter result in smaller pores since a higher amount of fibres is necessary to form the material with the same weight, but increases the number of the pores and the specific surface area while the volume density remains identical. This results in a higher friction of air molecules [20]. Both physical characteristics improve the sound absorption [21–25]. The reason for this improved absorbency is the possibility of the sound waves entering the material, which reduces the reflection on the surface of the material [15]. The sound waves that enter the material trigger a vibration of the fibres and pores and subsequently an energy conversion into heat [18]. The combination of bast fibres and cotton combines the fibre parameters.

This study describes and investigates the representability of the airflow resistivity of NFRP with models for fibre materials found in the literature. The airflow resistivity can be calculated using parameters such as the fibre diameter and density. Furthermore,

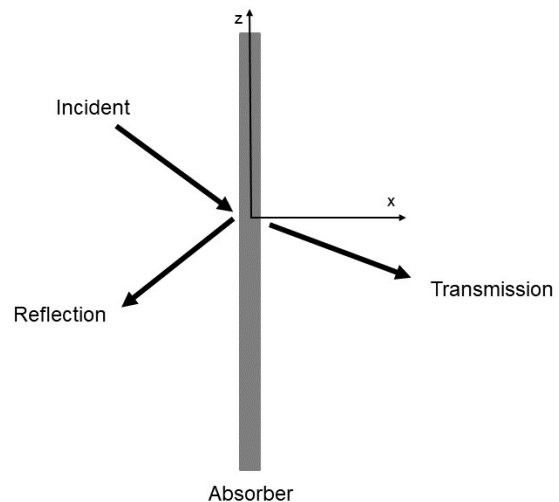


Figure 1. Functional principle of an absorber adapted from [15, 17].

the airflow resistivity and the absorption coefficient of the material are analysed. The relation of these parameters is discussed.

MATERIALS AND METHODS

Manufacturing of the fibre-reinforced composites

Fibres

The fibres utilized in this study consist of the matrix fibre polylactic acid (PLA) as the matrix fibre, along with bast fibres (LI) and cotton (CO). Specifically, the PLA fibres used are the TREVIRA® 400 6.7 dtex shiny rd 60 mm fibres, which possess optimal characteristics for the nonwoven production due to its crimping. The density measures at 1250 kg/m³. Flax fibres were sourced as bast fibres. The fibre diameters were measured with the optical measuring system FibreShape resulting in a mean diameter of 86.16 µm. The length of the fibres ranges from about 10 – 100 mm with a density of 1400 kg/m³ [26]. Additionally, two different types of cotton fibres were employed: long staple fibres from Giza and short staple fibres from Mali. These fibres vary in terms of fineness and length, allowing the evaluation of the distinct influences of each fibre type. The Micronaire which provides information about the maturity and the fibre fineness amounts to 4.14 (Mali) and 4.54 (Giza), the density to 1510 kg/m³ as described in [26]. The diameters, also measured with the FibreShape are on average 12.44 µm (Mali) and 12.30 µm (Giza). The Upper Half Mean Length (UHML) of the short staple fibre was measured at 29.54 mm, while the long staple fibre length was 32.46 mm.

Nonwovens

The nonwovens were manufactured by using a carding machine from TECHNOplants s.r.l. The fibres were opened and blended to ensure a homogenous mixture. Subsequently the carding machine

processed the fibres into webs by individualizing and parallelising the fibres. In the next step the webs were cross-laid and needle punched to form a nonwoven. The resulting nonwoven fabrics had a basis weight of 200 g/m² and a fabric width of 30 cm.

Nonwovens with various mixing ratios were manufactured. Different amounts of matrix fibres (25, 50, 75%) were used as well as assorted amounts of natural fibres. Test specimens without any cotton or bast fibre content were also produced. Short- and long-staple fibre cotton was also applied for the samples. The nonwoven layers, each weighing 200 g/m², were stacked to form a laminate structure prior to the thermoforming process.

Thermoforming

The nonwovens were layered into laminate structures prior to consolidation to increase the total surface weight. Variations of nonwovens with different blending ratios were also implemented. The nonwovens were layered with a 0°/90° layer structure (MD/CD) and then pressed. Different laminate structures were produced. These consisted of four layers of 200 g/m² each with a total basis weight of 800 g/m². The properties of the composites are depicted in Table 1.

The NFRP were produced by consolidating the nonwovens using a two-stage thermoforming process. Two tools were utilised for this purpose: One tool heated by a press melted the fibres under pre-pressure. Subsequently the material was transferred to another tool that consolidated the material by cooling the fibres and thus hardening them. Both tools consisted of a top and bottom plate that are fixed in a press.

The pre-pressure applied to the material by the heated tool was 50 bar. The materials were pressed at 195°C for 10 seconds and then transferred to an unheated press in which the material cooled and the PLA hardens. Thus, the matrix fibre PLA, formed a matrix around the natural fibres, which served as the reinforcing fibres, and solidified the composite, thereby forming a NFRP.

Analysing methods

Scanning electrode microscope (SEM)

The quality of the inner material was examined microscopically in order to be able to optimise the process quality. The degree of melting and the flow behaviour of the melted thermoplastic PLA were determined.

Table 1. Parameters of the composites.

Materials	Mixing ratio				Consolidation parameters		
	PLA	Flax	Cotton (short staple)	Cotton (long staple)	Temperature [°C]	Pressure [bar]	Time [s]
1	25	75	-	-	195	50	10
2	25	37.5	-	37.5			
3	25	-	-	75			
4	50	50	-	-			
5	50	25	25	-			
6	50	25	-	25			
7	50	-	50	-			
8	50	-	-	50			
9	75	25	-	-			
10	75	12.5	-	12.5			
11	75	-	-	25			

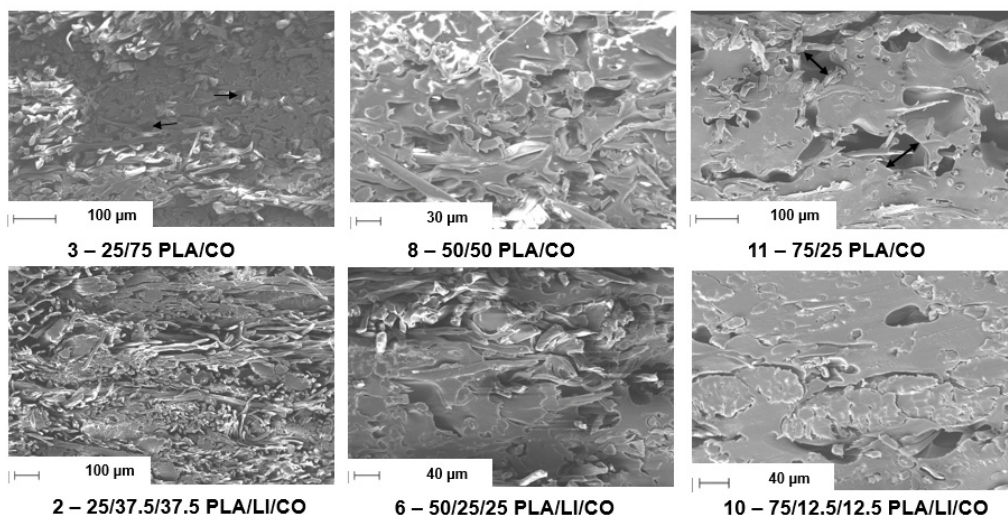


Figure 2. SEM images of the cross-section.

Table 2. Bulk and fibre density of the samples 1-11.

Samples	1	2	3	4	5	6	7	8	9	10	11
ρ_w [kg/m ³]	664	591	520	717	732	770	650	745	902	891	875
ρ_f [kg/m ³]	1363	1404	1445	1325	1353	1353	1380	1380	1288	1301	1315

Table 3. Calculated porosity of the samples 1-11.

1	2	3	4	5	6	7	8	9	10	11
0.51	0.58	0.64	0.46	0.45	0.52	0.52	0.46	0.35	0.31	0.33

The homogeneity and impregnation of the composite was also tested. Furthermore, the connection of the individual layers of the laminate structure was investigated in order to detect possible air pockets or defects.

Both the cross-section of the materials and the surface were examined.

Figure 2 shows a selection of microscopic images of the cross-section. On the top row the samples 2, 8 and 11 show the different proportion of the PLA combined with cotton fibres, the bottom pictures of the samples 2, 6 and 10 contain cotton fibres as well as flax fibres.

The images show that the PLA fibres are homogeneously fused. No accumulation of matrix can be seen inside the material. The fibres are evenly distributed. The fibres as well as the pores (dark spots) contained in the material are homogeneously distributed in the composite. Due to the layer structure of MD/CD, the directions of the fibres are recognisable, but the connection of the layers appears seamless.

In the cross-section of the material, the SEM images show that the pores are smaller and more frequent in the material with a higher natural fibre content. When the upper left image of sample three is compared to the upper right image of sample 11 with a high amount of PLA, the pores are significantly larger (see marks). This has a positive effect on the acoustic absorption.

The bulk density of the material ρ_w , which is calculated by the mass [kg] and the volume [m³] of the samples is pictured in the following table. The fibre density ρ_f is derived from the density of the fibres according to the amount of fibre in each sample as pictured in Table 1. For example, the fibre density of sample 1 is 1363 kg/m³ since it contains 25% PLA and 75% flax fibres. Samples with 50% cotton and 50% flax fibres as the natural fibre component include the density of flax as well as of cotton in equal parts and the respective amount of PLA. Those values are also listed in Table 2.

The porosity ϕ of the material can be derived from the bulk density of the material ρ_w of the samples and the density of the fibres ρ_f as seen in (1) [27].

$$\phi = 1 - \frac{\rho_w}{\rho_f} \tag{1}$$

The results from the calculation for each of the samples are depicted in Table 3.

The porosity of the samples rises with a decreasing quantity of the matrix. The specimen 1-3 with an amount of 25% PLA have the highest porosity compared with their respective samples. The natural fibre content also has an influence on the porosity, as sample with more cotton than flax fibres exhibit a higher porosity. The highest porosity according to the PLA amount is seen in the materials 3, 7, 8 and 11 containing exclusively cotton fibres.

Figure 3 shows the surface of the test specimen 2, 8 and 11 with different amounts of PLA. The matrix and fibre distribution is mostly homogenous, a small collection of PLA is visible on the surface of the sample 11 with a higher PLA content. This can be counteracted by reducing the consolidation time. On the surface of the test specimens, it can be seen clearly that the PLA matrix closes more of the surface with a higher PLA fibre content and therefore reduces the amount of the pores, thus increasing the airflow resistivity. The lower the PLA amount, the more fibres are visible on the surface.

Computed Tomography (CT)

The pores were examined by computed tomography to evaluate the acoustic properties. The CT images were taken with the GE Phoenix V by Baker Hughes system. The measurement time was 20 seconds with 1801 projections.

The sectional image and the volume are shown in Figure 4.

The areas shown in black are hollow spaces in the material. Thus, it is clear that specimen 4 with a mixing ratio of 50/50 PLA/LI has fewer but larger pores than test specimen number 6 with 25% cotton. This observation is also consistent with the analysis of the SEM images. The surface remains open, which preserves the air permeability.

Airflow resistivity

The airflow resistivity was tested according to DIN EN ISO 9053-2:2021-02 Acoustics - Determination of airflow resistance - Part 2: Air exchange flow method [28], with the test device Nor1517A by the Norsonic-

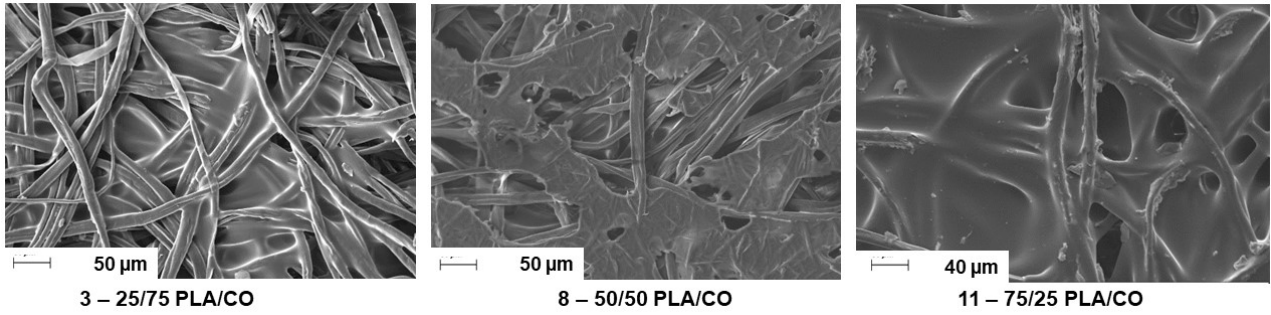


Figure 3. SEM images of the surface of the samples 2, 8 and 11.

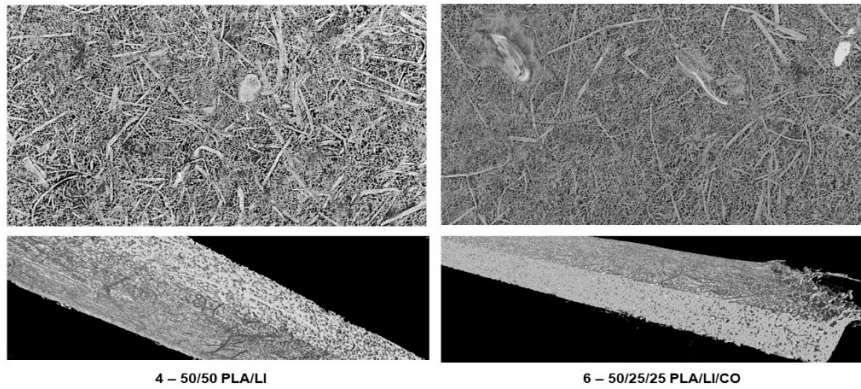


Figure 4. CT images of the sectional view (top) and the volume view (bottom) of the samples 4 and 6.

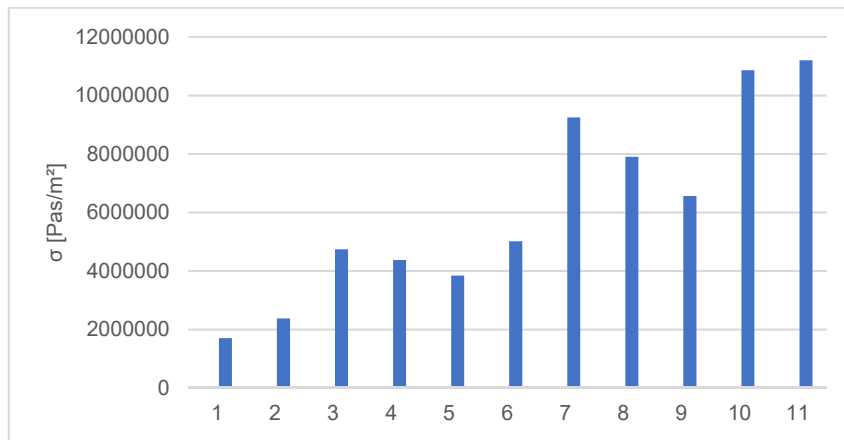


Figure 5. Airflow resistivity of the specimen 1 -11.

Tippkemper GmbH. An air alternating current with a frequency of 2 Hz is generated by means of a pressure vessel and a piston. The alternating current is detected by a microphone. The specific flow resistance R_s [Pas/m] is measured, whereby the airflow resistivity σ [Pas/m²] is calculated by using the thickness d [m] with

$$\sigma = R_s/d \quad (2)$$

The measurements of the specimen are pictured in Figure 5.

The airflow resistivity increases significantly with an increasing proportion of PLA. Test specimens 1-3 with a PLA content of 25% have a lower airflow resistivity according to the relating natural fibre

amount than test specimens 4-5 with a 50% PLA content and test specimens 9-11 with a PLA content of 75%. This is due to the fact that the matrix fibre wraps around the natural fibres as a result of melting during the thermoforming process and closes the pores in the material and on the surface. This behaviour is also visible in the SEM images in Figure 2 and Figure 3.

Materials with cotton have a higher airflow resistivity than those with flax fibres. When compared, specimens 1, 4 and 9 with flax fibres and specimens 3, 8 and 11 with cotton, it can be seen that the airflow resistivity is significantly higher. The properties of cotton, such as the fineness of the fibre and the

increased crimping of this fibre, have a positive effect on increasing the airflow resistivity.

Test specimens 5 and 7 with short-staple-fibre cotton and 6 and 8 with long-staple-fibre cotton show that the use of different breeds of cotton results in difference of the airflow resistivity. This is due to the properties of the fibres such as the fibre diameter, the wax content or the maturity.

Acoustic properties

The absorption capacity was examined using an impedance tube according to DIN EN ISO 10534-2 [29]. The absorption coefficient between the frequencies 1000 and 6000 Hz was tested. The sample is clamped in a Kundt's tube without any compression in front of a reverberant wall. White noise in the frequency range mentioned above is excited via a loudspeaker. The acoustic wave is partly reflected by the sample. Two microphones measure the sound pressure, which is a superimposition of the incoming and reflected waves. The absorption coefficient α is calculated by the surface impedance Z_s and the reflection factor r as followed [30]:

$$\alpha = 1 - |r|^2 \text{ and } r = \frac{1 + \widetilde{Z}_s}{1 - \widetilde{Z}_s} \quad (3)$$

The acoustic properties were determined based on the absorption coefficient α . The Figure 6 pictures the samples 1 – 11.

The absorption coefficient decreases with increasing PLA content, which is due to the surface properties of the specimens with a high matrix content. The higher amount of the thermoplastic matrix reduces the number of pores on the inside and on the surface of the material which increases the reflection of the sound waves. The air pockets inside the samples that diffuse the sound waves are reduced significantly as well. This is seen in samples 2, 6 and 10 with the PLA amounts of 25, 50 and 75% and an even amount of flax and cotton fibres. When comparing the samples 1, 4 and 9 with solely flax fibres as the natural fibre component a similar effect is visible.

The fibres of the samples 9, 10 and 11 that contain 75% PLA are well integrated into the thermoplastic matrix, which leads to a low absorption coefficient, in view of the fact that only a small amount of the sound wave is able to enter into the material and less pores can be found in the material.

Furthermore, the results show, that the material with flax and 25% PLA has a lower absorption compared to the samples which include cotton fibres. The absorption coefficient rises with samples number 2 and 3. The reduced and larger pores of the material with flax due to the larger fibre diameter reduces the sound absorption.

Samples 4, 5, 6, 7 and 8 exhibit a large scattering of the measurements. Nonetheless a rise of the absorption is visible with an increasing amount of cotton fibres.

Concisely materials with a higher amount of cotton fibres exhibit better acoustic properties than those with flax fibres because of the smaller fibre diameter that results in more and smaller pores in the material. The absorption coefficient rises with a decreasing amount of PLA, since the absorber contains more pores inside and on the surface of the material which reduces the reflection.

The relation of the properties can be described as:

$$\alpha_{CO} > \alpha_{CO+LI} > \alpha_{LI} \quad (4)$$

Calculation models of the airflow resistivity

The airflow resistivity σ is an indicator of the acoustic properties of a material. By determining the airflow resistivity, the absorption coefficient α can be modelled to estimate the acoustic absorption. Equally, it is possible to model the airflow resistivity of different materials by incorporating different fibre properties such as the density and fibre diameter. Further parameters needed are the dynamic viscosity of air η (0.82·10⁻⁶ Pas), the massivity μ which can be derived from the following equation [31].

$$\mu = 1 - \phi \quad (5)$$

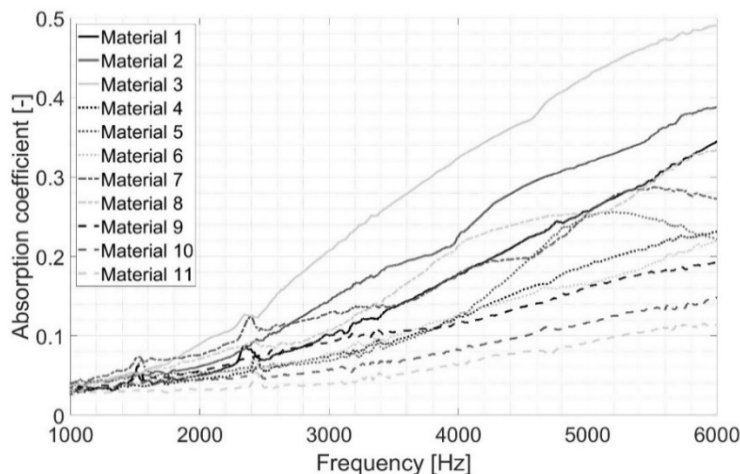


Figure 6. Absorption coefficient of the specimen 1 -11.

There are numerous papers that investigate the correlation of the fibre parameters and the airflow resistivity.

This study presents selected models to calculate the airflow resistivity of fibres and assesses the transferability of these models to NFRPs. The fibre parameters applied for the calculation of the models are listed in chapter 2.1.1.

Various models for calculating the airflow resistivity σ of fibre materials are described in [31] using empirical data from Sullivan. The model (6), here called Mechel Sullivan 1, considers fibre materials for parallel fibre orientation, whereas different fibre radii are being regarded. For this purpose, the parameters fibre radius a [m] as well as the bulk density ρ_w and the density of the fibres ρ_f are used. The airflow resistivity can be calculated from the dynamic viscosity of the air η , the massivity μ determined by the porosity of the material as seen in equation (6).

$$\sigma = \begin{cases} 10.56 \frac{\eta \mu^{1.531}}{a^2 (1-\mu)^3}; a \approx 6 - 10 [\mu\text{m}] \\ 6.8 \frac{\eta \mu^{1.296}}{a^2 (1-\mu)^3}; a \approx 20 - 30 [\mu\text{m}] \end{cases} \quad (6)$$

(6)

For the application to the specimens produced in this study, the model for fibre radii of 6-10 μm is used for the cotton content, the flax fibre content is applied to the model with fibre diameters of 20-30 μm . An interpolation is then carried out according to the fibre proportions in order to obtain the result of the " σ " value.

Another model by Mechel Sullivan (7) (Mechel Sullivan 2) considers fibre materials with mono-valued fibre radii and random fibre orientation. This model is also not designed for NFRP. The input parameters are the fibre radius a as well as the density ρ_w and the density of the fibres ρ_f of the material [31].

$$\sigma = 4 \frac{\eta}{a^2} \left[0.55 \frac{\mu^{4/3}}{(1-\mu)} + \sqrt{2} \frac{\mu^2}{(1-\mu)^3} \right] \quad (7)$$

The Ballagh model [21] is applied to the parameters and compared with the test results. The model is shown under (8). In addition to the density of the material ρ_w , Ballagh uses the fibre radius to calculate σ .

$$\sigma = 490 \rho_w^{1.404} / 10^6 a^2 \quad (8)$$

Bies and Hansen [32, 25] work with glass fibres to model the airflow resistivity through porous media by applying the parameters density and the fibre radii. The equation of the model can be seen in (9).

$$\sigma = 27.3 \mu^{1.53} (\eta / 4a^2) \quad (9)$$

Manning and Panneton present different models for the prediction of the airflow resistivity from the density and fibre diameter D [m] in their work [33]. The model is adjusted to mechanically, resin and thermally bonded fibres. (10) shows the equation for the

thermally bonded fibres as this consolidation method is closest to the method applied in this paper.

$$\sigma = \frac{1.94 \cdot 10^{-8} \rho_w^{1.516}}{D^2} \quad (10)$$

A model adjusted to multi component polyester fibres is presented in [34]. Yang et al. use three different kind of polyester fibres (regular, hollow and bi-component fibres).

$$\sigma = \frac{1.3395 \cdot 10^{-8} \rho_w^{1.565}}{D^2} \quad (11)$$

The approach of a capillary channel theory to predict the airflow resistivity is used by Pelegrinis et al. [35] The porous media is portrayed as a conduit flow between parallel cylindrical capillary tubes. This model adapts the Kozney-Carman model [36] for polyester fibres by an equation (12) that includes fibre diameter and the density of the material, which is used to calculate the massivity as seen in equation and (5).

$$\sigma = \frac{180 \eta \mu^2}{D^2} \quad (12)$$

MODELLING OF THE AIRFLOW RESISTIVITY

The calculation models presented in chapter 2.3 were applied to the manufactured test specimens and are shown in the graph below. A comparison was made with the test results of the front and back of the specimen. These are also shown in Figure 7.

The results of the models follow a similar trend compared to the airflow resistivity test results. However, the test results achieve higher results than the modelled values, which shows that the experimental findings cannot be clearly mapped with the models used. This means that there is a need for an adaptation or model for NFRPs.

CONCLUSIONS

NFRP are often made with technical flax. It has been demonstrated that replacing or supplementing the flax fibre material with cotton fibres improves the acoustic absorption of the materials. Increasing the amount of natural fibres as well as the quantity of the cotton fibres has a positive effect as well.

It is evident that the absorption coefficient and the airflow resistivity increase by similar proportions with an increasing cotton content (samples 1-3). The airflow resistivity of the sample 2 is 40% greater than of sample 1, and sample 3 is nearly thrice as high. The absorption coefficient increases at 4000 Hz approx. 40% when comparing samples 1 and 2. Sample 3 is almost twice as high as sample 1. This confirms the correlation of the two parameters. Samples with a high amount of PLA increase the airflow resistivity for the reason that the PLA decreases the permeability of the samples. This effect reduces the absorption coefficient.

The airflow resistivity was mapped with different models based on the density and the fibre radius. The results show that the models for fibre materials, while depicting

a trend, cannot fully represent the airflow resistivity of NFRP.

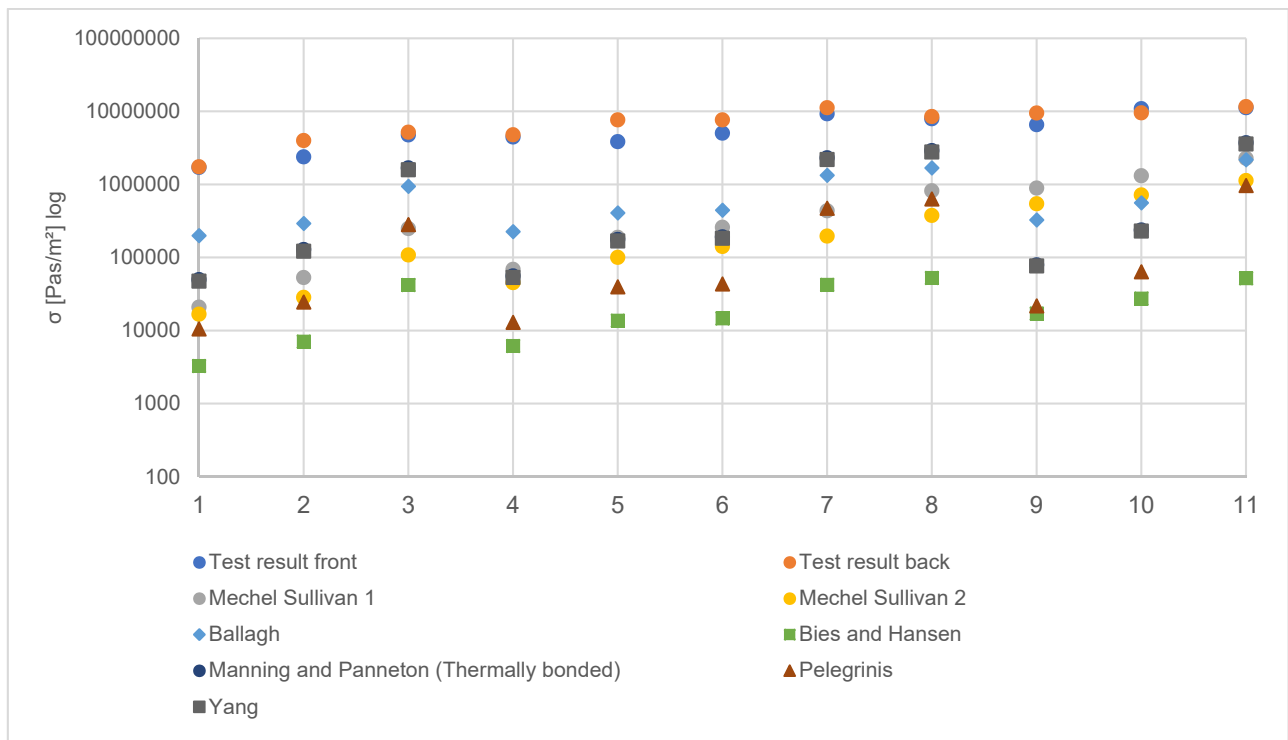


Figure 7. Test results and results of the modelling of the airflow resistivity.

Acknowledgement: The authors gratefully acknowledge the funding by the Federal Ministry of Food and Agriculture under the grant number 2220NR256A. The responsibility for the content of this publication lies with the authors. The authors declare there is no conflict of interest.



REFERENCES

- Berger W., Faulstich H. Fischer P., et al.: Textile Faserstoffe. Springer Berlin Heidelberg, Berlin, Heidelberg, 1993.
- Hottle T. A., Bilec M. M., Landis A. E.: Sustainability assessments of bio-based polymers. In: Polymer Degradation and Stability, 98(9), 2013, pp. 1898-1907. <https://doi.org/10.1016/j.polymdegradstab.2013.06.016>
- Trivedi A. K., Gupta M. K., Singh H.: PLA based biocomposites for sustainable products: A review. In: Advanced Industrial and Engineering Polymer Research, 6(4),2023, pp. 382-395. <https://doi.org/10.1016/j.aiepr.2023.02.002>
- Die Zukunft der Bauforschung, 2011, online: <https://www.detail.de/artikel/die-zukunft-der-bauforschung-4517/> [cit. 18.09.2023],
- Ardente F., Beccali M., Cellura M., et al.: Building energy performance: A LCA case study of kenaf-fibres insulation board. In: Energy and Buildings, 40(1), 2008, pp. 1-10. <https://doi.org/10.1016/j.enbuild.2006.12.009>
- Asdrubali F.: The role of Life Cycle Assessment (LCA) in the design of sustainable buildings: thermal and sound insulating materials, EURONOISE, 2009, Edinburgh, Scotland.
- Zabalza Bribián I., Valero Capilla A., Aranda Usón A.: Life cycle assessment of building materials: Comparative analysis of energy and environmental impacts and evaluation of the eco-efficiency improvement potential. In: Building and Environment, 46(5),2011, pp. 1133-1140. <https://doi.org/10.1016/j.buildenv.2010.12.002>
- Kayser O., Aversch N.: Technische Biochemie. Springer Fachmedien Wiesbaden, Wiesbaden, 2015.
- Bauer M., Friede P., Uhlig C.: Sandwiches with Nap Cores. In: Kunststoffe International, 2006, pp. 95-97.
- Gerber N., Dreyer C., Bauer M.: Noppenwabe als Kernmaterial - Kontinuierlich herstellbares Kernmaterial zur Funktionsintegration in Sandwichbauteilen. In: Konstruktion 3, 2015, pp. 14-16.
- Ha G. X., Bernaschek A., Zehn M. W.: Experimentally examining the mechanical behaviour of nap-core sandwich material – A novel type of structural composite. In: Journal of Reinforced Plastics and Composites, 38(8), 2019, pp. 369-378. <https://doi.org/10.1177/0731684418820437>
- Fachagentur Nachwachsende Rohstoffe e. V. (Hrsg.): Biokunststoffe – Pflanzen, Rohstoffe, Produkte, 2020.
- Karosseriebautage Hamburg, Proceedings, 2014. <http://dx.doi.org/10.1007/978-3-658-05980-4>
- Wu Y., Gao X., Wu J., et al.: Biodegradable Polylactic Acid and Its Composites: Characteristics, Processing, and Sustainable Applications in Sports. In: Polymers, 15(14), 2023. <https://doi.org/10.3390/polym15143096>
- Cox T. J., D'Antonio P.: Acoustic absorbers and diffusers – Theory, design, and application. Taylor & Francis, London, 2009.
- Einführung in die Akustik, 2023, online: <https://bauakustik-fachkreis.com/einfuehrung-in-die-akustik/> [cit. 18.09.2023].
- Möser M.: Technische Akustik. Springer Berlin Heidelberg, Berlin, Heidelberg, 2015.
- Crocker M. J. (ed.): Handbook of noise and vibration control. John Wiley, Hoboken N. J., 2007.
- Sciencetrans (Hrsg.): Proceedings of the 6th International Conference on Natural Fibers - Nature Inspired Sustainable Solutions, Portugal, 2023.

20. Mamtaz H., Fouladi M. H., Al-Atabi M., et al.: Acoustic Absorption of Natural Fiber Composites. In: Journal of Engineering, 2016.
<https://doi.org/10.1155/2016/5836107>
21. Ballagh K. O.: Acoustical properties of wool. In: Applied Acoustics, 48(2), 1996, pp. 101-120.
[https://doi.org/10.1016/0003-682X\(95\)00042-8](https://doi.org/10.1016/0003-682X(95)00042-8)
22. Ingard K. U.: Notes on sound adsorption technology. Noise Control Foundation, Poughkeepsie, NY, 1995.
23. Hui Z., Fan X.: Sound Absorption Properties of Hemp Fibrous Assembly Absorbers. In: Sen'i Gakkaishi, 65(7), 2009, pp. 191-196.
<https://doi.org/10.2115/fiber.65.191>
24. Samsudin E. M., Ismail L. H., Kadir A. A.: A REVIEW ON PHYSICAL FACTORS INFLUENCING ABSORPTION PERFORMANCE OFFIBROUS SOUN D ABSORPTION MATERIAL FROM NATURAL FIBERS. In: ARPJ Journal of Engineering and Applied Sciences, 11(6), 2016.
25. Bies D. A., Hansen C. H., Howard C. Q. (eds.): Engineering noise control. CRC Press, Boca Raton, FL, 2018.
26. Bast and other plant fibres. Textile Institute (Australia), Woodhead Publishing series in textiles no. 39, Woodhead, Cambridge, 2005.
27. ASTM-C0830-00R23: ASTM-C830: Standard Test Methods for Apparent Porosity, Liquid Absorption, Apparent Specific Gravity, and Bulk Density of Refractory Shapes by Vacuum Pressure. Ausgabe August 2023.
28. DIN EN ISO 9053-2:2021-02, Akustik_ - Bestimmung des Strömungswiderstandes_ - Teil_2: Luftwechselstromverfahren (ISO_9053-2:2020); Deutsche Fassung EN_ISO_9053-2:2020.
29. DIN EN ISO 10534-2:2001-10, Akustik_ - Bestimmung des Schallabsorptionsgrades und der Impedanz in Impedanzrohren_ - Teil_2: Verfahren mit Übertragungsfunktion (ISO_10534-2:1998); Deutsche Fassung EN_ISO_10534-2:2001.
30. Müller G., Möser M.: Taschenbuch der Technischen Akustik. Springer Berlin Heidelberg, Berlin, Heidelberg, 2016.
31. Mechel F. P. (ed.): Formulas of Acoustics, SpringerLink Bücher, Springer Berlin Heidelberg, Berlin, Heidelberg, 2008.
32. Bies D. A., Hansen C. H.: Flow resistance information for acoustical design. In: Applied Acoustics, 13(5), 1980, pp. 357-391.
[https://doi.org/10.1016/0003-682X\(80\)90002-X](https://doi.org/10.1016/0003-682X(80)90002-X)
33. Manning J., Panneton R.: Acoustical model for Shoddy-based fiber sound absorbers. In: Textile Research Journal, 83(13), 2013, pp. 1356-1370.
<https://doi.org/10.1177/0040517512470196>
34. Yang T., Mishra R., Horoshenkov K. V., et al.: A study of some airflow resistivity models for multi-component polyester fiber assembly. In: Applied Acoustics, 139, 2018, pp. 75-81.
<https://doi.org/10.1016/j.apacoust.2018.04.023>
35. Pelegrinis M. T., Horoshenkov K. V., Burnett A.: An application of Kozeny–Carman flow resistivity model to predict the acoustical properties of polyester fibre. In: Applied Acoustics, 101(5), 2016, pp. 1-4.
<https://doi.org/10.1016/j.apacoust.2015.07.019>
36. DallaValle J. M.: Flow of Gases through Porous Media . P. C. Carman. Academic Press, New York; Butterworths, London, 1956. 182 p. Illus. \$6. In: Science 124(3234), 1956, pp. 1254-1255.
<https://doi.org/10.1126/science.124.3234.1254.b>

AIMS AND SCOPES

“Vlákna a Textil” is a peer-reviewed scientific journal serving the fields of fibers, textile structures and fiber-based products including research, production, processing, and applications.

The birth of this journal is connected with three institutions, Research Institute for Man-Made Fibers, Svit (VÚCHV), Research Institute of Chemistry of Textiles (VÚTCH) in Žilina and Department of Fibers and Textiles at the Faculty of Chemical Technology, Slovak Technical University in Bratislava, having a joint intention to provide, utilize and deposit results obtained through the research, development and production activities dealing with the aforementioned scopes. „Vlákna a Textil“ journal has been launched as a consequence of a joining of existing magazines „Chemické vlákna“ (VÚCHV) and „Textil a chémia“ (VÚTCH). Their tradition should provide a good framework for the new journal with the main aim to create a closer link between the basic element of the product - fibre and its fabric - textile.

Since its founding in 1994, the journal introduces new concepts, innovative technologies and better understanding of textile materials (physics and chemistry of fiber forming polymers), processes (technological, chemical and finishing), garment technology and its evaluation (analysis, testing and quality control) including non-traditional applications, such as technical textiles, composites, smart textiles or garment, and nano applications among others. The journal publishes original research papers and reviews. Original papers should present a significant advance in the understanding or application of materials and/or textile structures made of them.

VLÁKNA A TEXTIL

Volume 31, Issue 1, June 2024

CONTENT

- 3 **TRAN, THI MINH KIEU; TRAN, THI NGOC HUE; NGUYEN, THANH TUNG AND HOANG, SY TUAN**
ANALYSIS OF VIETNAMESE WOMEN'S BODY SHAPE FROM ANTHROPOMETRIC DATA
- 13 **SHAHIDI, SHELA; MOAZZENHI, BAHAREH; KALAHROODI, HOSSEINI KIMASADAT AND MONGKHOLRATTANASIT, RATTANAPHOL**
WOUND DRESSING WITH TEXTILE DRESSING APPROACH: A REVIEW
- 26 **THO, LUU THI; PHUONG, DUONG THI AND HUONG, CHU DIEU**
EFFECT OF COMMERCIAL WATER REPELLENT AGENTS ON FUNCTIONAL PROPERTIES OF POLYESTER WOVEN FABRIC USED FOR WASHABLE MEDICAL MASKS
- 37 **STEHLE, FRANZISKA; GILLNER CHRISTIANE; DILBA BORIS; KEUCHEL SÖREN AND HERRMANN, AXEL S.**
ANALYSIS OF AIRFLOW RESISTIVITY AND ACOUSTIC ABSORPTION OF FIBRE-REINFORCED PLASTIC COMPOSITES MADE OF POLYLACTIC ACID AND NATURAL FIBRES

